National Library
of Canada

Bibliothèque nationale
du Canada

Canadian Theses Service

Service des thèses canadiennes

Ottawa, Canada
K1A 0N4

NOTICE

The quality of this microform is heavily dependent upon the quality of the original thesis submitted for microfilming. Every effort has been made to ensure the highest quality of reproduction possible.

If pages are missing, contact the university which granted the degree.

Some pages may have indistinct print especially if the original pages were typed with a poor typewriter ribbon or if the university sent us an inferior photocopy.

Reproduction in full or in part of this microform is governed by the Canadian Copyright Act, R.S.C. 1970, c. C-30, and subsequent amendments.

AVIS

La qualité de cette microforme dépend grandement de la qualité de la thèse soumise au microfilmage. Nous avons tout fait pour assurer une qualité supérieure de reproduction.

S'il manque des pages, veuillez communiquer avec l'université qui a conféré le grade.

La qualité d'impression de certaines pages peut laisser à désirer, surtout si les pages originales ont été dactylographiées à l'aide d'un ruban usé ou si l'université nous a fait parvenir une photocopie de qualité inférieure.

La reproduction, même partielle, de cette microforme est soumise à la Loi canadienne sur le droit d'auteur, SRC 1970, c. C-30, et ses amendements subséquents.

NL-339 (r. 88/04) c

Canada

UNIVERSITY OF ALBERTA

SOL-GEL PROCESSING OF HIGH-T_C SUPERCONDUCTORS IN THE SYSTEM Bi-(Pb)-Sr-Ca-Cu-O

BY

KUNSONG MA

A THESIS SUBMITTED TO THE FACULTY OF GRADUATE STUDIES AND RESEARCH IN PARTIAL FULFILLMENT OF THE REQUIREMENTS FOR THE DEGREE OF MASTER OF SCIENCE

IN

METALLURGY

DEPARTMENT OF MINING, METALLURGICAL AND PETROLEUM ENGINEERING

EDMONTON, ALBERTA

SPRING, 1992

National Library of Canada
Canadian Theses Service
Ottawa, Canada
K1A 0N4

Bibliothèque nationale du Canada
Service des thèses canadiennes

The author has granted an irrevocable non-exclusive licence allowing the National Library of Canada to reproduce, loan, distribute or sell copies of his/her thesis by any means and in any form or format, making this thesis available to interested persons.

The author retains ownership of the copyright in his/her thesis. Neither the thesis nor substantial extracts from it may be printed or otherwise reproduced without his/her permission.

L'auteur a accordé une licence irrévocable et non exclusive permettant à la Bibliothèque nationale du Canada de reproduire, prêter, distribuer ou vendre des copies de sa thèse de quelque manière et sous quelque forme que ce soit pour mettre des exemplaires de cette thèse à la disposition des personnes intéressées.

L'auteur conserve la propriété du droit d'auteur qui protège sa thèse. Ni la thèse ni des extraits substantiels de celle-ci ne doivent être imprimés ou autrement reproduits sans son autorisation.

ISBN 0-315-73144-3

Canada

UNIVERSITY OF ALBERTA

RELEASE FORM

NAME OF AUTHOR: KUNSONG MA

TITLE OF THESIS: **SOL-GEL PROCESSING OF HIGH-T_C SUPERCONDUCTORS IN THE SYSTEM Bi-(Pb)-Sr-Ca-Cu-O**

DEGREE: MASTER OF SCIENCE

YEAR THIS DEGREE GRANTED: SPRING, 1992

PERMISSION IS HEREBY GRANTED TO THE UNIVERSITY OF ALBERTA LIBRARY TO REPRODUCE SINGLE COPIES OF THIS THESIS AND TO LEND OR SELL SUCH COPIES FOR PRIVATE, SCHOLARLY OR SCIENTIFIC RESEARCH PURPOSES ONLY.

THE AUTHOR RESERVES ALL OTHER PUBLICATION AND OTHER RIGHTS IN ASSOCIATION WITH THE COPYRIGHT IN THE THESIS, AND EXCEPT AS HEREINBEFORE PROVIDED NEITHER THE THESIS NOR ANY SUBSTANTIAL PORTION THEREOF MAY BE PRINTED OR OTHERWISE REPRODUCED IN ANY MATERIAL FORM WHATEVER WITHOUT THE AUTHOR'S PRIOR WRITTEN PERMISSION.

SIGNATURE: Ma Kunsong

PERMANENT ADDRESS:

113# - 37BLG. UNIVERSITY OF
SCIENCE AND TECHNOLOGY
BEIJING, P.R. CHINA (100083)

DATE: Oct. 17. 1991

UNIVERSITY OF ALBERTA

FACULTY OF GRADUATE STUDIES AND RESEARCH

THE UNDERSIGNED CERTIFY THAT THEY HAVE READ, AND RECOMMEND TO THE FACULTY OF GRADUATE STUDIES AND RESEARCH FOR ACCEPTANCE, A THESIS ENTITLED, **SOL-GEL PROCESSING OF HIGH-T_C SUPERCONDUCTORS IN THE SYSTEM Bi-(Pb)-Sr-Ca-Cu-O**, SUBMITTED BY KUNSONG MA IN PARTIAL FULFILLMENT OF THE REQUIREMENTS FOR THE DEGREE OF MASTER OF SCIENCE IN METALLURGICAL ENGINEERING.

JmWhiting

DR. J. WHITING, COMMITTEE CHAIRMAN

DR. A.C. PIERRE, SUPERVISOR

J. Jung

DR. J. JUNG, COMMITTEE MEMBER

DR. N.O. EGIEBOR, COMMITTEE MEMBER

DATE: Oct. 17. 1991

ABSTRACT

Superconducting materials in the Bi-(Pb)-Sr-Ca-Cu-O system have been synthesized by sol-gel processing from nitrates by complexation with citric acid. The gelation process and the structures of the gels obtained have been studied through titration and SEM observation. Their phase transformations and microstructure development, during heat treatment, have been investigated by X-ray diffraction, SEM, and BET from 220°C to 860°C. The 2-2-0-1 phase forms at a lower temperature by this sol-gel processing than by conventional processing while the 2-2-1-2 and 2-2-2-3 phases form at about the same temperature. The 2-2-0-1 and 2-2-1-2 phase formations are by progressing intercalation of the other cations between the Cu-O layer of the copper oxide while that of the 2-2-2-3 phase is by nucleation and growth from the 2-2-1-2 phase. Sintering appears to be in competition with grain growth and phase transformation to the 2-2-2-3 phase. The later was promoted by the presence of liquid phases. The 2-2-1-2 and 2-2-2-3 grains had a plate-like shape. The later was promoted by the presence of liquid phases. The superconducting properties are sensitive to the addition of lead in this sol-gel processing. The higher the proportion of the 2-2-2-3 phase, the higher the critical temperature $T_{c,0}$ above 100K.

ACKNOWLEDGEMENT

I am most grateful to Professor Alain.C. Pierre for his supervision and guidance during this research and for writing the thesis, without which I could not finish this study.

This thesis and research are granted by the NATIONAL SCIENCE AND ENGINEERING RESEARCH COUNCIL OF CANADA (NSERC). Its support is fully acknowledgeed.

I should like to express my thanks to Ms. Tina Baker who took micrographs by SEM and all the help she gave me, and also to Mr.Skrzypek Henryk who help to prepare the samples.

I wish to acknowledge Mr. Terry Nickerson who guided me to prepare the gels and set up equipments used in the experiment, and Mr. Stefaniuk Rob and Mr Booth Doug who made the equipment for measuring critical temperatures.

I am deeply grateful to my wife Ding Yuan for all her help during this study and valuable comments on the results.

TABLE OF CONTENTS

CHAPTER PAGE

1. INTRODUCTION ... 1

2. LITERATURE REVIEW ... 3

2.1) SUPERCONDUCTING MATERIALS ... 3

2.1.1) Short history ... 3
2.1.2) The phenomenon of superconductivity ... 6
a) Critical properties of superconductors ... 6
b) Theory of superconductivity ... 10
2.1.3) Application ... 13
2.1.4) New high-T_c superconductors ... 15

2.2) THE Bi-(Pb)-Sr-Ca-Cu-O SYSTEM ... 16

2.2.1) Crystal structures ... 16
a) The 2-2-0-1 phase ... 17
b) The 2-2-1-2 phase ... 17
c) The 2-2-2-3 phase ... 17
d) Place of Pb in the 3 superconducting phases ... 21
e) Incommensureability of superconductors in the Bi-(Pb)-Sr-Ca-Cu-O system ... 23

2.2.2) Phase transformation and processing ... 23
a) Thermodynamics ... 23
b) Kinetics ... 25
c) Processing ... 28
i) Calcination and solid state reaction ... 28
ii) Sintering behaviors ... 29
iii) Microstructure ... 31
iv) Atmosphere ... 33

2.2.3) Superconducting properties ... 34

a) Energy gap, $\Delta(0)$ ... 34
b) Characteristic lengths, ξ and λ ... 35
c) Critical magnetic field, H_{c1} and H_{c2} ... 36
d) Critical temperature, $T_{c,0}$ ... 37
e) Critical current density, J_c ... 40

2.3) SOL-GEL PROCESSING ... 42

2.3.1) Summary of sol-gel processing ... 42
2.3.2) Cases of sol-gel processing for high-Tc superconductors ... 44
a) Inorganic salts ... 45
b) Organic salts ... 46
c) Alkoxides and organometallics ... 48
d) Organic additives ... 50
2.3.3) Sol-gel processing in the Bi-(Pb)-Sr-Ca-Cu-O system ... 51

3. EXPERIMENTAL PROCEDURE ... 53

3.1) RESEARCH STRATEGY ... 53

3.2) EXPERIMENTAL PROCEDURE ... 54

3.2.1) Sample preparation ... 54
3.2.2) Choice of initial composition ... 55
3.2.3) Sol-gel processing ... 55
3.2.4) Calcining and pellitizating ... 55
3.2.5) Superconductors transformation studies ... 56

3.3) CHARACTERIZATION OF MATERIALS AND EQUIPMENT USED: ... 57

3.3.1) Titration experiment ... 57
3.3.2) X-ray diffraction ... 57
a) Equipment ... 57
b) Phase identification ... 58
3.3.3) Density measurement ... 58

3.3.4) SEM and optical microscopy ... 60
a) Equipment ... 60
b) Sample preparation ... 60
c) Estimation of grain growth ... 60

3.3.5) BET method ... 61

3.3.6) The dc four probe method ... 61

4. RESULTS ... 64

4.1) SOL-GEL PROCESSING ... 64
4.1.1) Gelation ... 64
4.1.2) Gel structure and properties ... 64

4.2) PHASE TRANSFORMATION ... 70
4.2.1) During calcination of the gels up to 800°C ... 70
4.2.2) In superconductors above 800°C ... 70

4.3) SUPERCONDUCTOR PELLET'S MICROSTRUCTURE ... 89

4.3.1) Sintering behaviors ... 89
4.3.2) Microstructure observation under the SEM ... 94
4.3.3) Grain growth and oriented microstructure ...105

4.4) CRITICAL TEMPERATURE, $T_{c,0}$ ...110

5. DISCUSSION ...114

5.1) GELATION AND ULTRASTRUCTURE OF GELS ...114

5.2) PHASE TRANSFORMATION ...117

5.3) MICROSTRUCTURE AND SINTERING BEHAVIORS ...124

5.4) SUPERCONDUCTIVITY ...127

6. CONCLUSIONS ...129

7. FURTHER WORK ...131

REFERENCE ...132

APPENDIX ...141

LIST OF TABLES

PAGE

Table 2.1. Important events in developments of superconducting techniques ... 4

Table. 2.2 Application of various superconducting devces ... 14

Table. 2.3 Calculated and observed X-ray powder diffraction date of the 2-2-0-1 phase with a = b = 5.389Å and c = 24.64Å after Saggio, et al. ... 19

Table. 2.4. Calculated and observed X-ray powder diffraction date of the 2-2-1-2 phase with a = b = 5.42 ± 0.3 Å and c = 30.71 ± 0.15 Å after Srinivasan, et al. ... 20

Table. 2.5 Estimation of the X-ray powder diffraction data of the 2-2-2-3 phase after Koyama, et al. ... 21

Table. 2.6 Creitical temperature of the 3 superconducting phase in the Bi-(Pb)-Sr-Ca-Cu-O system ... 37

Table. 2.7 Relationship between sintering conditions and critical temperatures of the 2-2-0-1 type superconductors by conventional ceramic processing ... 38

Table. 2.8 Relationship between sintering conditions and critical temperaturesof the 2-2-1-2 type superconductors by conventional ceramic processing ... 38

Table. 2.9 Relationship between sintering conditions and critical temperatures of the 2-2-2-3 type superconductors by conventional ceramic processing ... 39

Table. 2.10 Critical current density J_c obtained in the Bi-(Pb)-Sr-Ca-Cu-O system by different methods ... 41

Table. 2.11 Relationship between sintering conditions and critical temperatures in sol-gel processes ... 52

Table. 3.1 The intial compositions of gel(a), (b) and (c) in the present reserch ... 55

Table. 3.2 Summary of heat-treatment studies of superconductors from the gel(a), (b), and (c) ... 56

LIST OF TABLES

Table. 4.1 Estimate of n, from the data on grain growth ...106

Table. 4.2 Critical temperature ($T_{c,0}$) where the resistivity cancels, for gel(a), (b) and (c) superconductors ...110

LIST OF FIGURES

PAGE

Fig. 2.1 Variation of the electric resistance of mercury with temperature ... 3

Fig. 2.2 Progress in the highest critical temperature of superconductors since their discovery ... 5

Fig. 2.3 Domain, as a function of the magnetic field H, temperature T and electric current density J, where a material is a superconductor ... 6

Fig. 2.4 Magnetization as a function of the applied magnetic field for a bulk superconductor; (a) type-I superconductor; (b) type-II superconductor ... 7

Fig. 2.5 (a) Slab of superconducting materials submitted to an external magnetic field H, (b) variation of the induction B, with distance y, inside the superconductor ... 9

Fig. 2.6 The mixed state in a type-II superconductors, showing normal cores and encircling superconducting vortices ... 10

Fig. 2.7 Electron-phonon coupling of a Cooper's pair in the BCS theory ... 11

Fig. 2.8 (a) Conduction band in the normal state; (b) Formation of energy gap at the Fermi level in the superconducting state ... 12

Fig. 2.9 Structural models of the average structure of $Bi_2Sr_2Ca_{n-1}Cu_{n+1}O_{4+2n+\delta}$ phases for n = 1 (a), n = 2 (b) and n = 3 (c). Cations are indicated by the symbol of the element in one half of the cell and small circles indicate oxygen atoms ... 18

Fig. 2.10 Crystal structure of the high-T_c phase in the Bi-Pb-Sr-Ca-Cu-O system ... 22

Fig. 2.11 (a) Quasi quaternary tetrahedron, showing the existence of the three superconducting phases (full lines). 1, 2, and 3 are representive for the 2-2-0-1, 2-2-1-2 and 2-2-2-3 phases. Phase diagram in the Bi-Sr-Ca-Cu-O system at 750°C (b); at 800°C (c); at 850°C (d) ... 26

Fig. 2.12 T-T-T diagrams of the Bi-Pb-Sr-Ca-Cu-O thin films, showing the formation domains of the 2-2-0-1, 2-2-1-2, and 2-2-2-3 phase ... 26

Fig. 2.13 Density achieved in 2-2-1-2 samples as a function of sintering temperature ... 30

Fig. 2.14 Variation of bulk density with sintering time 845°C, in $(Bi,Pb)_2Sr_2Ca_2Cu_3O_{10}$ made by conventional processing ... 30

Fig. 2.15 Oxygen partial-pressure dependence of the processing window ΔT for obtaining the Bi-Sr-Ca-Cu-O 2-2-2-3 phase ... 34

Fig.2.16 Simplified chart of sol-gel processing from A.C. Pierre ... 43

Fig. 3.1 Flow chart for the preparation of superconductors in the Bi-(Pb)-Sr-Ca-Cu-O system ... 54

Fig. 3.2 Illustration of T_c measurement equipment set-up for a dc four probe method ... 62

Fig. 3.3 Illustration of a sample with Indium connection for T_c measurement ... 63

Fig. 4.1 Illustration of gel(a), (b) and (c) ... 66

Fig. 4.2 Titration curves of nitrates with aqueous ammonia: (a) Bi, Pb, Sr, Ca, Cu nitrate titrated individually; (b) mixtures of Bi, Pb, Sr, Ca, Cu nitrates with composition of gel(c)- titrated with or without citric acid ... 67

Fig. 4.3 Microstructures of gel(a) are observed under a SEM. The gel was dried (a) at 20°C; (b) and (c) at 65°C ... 68

Fig. 4.4 The appearance of the gel(c): (a) before heat-treatment; (b) after heat-treatment at 220°C for 2 hours ... 69

Fig. 4.5 Black gels obtained by redissolving the gels heat-treated at (a)180°C; (b) 210°C, and (c) 240°C ... 69

Fig. 4.6 X-ray powder diffraction patterns of gel(a) heat-treated at different temperature for 12 hours ... 72

Fig. 4.7 X-ray powder diffraction patterns of gel(b) and (c) heat-treated at 700, 750, and 800°C for 12 hours ...73

Fig. 4.8 X-ray diffraction patterns of gel(a) pellets heated at 815, 830, 845, and 860°C for 24 hours ... 74

Fig. 4.9 X-ray diffraction patterns of gel(b) pellets heated at 815, 830, 845, and 860°C for 24 hours ... 75

Fig. 4.10 X-ray diffraction patterns of gel(c) pellets heated at 815, 830, 845, and 860°C for 24 hours ...76

Fig. 4.11 X-ray diffraction patterns of gel(a) pellets heat-treated at 815°C for increasing times ... 79

Fig. 4.12 X-ray diffraction patterns of gel(b) pellets heat-treated at 815°C for increasing times ... 80

Fig. 4.13 X-ray diffraction patterns of gel(c) pellets heat-treated at 815°C for increasing times ...81

Fig. 4.14 X-ray diffraction patterns of gel(a) pellets heat-treated at 830°C for increasing times ... 82

Fig. 4.15 X-ray diffraction patterns of gel(b) pellets heat-treated at 830°C for increasing times ... 83

Fig. 4.16 X-ray diffraction patterns of gel(c) pellets heat-treated at 830°C for increasing times ... 84

Fig. 4.17 X-ray diffraction patterns of gel(a) pellets heat-treated at 845°C for increasing times ... 85

Fig. 4.18 X-ray diffraction patterns of gel(b) pellets heat-treated at 845°C for increasing times ... 86

Fig. 4.19 X-ray diffraction patterns of gel(c) pellets heat-treated at 845°C for increasing times ... 87

Fig. 4.20 Estimatation of volume fraction of the 2-2-2-3 phase by $I_h(0010)/I_h(0010)+I_l(008)$ from X-ray powder diffraction data ... 88

Fig.4. 21 Evolution of bulk density of gel(a), (b) and (c) samples with time: at (a) 815°C, (b) 830°C, (c) 845°C ... 91

Fig. 4.22 Evaluation, with temperature, of the bulk density attained after 24 hours heat treatments for the 3 superconductors ... 92

Fig. 4. 23 Pore structure evolution during heat treating at 845°C, for gel(a) and (b) superconductors: (a) specific surface area; and (b) average pore radius ... 93

Fig. 4.24 Scanning electron micrograph and semi-quantitative EDAX analysis of a gel(b) superconductor heat-treated at 845°C for 144 hours ... 96

Fig. 4.25 Formation of slit shaped microcracks inside a gel(c) superconductor heat treated at 830°C ... 97

Fig. 4.26 SEM micrographs of gel(a), (b) and (c) superconductor pellets after 144 hours heat-treatment at 845°C ... 98

Fig. 4.27 Evolution of the microstructure under the SEM, for gel(b) superconductor pellets heat treated at 815°C for: (a) 24h; (b) 144h ... 99

Fig. 4.28 Evolution of the microstructure under the SEM, for gel(b) superconductor pellets heat treated at 830°C for: (a)24h; (b)48h; (c)144h; (d)288h ...100

Fig. 4.29 Evolution of the microstructure under the SEM, for gel(b) superconductor pellets heat treated at 830°C for: (a)24h; (b)48h; (c)144h; (d)288h ...101

Fig. 4.30 Evolution of the microstructure under the SEM, for gel(a) superconductor pellets heat treated at 830°C for: (a)144h; (b)288h ...102

Fig. 4.31 Evolution of the microstructure under the SEM, for gel(b) superconductor pellets heat treated at 845°C for: (a)24h; (b)96h; (c)144h; (d)288h ...103

Fig. 4.32 Evolution of the microstructure under the SEM, for gel(c) superconductor pellets heat treated at 845°C for: (a)24h; (b)96h; (c)144h; (d)288h ...104

Fig. 4.33 Grain growth kinetics in superconductors: (a) gel(c) superconductors at different temperature; (b) gel(a), (b), and (c) superconductors at 845°C ...107

Fig. 4.34 Grain growth data plotted with log(D) as a function of log(t) ...108

Fig. 4.35 Estimation of the orientation degree of superconductor pellets from X-ray diffraction pattern; (a) at 815°C; (b) at 830°C ...109

Fig. 4.36 Variation of the resistance with temperature for the gel(a) sample sintered at 845°C for 144 hours ...111

Fig. 4.37 Variation of the resistance with temperature for the gel(b) sample sintered at 845°C for 96 hours ...111

Fig. 4.38 Variation of the resistance with temperature for the gel(b) sample sintered at 845°C for 144 hours ...112

Fig. 4.39 Variation of the resistance with temperature for the gel(c) sample sintered at 830°C for 144 hours ...112

Fig. 4.40 Variation of the resistance with temperature for the gel(c) sample sintered at 845°C for 144 hours ...113

Fig. 4.41 Variation of the resistance with temperature for the gel(c) sample sintered at 845°C for 288 hours ...113

CHAPTER 1: INTRODUCTION

The phenomenon of superconductivity was discovered 80 years ago. Since that time, superconductivity have been studied extensively in many ways, and many applications of superconductors have been developed or are considered.

The most traditional superconductors are metallic alloys and must be cooled to a very low temperature of about 4K in liquid helium. However, since 1986, new superconducting materials have been discovered, which can be used in liquid nitrogen at about 77K. They are complex ceramics of the perovskite type. They have attracted an enormous number of investigations. Many investigation aim to understand the physics of superconductores, and its origin in these materials. Others address their complex structures. Some are application oriented. A very important group concerns their processing; as monoliths, ribbons, coating, or wires, which is a difficult task given their very brittle and anisotropic nature. The present study belongs to this last group.

Most recently, the possibility of making superconductors in the Bi-(Pb)-Sr-Ca-Cu-O system by a sol-gel processing has been explored. The system considered is one of the most promising , and yet one of the most difficult to process. However, sol-gel processing is a relatively new field in the engineering of ceramics, which offers interesting possibilities for fabricating ceramic wires, ribbons, coating or powder sintering at a temperature lower than with conventional processing.

A complete sol-gel process, from the chemical synthesis of gels, to the final superconductors, including phase transformation of the gels and sintering, is followed here step by step.

The thesis is organized as follows. The next chapter gathers a literature review summarizing the field of superconductors and the phenomena of superconductivity. Recent research on the new high temperature superconductors, especially on the Bi-(Pb)-Sr-Ca-

Cu-O system, are presented. In chapter 3 the experimental procedures and equipments used in the present work are described, and the results are presented in chapter 4. They concern the structures and properties of the materials in the successive steps of this sol-gel process. The techniques used comprise X-ray diffraction, density measurement and pore structure analysized by the BET method, microstructures observed under a SEM and an optical microscope, and determination of the critical temperature ($T_{c,0}$) by a dc four probes method. These results are discussed in chapter 5. After conclusion in chapter 6, some suggestions are proposed for further research on improving the quality of the superconductors made by the sol-gel processing, and understanding the phase transformation mechanisms as well as the relation between microstructure and superconducting properties.

CHAPTER 2: LITERATURE REVIEW

The present work is placed within the general field of superconductivity, which is first reviewed briefly. Two domains are more deeply involved: the system Bi-(Pb)-Sr-Ca-Cu-O; and the sol-gel processing in this system. They are addressed in the two following sections of this literature review.

2.1) SUPERCONDUCTING MATERIALS

2.1.1) Short history

The electrical resistivity of many metals, alloys and ceramics goes down suddenly to zero when the samples are cooled to a sufficiently low temperature. This phenomenon, called superconductivity, was observed firstly by Karmerlingh Onnes[1] in Leiden in 1911. Below a critical temperature T_c the sample undergoes a phase transition from a normal electrical resistivity state to a superconductivity state with zero resistance (Fig. 2.1)[1, 2].

The materials involved has been removed because of copyright restrictions.

Fig. 2.1 Variation of the electric resistance of mercury with temperature[2].

Since that time the phenomenon has attracted many scientists and engineers. The main historical events in the development of superconductors are summarized in Table. 2.1. Many applications have been found and will be summarized in the next section.

Table 2.1. Important events in developments of superconducting techniques[3, 4, 5]

Year	Events in developments of superconducting techniques	Reference
1908	Helium liquefaction by Kamerlingh Onnes.	[5]
1911	Onnes discovered superconductivity in Hg at $T_c = 4.1K$	[1]
1913	Pb found to be superconducting at $T_c = 7.2K$.	[5]
1914	Superconductivity could be undermined by the presence of magnetic fields and low currents.	[5]
	Onnes made the first superconducting magnet.	[5]
1930's	Discovery of Meissner effect and the type-II superconductors in alloys	[6]
	The London Theory	[7]
1950	The Ginzburg-Landau theory	[8]
1957	Bardeen, Cooper and Schrieffer established the BCS theory	[9]
	Theory of the type-II superconductors	[10]
1960's	Discovery of Josephson effect.	[11]
1970's	Nb_3Ge with $T_c = 23.2K$	[12]
1986	Bednorz and Müller made a scientific breakthrough in the La-Ba-Cu-O system with $T_c = 30\text{-}40K$.	[13]
1987	Superconductors in the Y-Ba-Cu-O system with T_c=80-90K, above the temperature of liquid nitrogen.	[14]
1988	Superconductors in the Bi-(Pb)-Sr-Ca-Cu-O system with $T_c = 110K$ and in the Tl-Ba-Sr-Ca-Cu-O with $T_c = 120K$	[15, 16]

After the discovery of superconductivity a number of important properties have been progressively found, for instance, the Meissner effect, the type-I and the type-II superconductors, and the isotope effect. These have provided the ground to develop theories allowing to understand the phenomena associated with superconductivity.

In 1934, Gorter and Casimir[17] developed a two-fluid model to explain the thermal properties and zero resistance of superconductors successfully. It assumed that normal state electrons coexist with superconducting electrons, in a superconductor. In 1935, F. and H. London [7] derived the London equations to explain an effect called Meissner effect and described later. In 1950, V.L. Ginzburg and L.D. Landau [8] applied the Landau phase transition theory to the derivation of the Ginzburg-Landau equations and explained the thermal, electrical and electromagnetic properties of a superconductor. In 1957, A.A. Abrikosov[10] solved these Ginzburg-Landau equations and explained the difference between the type-I and type-II superconductors.

The materials involved has been removed because of copyright restrictions.

Fig. 2.2 Progress in the highest critical temperature of superconductors since their discovery[4].

The superconductivity in metals and alloys is now very well understood by the BCS theory[9], call after the name initial of Bardeen, Cooper and Schrieffer.

In 1986 a breakthrough in the discovery of high-T_c superconductors in ceramics triggered extensive researches to find superconductors with a higher critical temperature, possible at room temperature[13]. The Fig. 2.2 shows the progresses in the raising of the critical temperature since the beginning of the discovery of superconductivity[4]. The discovery of superconductors in the Y-Ba-Cu-O system, with a critical temperature above 77K, is an important achievement because liquid nitrogen is much cheaper and more abundant than liquid helium. Before, the use of liquid helium as a coolant was necessary .

2.1.2) The phenomenon of superconductivity

a) Critical properties of superconductors[2, 4, 12, 18, 19, 20]

A superconductor is characterized by a zero electrical resistance when it is submitted to a temperature, a magnetic field and an electric current below critical values. These critical values define a domain, summarized on Fig. 2.3[19], where superconductivity maintains.

The materials involved has been removed because of copyright restrictions.

Fig. 2.3 Domain, as a function of the magnetic field H, temperature T, and electric current density J, where a material is a superconductor[19].

The critical temperature (T_c) is the temperature below which the electric resistance of the materials varnishes. In practice the resistance begins to drop at an " onset critical temperature" $T_{c,onset}$ and cancels out completely at a lower temperature $T_{c,0}$. The values of T_c depends on the magnetic field.

The critical current density (J_c) is the largest current density the material can carry under zero voltage in the superconducting state. Actually J_c depends on the magnetic field to which it is submitted and on the temperature of operation.

The critical magnetic field (H_c) is the lowest magnetic field (**H**) which destroys the superconducting state at a given temperature and a given current density.

The variation of magnetization **M** inside a superconductor, when a magnetic field **H** is applied, is summarized as Fig. 2.4. Type-I superconductors exhibit a sharp transition described by a unique critical magnetic field-H_c (Fig. 2.4(a)). Below the H_c (type-I) or H_{c1} (Type-II), the magnetic induction B inside the superconductor is[19, 20];

$$\mathbf{B} = \mu_o(\mathbf{H}+\mathbf{M}) = 0 \qquad (2.1)$$

where B is an induced magnetic field and μ_o is constant, that is to say

The materials involved has been removed because of copyright restrictions.

Fig. 2.4 Magnetization as a function of the applied magnetic field for a bulk superconductor; (a) type-I superconductor; (b) type-II superconductor[18].

$$\mathbf{M} = -\mathbf{H} \tag{2.2}$$

where **M** is the magnetization. However, type-II superconductors undergo a progressive transition from the superconductive to a normal state, between a lower critical field H_{c1} and a upper critical field H_{c2}, as shown in Fig. 2.4(b).

Superconductors are "superdiamegnetic" materials which expel any applied magnetic field from the sample. This effect, called the Meissner effect, often helps to unambiguously demonstrate the occurrence of superconductivity with the familiar sight of a small bar magnet raising over the surface of a superconductor.

The London and Ginzburg-Landau theories have brought one important parameter characterizing the penetration depth of a magnetic field - the London penetration depth (λ). When a type-I superconductor is submitted to a magnetic field **H**, the induction field **B** does not change discontinuously from its value outside the sample to a zero value inside. Rather, its magnitude decreases exponently with the distance from sample external surface. The situation is illustrated in Fig. 2.5, and can be described by the following equation derived from the London equations.

$$B_z(y) = B_z(0)e^{-y/\lambda} \tag{2.3}$$

Where $B_z(0)$ is the magnetic induction at the sample surface and

$$\lambda^2 = \frac{m}{\mu_o n_s e^2} \tag{2.4}$$

The parameter λ, called the London penetration depth, is a measure of the distance the induction field penetrates into the sample[2]. The magnitude of λ is in order of 100-1000Å typically in conventional metallic superconductors[20].

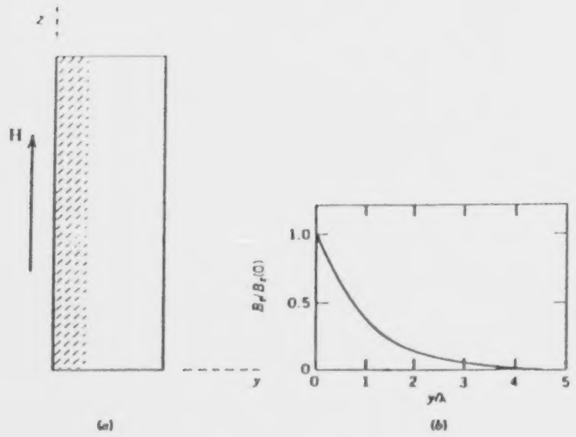

Fig. 2.5 (a) Slab of type-I superconducting materials submitted to an external magnetic field H, (b) variation of the induction B, with distance y, inside the superconductor.

In a type-II superconductor, a magnetic flux penetrates a superconductor in a quantified manner. This is also true for the magnetic field induced by a current passing in the superconductor. Each quantum is called a fluxoid. Its value is[18]

$$\phi_o = 2\pi h/2e = 2.0678 \times 10^{-15}\ \text{tesla}\cdot\text{m}^2 \tag{2.5}$$

According to the quantum theory , the minimum permissible quantum magnetic flux for one free electron is half of the value of (2.5). This double value for the fluxoid comes from the presence of 2 electrons in a Cooper's pair[12, 18].

The number of fluxoids change with applied magnetic field **H** and temperature T, for a magnetic field between H_{c1} and H_{c2}. This mixed state is described in Fig. 2.6, where the shaded cores are normal state fluxoid and a current flows in vortices of thickness λ around each fluxoid. Each current generates a magnetic flux with the value of a fluxoid.

Concerning the coherence length ξ, its physical mean will be discussed in the next section. Ginzburg-Landau has defined a characterization of the type of superconductors by the ratio;

$$\chi = \lambda/\xi \tag{2.6}$$

For a type-I superconductors $\chi < 0.71$. For a type-II superconductor $\chi > 0.71$.

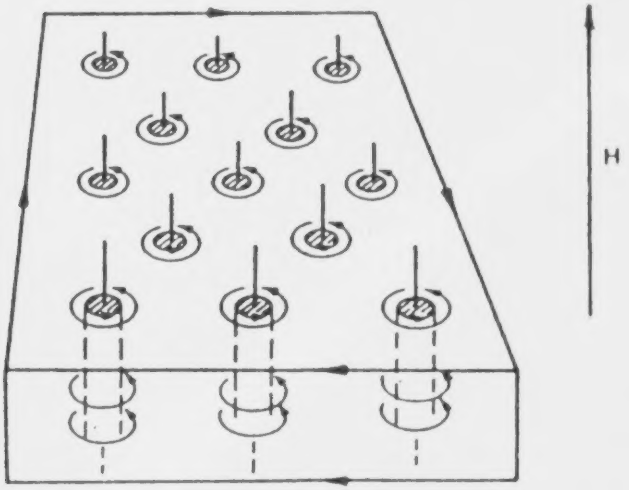

Fig. 2.6 The mixed state in a type-II superconductors, showing normal cores and encircling supercurrent vortices.

b) Theory of superconductors[2, 9, 12, 18, 20]

The basis for the classical theory of superconductivity was laid in 1957 by Bardeen, Cooper, and Shrieffer[9], and is called the BCS theory.

According to this theory, superconductivity is due to an attractive force between electrons by the intermediate of the charged atoms nuclei. The coulomb attraction between the electrons and the atom nuclei enhances the atomic vibration of the material. This energy is restituted to a second electron with an opposite spin. Two electrons happen therefore to be coupled by electron-phonon interactions. This phenomenon is illustrated on Fig. 2.7. The corresponding coupling energy is maximum when the two electrons have momentum identical in magnitude and opposite in direction and also opposite spins, in which case the total momentum of the electrons pair is zero. Pairs of electrons that meet these conditions, called Cooper pairs, are the fundamental superconducting charge carriers in the BCS theory. The Cooper-pair has a lower free energy than the previously free electrons[2, 21].

The materials involved has been removed because of copyright restrictions.

Fig. 2.7 Electron-phonon coupling of a Cooper's pair in the BCS theory[2].

Successful theoretical results have been achieved on the discovery of Cooper's pair, when they form by condensation of electrons near the Fermi surface according to the Fermi-Dirac distribution[2, 9, 18].

The electron-lattice-electron interaction leads to the formation of an energy gap (in Fig. 2.8[18]) with a magnitude, $\Delta(0)$ at 0K given by[12]

$$\Delta(0) = 2h\omega_{\theta}\exp(-1/UD(\mathbf{e_F})) \qquad (2.7)$$

In the above equation ω_θ is the Debye angular frequency, U the electron-lattice interaction, and D the electron orbital density of one spin at the Fermi level, typically $\Delta \sim 10^{-4}\,\varepsilon_F$[18].

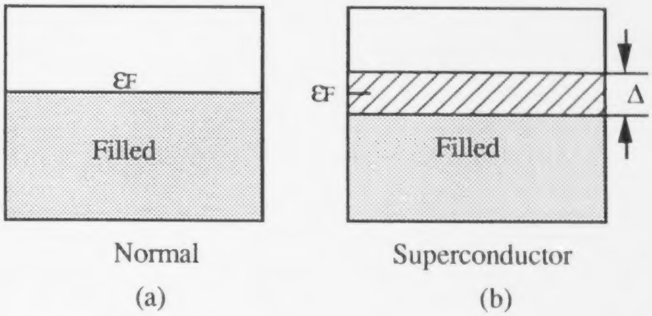

Fig. 2.8 (a) Conduction band in the normal metallic state; (b) Formation of energy gap at the Fermi level in the superconducting state.

An important length, called the coherence length (ξ) measures the average separation between the two electrons in a Cooper's pair. The intrinsic, also called Pippard's value, of the coherence length, denoted by ξ_o, can be expressed as:

$$\xi_0 = \frac{hv_F}{2\Delta} \tag{2.8}$$

where v_F is the average velocity of electrons at the Fermi surface, Δ is the superconducting energy gap and h is Planck's constant[2, 18].

The critical temperature T_c of an element or alloy depends on the electron orbital density $D(\varepsilon_F)$ of one spin at the Fermi level and on the electron-lattice interaction U. The latter can be estimated from the resistivity at room temperature which depends itself on the electron-phonon interaction. For $UD(\varepsilon_F) << 1$ the BCS theory predicts[12,18]

$$K_BT_c = 1.13h\omega_\theta \exp[-1/UD(\varepsilon_F)] \tag{2.9}$$

This result is in qualitative agreement with the experimental data. An apparent paradox must be noticed: the higher the resistivity of a metallic conductor at room temperature, the higher U, and hence the higher the critical temperature T_c where the material become a superconductor.

A comparison of equations (2.7) and (2.9), gives the following relation:

$$\frac{2\Delta}{K_B T_c} = 3.53 \qquad (2.10)$$

This indicates the critical temperature is proportional to the energy gap. The coefficient 3.53 represents the Cooper's pair coupling according to the BCS theory[12, 18].

All electrons, including the Cooper's pairs, are characterized by a perfectly isotopic distribution of their momentum, when no current flows. However, when a superconductor carries a current, all Cooper's pairs have the same momentum. Because of coupling, the current is carried by pairs, and the momentum is not lost in a scattering processing. In other words, there is no resistance as long as the current is carried by Cooper's pairs. The only way to destroy this superconducting state is to tear up the Cooper's pairs. The energy of a Cooper's pair increases when it carries a current or is submitted to an applied electrical field, or/and an applied magnetic field. If this energy exceeds that the Cooper's pair coupling energy, the Cooper's pair is destroyed. Hence, critical temperature, critical current density, and critical magnetic field are related to each other in a superconductor[12, 18].

2.1.3) Applications

Superconductors can be used in many applications, for instance, power transmission with a low energy loss, high energy accelerators and techniques requiring powerful magnets.

Table 2.2. Predicted Times for real applications of various Superconducting Devices [19]

Domain	Applications
High energy	Magnetic levitation train
	Superconductor-driven ship
	Power line
	Power generator
	Power storage
	Superconducting magnet
	Particle accelerator
	NMR/MRI
	Magnetic shielding
Low energy	Josephson device as switches
	Logic gates
	Computer memory
	SQUIDS
	IC package / substrate
	Superconductor,semiconductor IC
	IR sensors

The number of possible attractive applications of superconductors is large and the discovery of high-T_c ceramic superconductors, able to work in the liquid nitrogen temperature, has increased their interests. A partial listing of applications is given in Table 2.2. It has excited a very active competition between most developed countries.

The effect called Josephson, mentioned in Table 2.2, consists in a tunneling of a Cooper's pair from a superconductor to another superconductor, either through a thin insulating layer or through a narrow superconducting contact called a weak link where only one magnetic fluxion can pass. This effect provides the theoretical basis for superconducting quantum interference devices (SQUIDS) and many electric applications[11, 12].

2.1.4) New high-T_c superconductors

Since Bednorz and Müller[13] discovered the high-T_c superconductor in the La-Ba-Cu-O system, with a T_c between 30-40K in 1986, several other high-T_c superconducting systems have been found. They include the Y-Ba-Cu-O system with a critical temperature T_c in the range of 90-100K[14], the Bi-(Pb)-Sr-Ca-Cu-O system with a highest T_c =110K[15] and the Tl-Ba-Sr-Ca-Cu-O system with a T_c in the range of 120-125K [16]. The Bi-(Pb)-Sr-Ca-Cu-O system presents several advantages. In particular it does not contain rare-earth elements. Its phases are chemically stable and not dangerous for health like the Tl superconductors. The system will be discussed in more detail in the following sections.

These superconductors have to be fabricated in configurations that depend on the specific applications, that is (i) thin films for SQUIDS, Josephson junction switches, infrared (IR) sensors, (ii) thick films for circuit interconnection and current switches, (iii) bulk materials for magnetic bearings or microwave cavities, and (iv) fine wires and fibers or whiskers for high-field magnets, motors and generators, or power transmission[22].

Thin films (less than about 3000Å thickness) are usually made by epitaxial growth on single-crystal substrates such as $SrTiO_3$, $LaGaO_3$, $LaAlO_3$ or MgO. This includes a number of different processing methods such as sputtering, molecular beam epitaxy, chemical vapor deposition, metal organic chemical vapor deposition, sol-gel process, and laser ablation. The deposition is followed by heat treatment (usually at $T \leq 900°C$), in different atmospheres[22]. High-quality monocrystalline layers with the c-axis perpendicular to the substrate surface have been grown in the Y-Ba-Cu-O, Bi-(Pb)-Sr-Ca-Cu-O, and Tl-Ba-Sr-Ca-Cu-O systems. Their critical current density J_c can be as high as 10^6 A/cm^2 at 77K, under a magnetic field $H = 0$[23]. A review paper on the subject has been written by Humphreys, et al. [24].

Thick films have successfully been prepared by screen printing, from slurries[25, 26.1], and by plasma coating[26.2]. The thick films made so far have a low critical current density (100-1000A/cm^2 at 77K, H = 0)[22].

There are many methods to fabricate bulk high-T_c superconductors. They can be classified in conventional solid state reaction , sol-gel, and melt-quenching processes. The main problem with bulk superconductors is also their low critical current density. The number of publications on this subject is enormous and will not be addressed.

The fabrication of wires, fibers or whiskers of high-T_c ceramic superconductors is required for a number of important applications, for example, power transmission. High-T_c ceramic superconductors are mechanically brittle and cannot be drawn easily into fine wires. However, several different approaches have been studied to overcome this problem. They include metal-clad composite wires with the superconducting powder placed in a metal tube, metal-core composite wires where a metal wire is coated with the superconductors, and all ceramic wires and tapes made by slurry-extrusion, tape-casting, melt-spin or metal precursor melt-spinning[22], sol-gel[27], laser heated pedestal growth processes[28], and drawing in glass[29].

2.2) THE Bi-(Pb)-Sr-Ca-Cu-O SYSTEM

2.2.1) Crystal Structures

The structure of superconductors in the Bi-(Pb)-Sr-Ca-Cu-O system can be described by reference to the simpler Bi-Sr-Ca-Cu-O system. The latter comprises three different superconducting phases with structure similarities. Their chemical composition can be expressed as $Bi_2Sr_2Ca_{n-1}Cu_nO_{4+2n+\delta}$ with n = 1, 2, and 3 for these called 2-2-0-1, 2-2-1-2 , and 2-2-2-3 phases respectively. The structures can be understood in terms of BiO double layers and perovskite-type cuboids which are sandwiched between the BiO layers [Perovskites, Appendix A]. Each perovskite cubic comprises respectively 1, 2, and 3 CuO layer in the 3 phases. This gives a stacking sequence parallel to the c-axis, shown in Fig. 2.9[30].

a) The 2-2-0-1 Phase

Its exact chemical composition is $Bi_2Sr_2CuO_{6+\delta}$. This phase is characterized by the lowest T_c (between 3.5 - 22 K). It is recognized as a tetragonal structure with lattice parameters a = b = 5.389Å and c = 24.64Å [31]. However, some authors have reported it as being a pseudotetragonal structure with slightly different values for a and b[32].

A complete X-ray powder diffraction data of this phase is reported in Table 2.3[31, 33] and the structure is shown in Fig.2.9(a)[30]

b) The 2-2-1-2 Phase

Its exact chemical composition is $Bi_2Sr_2CaCu_2O_{8+\delta}$. It has also a tetragonal structure and its lattice parameters with T_c = 80K have been reported by Carim[32] and Srinivasan[34]. Table 2.4 gives the X-ray powder diffraction data according to the second author. The corresponding lattice parameters are a = b = 5.42±0.3Å and c =30.71±0.15Å[34]. The crystal structure is derived from the perovskite, like the 2-2-0-1 phase but two CuO planes are intercalated between BiO sheets as shown in Fig.2.9(b).

c) The 2-2-2-3 Phase

It has the highest $T_{c,0}$ = 110K. Its crystal structure is tetragonal with lattice parameters: a = b = 5.396Å and c = 37.180Å[35]. Because of difficulties in obtaining the pure 2-2-2-3 phase the exact X-ray powder diffraction is still controversial. Table 2.5 shows the X-ray powder diffraction data estimated from the X-ray diffraction pattern by Koyama[35]. It comprises three CuO planes, of which is not distorted and two are distorted[36].

The materials involved has been removed because of copyright restrictions.

Fig. 2.9 Structural models of the average structure of $Bi_2Sr_2Ca_{n-1}Cu_nO_{4+2n+\delta}$ phases for n =1 (a), n = 2 (b) and n = 3 (c). Cations are indicated by the symbol of the element in one half of the cell and small circles indicate oxygen atoms[30].

Table. 2.3 Calculated and observed X-ray powder diffraction date of the 2-2-0-1 phase with a = b = 5.389Å and c = 24.64Å after Saggio, et al.[31]

$d_{obs.}$ (Å)	$d_{calc.}$ (Å)	*h*	*k*	*l*	I/I_0
12.380	12.320	0	0	2	5
5.271	5.246	1	0	1	5
4.107	4.107	0	0	6	30
3.763	3.766	1	1	1	1
3.630	3.637	1	0	5	4
3.457	3.456	1	1	3	66
3.234	3.240	1	1	4	6
3.079	3.080	0	0	8	45
3.014	3.014	1	1	5	100
2.947	2.947	1	0	7	<1
2.693	2.694	2	0	0	48
2.629	2.632	2	0	2	1
2.584	2.586	1	1	7	7
2.464	2.464	0	0	10	14
2.414	2.410	2	1	0	4
2.247	2.244	2	1	4	5
2.027	2.028	2	0	8	31
1.929	1.931	1	1	11	26
1.905	1.905	2	2	0	16
1.793	1.791	3	0	1	1
1.728	1.728	2	2	6	<1
1.697	1.697	1	1	13	12
1.668	1.669	3	1	3	7
1.618	1.620	2	2	8	5
1.610	1.610	3	1	5	16
1.539	1.540	0	0	16	10
1.355	1.355	1	1	17	8

Table. 2.4. Calculated and observed X-ray powder diffraction data of the 2-2-1-2 phase with a = b = 5.42 ± 0.3 Å and c = 30.71 ± 0.15 Å after Srinivasan, et al.[34]

$d_{obs.}$ (Å)	$d_{calc.}$ (Å)	h	k	l	I/I_o
5.328	5.338	0	1	1	16
3.837	3.839	0	0	8	39
3.736	3.721	1	0	6	17
3.585	3.589	1	1	3	57
3.477	3.410	0	1	7	22
3.249	3.251	1	1	5	100
3.139	3.133	1	0	8	20
3.067	3.071	0	0	10	36
3.013	-	-	-	-	30
2.882	2.886	1	1	7	75
2.703	2.710	2	0	0	91
2.660	2.669	2	0	2	22
2.549	2.559	0	0	12	35
2.436	2.395	0	2	6	21
2.209	2.214	2	0	8	17
2.027	2.032	2	0	10	35
2.007	2.010	1	1	13	20
1.911	1.916	2	2	0	44
1.854	1.859	2	2	4	18
1.803	1.806	1	1	15	23
1.686	1.690	3	1	3	15
1.646	1.651	3	1	5	25
1.630	1.635	3	0	8	18
1.592	1.596	3	1	7	24
1.574	1.557	3	0	10	17
1.529	1.532	3	1	9	23
1.358	1.355	4	0	0	17

Table. 2.5 Estimate of the X-ray powder diffraction data of the 2-2-2-3 phase after Koyama, et al. [35]. (calculation with a = b = 5.39Å, c = 37.0Å) (incertitudes: $\Delta(2\theta) = \pm 0.1$; $\Delta\ (I/I_o) = \pm 2\%$)

$d_{calc.}$ (Å)	$2\theta_{calc.}$ (°)	$2\theta_{obs}$ (°)	*h*	*k*	*l*	I/I_o
18.50	4.77	4.7	0	0	2	30.0
9.25	9.55	9.5	0	0	4	3.0
4.63	19.17	19.1	0	0	8	10.0
3.70	24.02	24.0	0	0	10	100.0
3.39	26.27	26.2	1	1	5	10.0
3.08	28.92	29.0	0	0	12	75.0
2.79	31.98	32.0	1	1	9	15.0
2.70	33.23	33.0	2	0	0	10.0
2.64	33.88	34.0	0	0	14	92.0
2.52	35.55	35.6	1	1	11	15.0
2.31	38.90	39.0	0	0	16	7.0
2.28	39.47	39.5	1	1	13	2.0
2.06	44.00	44.0	0	0	18	5.0
2.03	44.60	44.6	2	0	12	8.0
1.91	47.60	47.4	2	2	0	6.5
1.89	48.10	47.9	1	1	17	13.0
1.85	49.19	49.2	0	0	20	8.0
1.73	52.80	52.7	1	1	19	12.0

d) Place of Pb in the 3 superconducting phases

Many experiments have indicated that Pb helps the formation of the 2-2-2-3 phase in the Bi-Sr-Ca-Cu-O system. Pb atoms substitutes for the Bi, Sr, Ca, atoms with respective proportions of 9%, 7%, 3%[36]. Also, the addition of Pb modifies the lattice parameters. For instance, the c parameter increases by about 1% in the 2-2-2-3 phase and decreases by 1% in the 2-2-1-2 phase when x, in $Bi_{1-x}Pb_x$, increases from 0.1 to 0.4[37, 38]. Fig. 2.10 shows the crystal structure of the 2-2-2-3 phase with Pb element[30, 36].

The materials involved has been removed because of copyright restrictions.

Fig. 2.10 Crystal structure of the high-T_c phase in the Bi-Pb-Sr-Ca-Cu-O system[36]

e) Incommensurability of superconductors in the Bi-(Pb)-Sr-Ca-Cu-O System

The crystal phases of this system lack short-range lattice periodicity in at least one direction, but display a perfect long-range ordering. A number of reports indicate they are incommensurate[30, 39, 40, 41, 42, 43, 44]. This incommensurability has been observed in the 2-2-0-1, 2-2-1-2, and 2-2-2-3 phases. Its effect on superconductivity is not clear until now. However, it influences the electronic and magnetic properties of these compounds greatly[45]. Detailed descriptions on this issue are beyond this thesis.

2.2.2) Phase transformation and processing

The formation mechanism of superconducting phases in the Bi-(Pb)-Sr-Ca-Cu-O system is quite complex and is not understood completely until now. The thermodynamic and kinetic aspects are examined separately in the next section, before the actual processing techniques employed.

a) Thermodynamics

Several investigations have contributed to the determination of phase diagrams in the Bi-Sr-Ca-Cu-O system[31, 42, 46, 47, 48, 49, 50, 51]. Ternary system phase diagrams such as Bi-Sr-Cu-O and Sr-Ca-Cu-O have been established, and the important characteristics in the phase transformations have also been discussed.

One group of phase diagrams in the Bi-Sr-Ca-Cu-O system is shown in Fig. 2.11[49]. In the quaternary system of the $BiO_{1.5}$, CaO, CuO and SrO, represented by the tetrahedron in Fig. 2.11(a), 13 binary oxide phases at least have been found in binary systems corresponding to the six edges, and 7 ternary oxide phases in the 4 ternary systems represented by the four faces[49]. The three superconducting quaternary oxide

The materials involved has been removed because of copyright restrictions.

(a) Quasi quaternary tetrahedron (b) at 750°C

The materials involved has been removed because of copyright restrictions.

(c) at 800°C (d) at 850°C

Fig. 2.11 (a) Quasi quaternary tetrahedron, showing the existence of the three superconducting phases (full lines). 1, 2, and 3 are representive for the 2-2-0-1, 2-2-1-2 and 2-2-2-3 phases. Phase diagram in the Bi-Sr-Ca-Cu-O system at 750°C (b); at 800°C (c); at 850°C (d)[49].

phases (the 2-2-0-1, 2-2-1-2, and 2-2-2-3 phases) within the tetrahedron, form one coexistence domain with one binary edge phase. Compounds with a fixed Sr-Ca ratio can be represented in a triangular domain $Sr_2Bi_2O_5$-CaO-CuO. The phase equilibria within this ternary system are shown on Fig.2.11(b), (c), and (d) at three different temperatures. The 2-2-0-1 phase is the only stable phase at 750°C on Fig. 2.11(b). It coexists with the 2-2-1-2 phase at 800°C (Fig. 2.11(c)) and finally all three superconducting phases, the 2-2-0-1, 2-2-1-2 and 2-2-2-3 phases, coexist at 850°C (Fig. 2.11(d)).

It is also known that the 2-2-0-1 phase is superconducting in a very narrow range of composition[31, 46]. The 2-2-0-1 composition phase starts to melt below 840°C and melt completely at 950°C[42, 46]. The 2-2-1-2 and 2-2-2-3 phases also start to melt at about 840°C[52, 53], the latter one also forms in a very narrow range of composition.

b) Kinetics

It seems that thermodynamics is insufficient to explain the nature of phase formed depending on the procedure. For instance, the formation of the 2-2-2-3 superconducting phase takes a long time, of the order of days[49]. Lin, et al.[54] have determine a temperature-time-transformation (T-T-T) diagram for materials with the initial Bi-(Pb)-Sr-Ca-Cu cation composition of 1.6-(0.4)-2-2-3. Although this diagram is for thin films obtained by DC sputtering, which may not be completely suitable for fabrication of bulk superconductors, it provides a guide for understanding the kinetics of the formation of the superconducting phases in the system.

This T-T-T diagram, shown in Fig.2.12[54] is composed of five ranges : (1) the 2-2-0-1 phase; (2) a mixture of 2-2-0-1 and 2-2-1-2 phases; (3) the 2-2-1-2 phase; (4) a mixture of 2-2-1-2 and 2-2-2-3 phases; (5) the 2-2-2-3 phase. The nose temperature of the 2-2-1-2 phase is at 830°C and that for the 2-2-2-3 phase at 840°C. But the temperature range where the 2-2-2-3 phase is the only one to form is very narrow, about 10°C, moreover, a long-time heat treatment is necessary.

The materials involved has been removed because of copyright restrictions.

Fig. 2.12 T-T-T diagram for Bi-Pb-Sr-Ca-Cu-O thin films, showing the formation domains of the 2-2-0-1, 2-2-1-2, and 2-2-2-3 phases[54].

Hatano and Hittich[49, 55] have found a significantly different result. The 2-2-2-3 phase would form from the 2-2-1-2 phase, then revert beck to this phase, according to the sequence:

$$2\text{-}2\text{-}1\text{-}2 \rightarrow 2\text{-}2\text{-}2\text{-}3 \rightarrow 2\text{-}2\text{-}1\text{-}2 \qquad (2.11)$$

A possible explanation by Huang, et al.[56] is that the 2-2-2-3 phase cannot grow directly from the 2-2-1-2 phase during heat treatment while in the solid state. The 2-2-1-2 phase has first to melt. Hence, its melting point must be lower than that of the 2-2-2-3 phase. This behavior can be enhanced by an increase in Ca content, or by a decrease of the oxygen partial pressure during calcination and sintering[56]. Tripathi, et al.[57] investigated the influence of silver and excess copper on the formation the 2-2-2-3 phase. They found that the addition of silver was detrimental for the phase formation and sintering while an excess copper markedly enhances the formations of both the 2-2-2-3 phase and the 2-2-1-2. This is coherent with the remark, by Shi, et al.[58], that the formation of the 2-2-2-3 phase requires some non-stoichiometry in the Ca and Cu of the 2-2-1-2 phase. The diffusion process is enhanced by excesses of both Ca and Cu in the starting composition. Actually, the preferred starting composition is often 1-1-1-2, instead of 2-2-2-3 with respect to Br-Sr-Ca-Cu[59].

The most successful additive is definitely Pb. It enhances considerably the 2-2-2-3 phase formation, as well as its stability[38, 60, 61]. The range $0.3 \leq x \leq 0.5$ with respect to a composition $Bi_{2-x}Pb_xSr_2C_2Cu_2O_{10-x/2}$ is the most effective and allows to achieve a critical temperature $T_c = 110K$[37,38,62]. An excellent initial composition is, for example, $Bi_{1.84}Pb_{0.34}Sr_{1.91}Ca_{2.03}Cu_{3.06}O_y$. [35, 63]. It seems that Pb helps the formation of a reactive liquid phase in the coexistence domain of the $Bi_2Sr_2CaCu_2O_y$, Ca_2PbO_4, and CuO phases[64]. From this liquid, the 2-2-2-3 superconducting phase grows more easily and faster[38, 60]. Also, at the microscopic level, the lead-free 2-2-2-3 crystals can be easily cleaved perpendicularly to the **c**-axis, near the BiO planes [65], and deteriorate easily. However, lead substitution improves the inter-layer bonding, which results in a stabilization of the 2-2-2-3 phase[38].

The formation rate of the 2-2-2-3 phase can also be improved by a better fabrication processing[66]. For instance, in the conventional method from oxides and carbonates, Jang, et al.[66] achieved a better result by mixing $SrCO_3$, $CaCO_3$, and CuO first, and letting them reacted at 910°C for 10h in air. Bi_2O_3 is added in a second step to limit its vaporization after CuO is fully decomposed at 875°C. Sol-gel processing offers also some good possibilities and is the subject of the present experimental study[63].

d) Processing

We have mentioned three main processing techniques. They are: conventional ceramic processing, sol-gel and melt-quenching processing.

Melt-quenching consists in: (1) melting the initial materials; (2) quenching the melt; (3) heat-treating the quenched materials. A number of quenching methods, such as between two rollers and by iron-pressing, etc. have been summarized by Liu, et al.[67]. Melt-quenching is an important fabrication technique. However, it is quite different from conventional and sol-gel ceramic processing.

Conventional processes include calcination, shaping, sintering and post-heat-treatment steps. Sol-gel processes differ from conventional processes in that the compounds are synthesized by chemical routes. The next sections will focus on conventional ceramic while sol-gel processing will be discussed in section 2.3.

i) Calcination and solid state reaction

The oxides Bi_2O_3, CuO, PbO, and carbonates $SrCO_3$, $CaCO_3$ have often been chosen as the starting materials (or precursors) in the conventional ceramic processing of the Bi-(Pb)-Sr-Ca-Cu-O superconductors. The calcination stage usually takes a long time from 10 to 24 hours at temperatures ranging from 700 to 800°C. This is necessary to fully transform the carbonates into oxides[68, 69]. The nitrates $Bi(NO_3)_3 \cdot 5H_2O$, $Pb(NO_3)_3$, $Sr(NO_3)_2$, $Ca(NO_3)_2 \cdot 4H_2O$, $Cu(NO_3)_2 \cdot 3H_2O$ have also been selected. They have to be calcined at 500°C for 2 hours at least, to convert them into oxides[34]. Calcination can be much faster at high temperatures , for instance, about 10 seconds at 1200°C under Argon, according to Liu et al. [68].

A possible succession of transformations occurring on the Bi-Sr-Ca-Cu-O system, during calcination, is the following:[69]

$$CuO + Bi_2O_3 \xrightarrow{\sim 500\,^{\circ}C} CuBi_2O_4 \qquad (2.12)$$

$$Sr_{1-x}Ca_xCO_3 \xrightarrow{> 600\,^{\circ}C} SrCO_3 + CaO \qquad (2.13)$$

$$2SrCO_3 + CuBi_2O_4 \xrightarrow{\sim 700\,^{\circ}C} Bi_2Sr_2CuO_6 + 2CO_2 \qquad (2.14)$$

$$Bi_2Sr_2CuO_6 + CaO + CuO \xrightarrow{> 800\,^{\circ}C}$$

$$Bi_2Sr_2CaCu_2O_8 \text{ (The 2-2-1-2 phase)} \qquad (2.15)$$

The phases formed are the same when Pb is added to the system. The only difference in solid state reactions is the formation of Ca_2PbO_4 at about 700°C[70].

ii) Sintering

It is desirable to achieve a density as high as possible, without altering the nature of the superconducting phase. Actually, the number of studies addressing this problem are scarce.

Johnson, et al.[71] investigated the densification behavior in the $Bi_2Sr_2CaCu_2O_8$ superconductors from oxides and carbonates. Their results are reported in Fig. 2.13. A retrograde densification occurs between 850°C and 890°C. It results from the formation of thin platelike crystalline 2-2-1-2 grains, which grow in a randomly oriented fashion, pushing the structure apart. This retrograde densification, together with the narrow temperature range available before melting, makes the materials a difficult one to process. A similar behavior occurs in the Bi-(Pb)-Sr-Ca-Cu-O superconductors made from oxides and carbonates, as shown in Fig. 2.14[72]. There, retrograde densification occurs simultaneously with the formation of the 2-2-2-3 phase, at 845°C. In this case, other factors explaining this behavior: first, the theoretical density of the 2-2-2-3 phase is lower

The materials involved has been removed because of copyright restrictions.

Fig. 2.13 Density achieved in 2-2-1-2 samples as a function of the sintering temperature[71].

The materials involved has been removed because of copyright restrictions.

Fig. 2.14 Variation of bulk density with sintering time 845°C, in (Bi, Pb)$_2$Sr$_2$Ca$_2$Cu$_3$O$_{10}$ made by conventional processing[72].

than that of the 2-2-1-2 phase; secondly, Bi and Pb leave at high temperature[72, 73]. This sintering behavior is improved by adding excess copper[57]. In $Bi_{1-x}Pb_xSrCaCu_{1.8}O_y$ superconductors, the best sintering capability of bulk samples (about 67% of the theoretical density) occurs for $0.4<x<0.7$[74].

iii) Microstructures

It is apparently difficult to take good optical micrographic pictures of Bi-(Pb)-Sr-Ca-Cu-O superconductors. One of the best observation published on the $Bi_2Sr_2CaCu_2O_y$ phase, taken with crossed polarizers, does not show well defined grain boundaries[75]. The grain contains a lot of parallel slits.

A SEM study by Gao, et al.[76] has shown the 2-2-2-3 phase exhibits a platelike shape and is dispersed in a featureless 2-2-1-2 phase. However, other reports indicate both the 2-2-2-3 and 2-2-1-2 phases consist of platelike grains[71, 27]. One prominent feature of a typical Bi-Sr-Ca-Cu-O grain is the presence of intergrowth with different c parameters inside the same grain, for example, c = 30.5Å and c = 30.7Å[83]. The variation in the nature of the repeat unit is due to local variation in the composition. As sintering is maintained for longer times, the platelike grain structures of the 2-2-1-2 and 2-2-2-3 phases improve. The addition of Pb promotes the growth of the 2-2-2-3 grains[64].

The presence of Josephson-type weak-links at the grain boundaries of polycrystalline high-T_c superconductors is now well known[77, 78]. The misoriention angle between adjacent grains influences the current carrying capability at the grain boundaries. Across most of the large-angle grain boundaries, the critical current is severely limited, especially in the presence of a magnetic field[22]. These orientations behave as weak links[79].

Actually, the origin of grain boundary weak-link properties is still not clearly understood. It may be related to: (1) disturbed crystal structure or altered interatomic distances near the grain boundaries, (2) chemical variations (cation or oxygen stoichiometry), (3) impurities such as carbonaceous compounds or amorphous materials, (4) microcracks caused by thermal contraction, or (5) anisotropy in superconductivity, especially at large-angle boundaries[22]. We know for instance that slight changes in the Cu-O bond distance or angle may wipe out the superconductivity[80].

In highly dense $Bi_2Sr_2CaCu_2O_{8+\delta}$ adjacent grains with their **c**-axis parallel to each other, and rotated by approximately 45° with respect to each other around this axis form coherent (001) grain boundaries. For a rotation angle of 90° around the **c**-axis, twin (00*l*) grain boundaries can be observed. In both cases, the interfaces lie between two adjacent BiO layers. polytypes, i.e. lamellae of phases which are not the 2-2-1-2 ones, are frequently observed at twin boundaries and also occur at small angle tilt boundaries. They allow to accommodate for the mismatch. Such compositional variations along the grain boundaries may be responsible for the weak-link behavior[81, 82]. The 2-2-2-3 grains shorter boundaries in the (**a**,**b**) plane are generally distorted. However, the grain boundaries along the long edge comprise a thin layer of the 2-2-1-2 superconducting polytype. Also, coherent intragranular boundaries exist[83]. This kind of grain boundaries are responsible for a lower critical current density, but have little effect on the critical temperature. However, from the above analysis, most (00*l*) grain boundaries in the $Bi_2Sr_2CaCu_2O_{8+\delta}$ superconductors are coherent. Consequently, the weak-link effect is less prominent than in the Y-Ba-Cu-O superconductors, where large-angle grain boundaries are common. This suggests that, if the polytypes along grain boundaries could be eliminated by selecting appropriate sintering conditions, the weak-link effect could be overcome[81, 82].

The main other defects in the Bi-(Pb)-Sr-Ca-Cu-O ceramic superconductors include: (1) point defects, mainly by cationic substitutions and; (2) dislocations.[81, 82, 83].

The relationship between these defects and superconducting properties are far beyond the scope of this thesis.

The formation of textured microstructures during shaping and sintering is a common phenomenon in the Bi-(Pb)-Sr-Ca-Cu-O superconductors. It is also desirable to attain high critical current density[84]. The degree of preferred orientation in a sample can be estimated from the intensity of the (00l) peaks in the X-ray diffraction patterns[84]. It has for instance be defined as[85]

$$Q = 1 - \frac{I(115)}{I(0010)} / \frac{I_o(115)}{I_o(0010)} \qquad (2.16)$$

where I denotes the X-ray intensity of the corresponding (hkl) peak for the sample being studied and I_0 that of a standard without preferred orientation.

The platelike grains already present in the calcined powders of $Bi_{1.6}Pb_{0.4}Sr_2Ca_2Cu_3O_y$ are already slightly oriented by pressing. The latter then act as nucleating agents during sintering and help the formation of preferred oriented microstructure in conventional ceramic processing[86]. The 2-2-1-2 type superconductors can be orientated by hot-pressing to more than 95%, according to the Q value[85]. Cold - pressing also is efficient[87, 88]. It has also been found that Ag can promote the preferred orientation along the c-axis in the 2-2-1-2 type superconductors[89].

iv) Atmosphere

The successful synthesis of the 2-2-2-3 phase typically requires a sintering temperature above the partial melting temperature but below the temperature of complete melting and decomposition. The processing of the Bi-(Pb)-Sr-Ca-Cu-O compound outside this temperature window usually results predominantly in the 2-2-1-2 phase with intergrowth structure and various second-phase particles[22]. The window is about 10°C in air [90], about 5°C in a 1atm O_2 environment[91], and about 20°C for Po_2 = 0.1 atm, as shown in Fig.2.15[91]. In practice a partial pressure Po_2 = 1/13 atm O_2 is often chosen[35, 62], sometimes mixed with Argon[92]. 2-2-1-2 type superconductors with $T_{c,0}$ = 85K can be obtained as low as 775°C under reduced oxygen pressure[73]. The reduced temperature is turn helpful to decrease the loss of Bi and Pb[73]. Another advantage of using a partial oxygen pressure is to minimize the chemical reaction of Ag with Pb when Ag is added to the system[93].

The materials involved has been removed because of copyright restrictions.

Fig. 2.15 Oxygen partial-pressure dependence of the processing window ΔT for obtaining the Bi-Sr-Ca-Cu-O 2-2-2-3 phase[91].

2.2.3) Superconducting properties

a) Energy gap, Δ(0)

The magnitude of the superconducting energy gap Δ and its temperature dependence are important to determine the strength of Cooper's pair coupling. Besides T is near T_c, the magnitude of Δ is not significantly different from Δ(0) at 0K[19].

More precisely, it has been mentioned previously that the coupling strength is related the value of the ratio of $2\Delta/K_BT_c$ where Δ is the energy gap of a superconductor and T_c is the critical temperature. A value of $2\Delta/K_BT_c$ near 3.5 like in the BCS theory indicates weak coupling, while values substantially larger are an evidence of strong coupling[19].

For the 2-2-1-2 superconductors, data by Raman spectroscopy[94, 95], tunneling effect[96, 97], photoemission[98, 99], far-infrared spectroscopy[100], and electron-energy-loss spectroscopy[98] have provided an energy gap 2Δ value between $\approx$ 24 m*e* V and $\approx$ 60 m*e* V for $T \ll T_c$. This corresponds to a ratio of $2\Delta/K_BT_c$ between 5.5 and 9, which indicates strong-coupling.

Raman and tunneling studies also show the superconducting gap of 2-2-1-2 crystals is strongly anisotropic[97, 101]. In average, $2\Delta_{a,b}(0)/K_BT_c \approx 6.0$ in the **a** or **b** direction and $2\Delta_c(0)/K_BT_c \approx 3.5$ in the **c**-direction[97, 101]. That is to say coupling is strong in the (**a**,**b**) plane and weak in the **c**-plane.

b) Characteristic lengths, ξ and λ

The coherence length $\xi(T)$ is relatively small in the Bi-(Pb)-Sr-Ca-Cu-O system superconductors, typically on the order of 10Å or less, by comparison with values on the order of 1000Å for conventional type-II superconductors. Since ξ may be considered as the distance over which coherence can be maintained across a normal region, it is a measure of the scale at which lattice defects can disrupt the supercurrent. The result is that even grain boundaries could be sufficiently thick to disrupt superconductivity in these peroviskites. This may partially explain the relatively low values of J_c typically observed in bulk ceramic superconductors[19, 102].

This situation is even aggravated by anisotropy. Estimates of $\xi_c(0)$ and $\xi_{ab}(0)$ are approximately 1.6Å and 38Å respectively along the **c**-axis and in copper-oxygen (**a**,**b**) plane, in the 2-2-1-2 superconductor[103]. These extremely short coherence lengths, on the order of the size of the 2-2-1-2 unit cell, make the superconductivity of the oxides quite sensitive to grain boundaries and local defects[104].

Being given the difficulty to synthesize 2-2-2-3 single crystal, only average values have been estimated. They are $<\xi(0)> = 31.1Å$ for the coherence length and $<\lambda(0)> = 1950Å$ for the penetration length[105].

c) Critical magnetic field, H_{c1} and H_{c2}

Because superconductors in the Bi-(Pb)-Sr-Ca-Cu-O system are of the type-II, two critical magnetic fields $H_{c1}(T)$ and $H_{c2}(T)$ have to be determined. Calling $H_c(0)$ the critical field at absolute zero, a useful approximation of H_c at a temperature T is:[19]

$$H_c = H_c(0)\left[1 - \left(\frac{T}{T_c}\right)^2\right] \qquad (2.17)$$

when $H_{c2}(0)$ is too high to be determined in practice, the following relation requires only to determine the slope of H_{c2} vs. temperature near the critical temperature T_c:[19]

$$H_{c2}(0) \approx 0.69T_c\left|\frac{dH_{c2}}{dT}\right|_{T=T_c} \qquad (2.18)$$

R. Job and M. Rosenberg[105] investigated in detail the lower critical field H_{c1} of the 2-2-1-2 and the 2-2-2-3 superconducting phases. At 4K, $H_{c1} \approx 0.03T$ for polycrystalline 2-2-2-3 superconducting samples and $H_{c1} \approx 0.01T$ for polycrystalline 2-2-1-2 superconducting samples. As the temperature increases, H_{c1} decreases rapidly. Also, the lower magnetic field H_{c1} is anisotropic. In the direction of the **c**-axis it is 5 or 6 larger than that in the **(a,b)** plane.

Batlogg, et al.[106] studied the upper critical field H_{c2} of 2-2-1-2 single crystals. The value of $-dH_{c2}/dT$ is between 0.55 T/K ($H_{c2}(0) \approx 30T$)[106] and 0.75 T/K[103] in the **c**-direction and is about 4.5 T/K ($H_{c2}(0) \approx 250T$)[106] parallel to the (**a,b**) plane. For the 2-2-2-3 type superconductors the average values of $H_{c2}(0)$ cover therefore a wide range, from 45 to 305T[107]. The results also indicate processing parameters have a strong effect on the upper critical field which is related to the critical current density.

d) Critical temperature, $T_{c,0}$

The critical temperature ranges of the three different phases (2-2-0-1, 2-2-1-2, and 2-2-2-3), as have determined by different authors, are summarized in Table 2.6. The processing conditions, which are diversed with respect to sintering temperature, duration and atmosphere, influence largely the superconducting properties, especially the critical temperature and critical current density. The effect on critical temperatures of materials made by conventional processing, is reported respectively in Table 2.7, 2.8, and 2.9 for the three phases.

Table 2.6 Critical temperatures of the 3 superconducting phase in the Bi-(Pb)-Sr-Ca-Cu-O system

Phase	$T_{c,0}$ (K)	Reference
2-2-0-1	3.5 - 22	[31, 33, 42, 46, 108, 109, 110]
2-2-1-2	80 - 85	[15, 32, 109, 111]
2-2-2-3	105 - 110	[36, 37, 112, 113]

The 2-2-0-1 compound (Table 2.7) must be stabilized in the temperature range of 800-880°C in air or oxygen atmosphere, where a liquid phase forms, to have its highest T_c. A higher processing temperature, i.e. above 900°C destroys its superconductivity[31]. A long sintering time is needed to get an ideal structure, otherwise , the phase is not superconductive[69].

Table. 2.7 Relationship between sintering conditions and critical temperature of 2-2-0-1 type superconductors made by conventional ceramic processing

Composition Bi:(Pb):Sr:Ca:Cu	Sintering Temp. (°C)	Sintering Time (h)	Phase	$T_{c,\ onset}$ (K)	$T_{c,\ 0}$ (K)	Ref
10.6 : 9.4 : 0 : 5	800, air	72	2-2-0-1		9	[31]
2 : 2-x : 0 :1, 0.1<x<0.25	800-830, air	0.1 - 400	2-2-0-1	6		[42]
2+x : 2-x : 0 : 1+y 0.1<x<0.6, 0<y<x/2	840, air	45 - 150	2-2-0-1		~10	[46]
2 : 2 : 0 : 1	850, air	16	2-2-0-1		6	[33]
1.49 : 1.68 : 0 : 3.0	860, O_2	7	?		3.5-5.4	[110]
1 : 1 : 0 : 1	880, air	12	2-2-0-1	8	4.7	[114]

Table. 2.8 Relationship between sintering conductions and critical temperatures of 2-2-1-2 type superconductors made by conventional ceramic processing

Composition Bi : (Pb) : Sr : Ca : Cu	Sintering Temp. (°C)	Sintering Time (h)	Phase	$T_{c,}$ onset (K)	$T_{c,\ 0}$ (K)	Ref
2 : 2 : 1 : 2-2.5	800, air	3	2-2-1-2			[115]
2 : 2-x :1+x:2, 0<x<0.5	850, air	16	2-2-1-2		75	[33]
4 : 3: 3 : 4 (Nitrate salts)	860+15,air	>12	2-2-1-2	85	66	[34]
2 : 2 : 1 : 2	870, air	12	2-2-1-2	93	82	[116]
2 : 2 : 1 : 2	888, 0_2	2	2-2-1-2		68	[71]
	901, 0_2	2	2-2-1-2		70	
	904, 0_2	2	2-2-1-2		78	
	911, 0_2	2	2-2-1-2		60	
2 : 2-y : 1 : 2	775, in10^4Pa O_2	8	2-2-!-2			[73]

The 2-2-1-2 compound has an optimum T_c after sintering in the temperature range from 800 to 911°C under an air or an oxygen atmosphere, as shown in Table 2.8. The 2-

2-1-2 phase can be formed as low as 800°C[115], but its critical temperature is then very low, apparently in relation with a different c parameters ($c = 30.55Å$ instead of $c = 30.70Å$[115]).

Table 2.9 shows the relationship between the sintering conditions and the critical temperatures with the 2-2-2-3 compound. Its value depends on the volume fraction of the 2-2-2-3 phase. In order to achieve a high critical temperature, a long sintering time in a very narrow temperature range, about 10°C at 850°C, is necessary. As we have seen in processing, the addition of Pb is helpful as well as the excess of Ca and Cu.

Table. 2.9 Relationship between sintering conditions and critical temperature of 2-2-2-3 type superconductors made by conventional ceramic processing

Composition Bi : (Pb) : Sr : Ca : Cu	Sintering Temp. (°C)	Sintering Time (h)	Phase	$T_{c,}$ onset (K)	$T_{c,0}$ (K)	Ref
1 : 1 : 1 : x, x=2, 3	852	0.5	2-2-1-2 +2-2-2-3	110	84	[118]
1 : 1 : 1 : 2	837,air				109.3	[119]
1 : 1 : 1 : 2	865±5,air	900	2-2-2-3		104	[120]
1 : 1 : 1 : 2	880	0.33	2-2-2-3			[15]
	870,air	200		105		
1 : 1 : 1 : 2	882	0.33	2-2-2-3			[47, 108]
	872,air	9			105	
1.73:(0.35):1.89:1.86:3	840,air	90	2-2-2-3		104	
1.6 : (0.4) : 2 : 2 : 3	845,air	64-250	2-2-2-3		110.7	[72]
1.75 : (0.45):1.7 : 1.8:3	860,air	210	2-2-2-3			[121]
1.4 : (0.6) : 2 : 2 : 3	870,air	240	2-2-2-3	113	108	
1.84 : (0.34) : 2 : 2 : 3	830-846, 1/13 Po_2	36-84	2-2-2-3		107	[38] [35]
1.84: (0.34) : 2.06-1.94 : 1.99-2.06 : 2.95-3	835, 1/13 Po_2	84	2-2-2-3		103 - 104	[62]

After sintering, the sample cooling rate influences the critical temperature. Zhuang, et al.[117] studied the influence of cooling rate on the critical temperatures of the samples without Pb and with Pb, and they reported that a rapid cooling increased $T_{c,0}$ of samples without Pb whilst it decreased $T_{c,0}$ in samples with Pb. The optimum cooling rate for the 2-2-2-3 type superconductors with Pb was in range from about 50°C/h to 100°C/h[69].

Annealing in a temperature range 300-825°C decreases the critical temperatures as well as the critical current density while non-superconducting phases like Ca_2PbO_4 are formed[122].

e) Critical current density, J_c

Although critical temperatures of new superconductors have been raised to 110°C, the bottleneck in the slow progress towards the major applications of bulk high-T_c superconductors is their low critical currents, especially in strong magnetic fields. Because of differences in measurement methods the J_c data are quite dispersed. However, at 77K and under a field H = 0, by the dc four-probe method, they go from 100 A/cm^2 to 6260 A/cm^2[76, 123, 124]. These low critical current density, compared with Nb_3Ge where they are of order of $10^7 A/cm^2$, eliminates some of the most attractive potential applications of high-T_c superconductors.

There are two major causes to the low J_c value in bulk polycrystalline high-T_c superconductors, that are (1) weak links at the grain boundaries because of the extremely short coherence lengths (<40Å), as analyzed previously[106], and (2) flux line movements within the grains[22].

The most successful methods allowing to overcome these problems try to achieve a high grain orientation. They are: (1) Melt-texturing, (2) Deformation texturing (i.e. by pressing), (3) Substrate-induced texturing, (4) Magnetic field alignment[22]. Deformation texturing process seems to be most successful in the Bi system.

Table. 2.10 summarizes the different processes studied to improve the critical current density in the Bi-(Pb)-Sr-Ca-Cu-O(Ag) superconductors. Deformation texturing seems to be most successful processing technique. The addition of Ag and pressing can increase its value about one order of magnitude from a few $100A/cm^2$ to a few $1000A/cm^2$[72, 76, 123, 124,].

Table. 2.10 Critical current density J_c obtained in the Bi-(Pb)-Sr-Ca-Cu-O system by different methods.

Composition Bi : (Pb) : Sr : Ca : Cu : (Ag)	Processing	Sintering Conditions	$T_{c,0}$ (K)	J_c (at 77K) (A/cm^2)	Ref
1.6 : (0.4) : 1.6 : 2 : 3	Conventional ceramic process	800-840°C, O_2+N_2 with Po_2 = 0.010-0.209 atm, 50h	>100	260, H=0	[125]
1.6 : (0.4) : 1.6 : 2 : 3 : (Y)			<100	1240-1520, H=0	
1.6:(0.4):2:3:4:(Y)	Conventional ceramic Process	810-840°C, 5%O_2 + 95%Ar	104-110	50 - 4000, H=0	[76, 123]
1.84:(0.34):1.91:2.03:3.06	Hot-press	(1)842°C,N_2,60h (2)844°C,N_2,100h (3)822°C,air,2h under $300kg/cm^2$	106	7000, H=10Oe	[125]
	Intermediate pressing	(1)842°C,N_2,60h (2) cold press under $5ton/cm^2$ (3)845°C, N_2, 5h	106	6260, H=0	
	Conventional ceramic process	842°C, N_2,60h	106	500, H=0	
1.6 : (0.4) : 2 : 2 : 3	Conventional ceramic process	845°C,air,64-250h	104	1000, H=0	[72]
1.84:(0.34):1.91:2.03:3.06	Cold multiple pressing	(1)850°C, air, 24h (2)cold press (3)850°C, air, 72h	107	10^4, H =0	[88]
2 : 2 : 2 : 2	Hot-pressing	850°C, air ,under 1000-1500 psi	85		[126]
1.84:(0.34):1.91:2.03:3.06	An Ag-sheath (tapes)	845°C,air,1-24h with intermediate press	110	8000, H=0	[127]
1.84:(0.48):2:2.2:3.2	As-drawn filament + sintering	(1)porilyzed at 500°C, 1h (2)840°C,air,14h (3)pressed and sintered at 840°C, 1/13 atm O_2 ,18h,	95	1200, H=0	[128]
1.84:(0.34):1.91:2.03:3.06			88	100, H=0	

2.3) SOL-GEL PROCESSING

2.3.1) Summary of sol-gel processing

A colloid is a suspension in which the dispersed solid phase comprises so small particles (~1-1000nm) that gravitational forces are negligible and interactions are dominated by short-range forces, such as van der Waals attraction and surface charges repilsion[129]. A sol can be defined as a stable dispersion of colloidal solid particles within a liquid[130]. One transforms a sol into a gel by passing through a so-called gel-point, where viscosity becomes infinite and elasticity appears. A gel can be defined as an infinite 3-dimensionally interconnected solid network expanded in a stable fashion through a liquid medium[130]. Powder for ceramics can be obtained from a gel , and then be treated by conventional processing (cold pressing, hot-pressing, sintering).

Therefore a sol-gel processing is defined as a colloidal route to synthesize ceramics in which intermediate stages include a sol and/or a gel state[130].

A typical sol-gel processing, as shown in Fig.2.16[130], includes: (1) selecting precursors of the future ceramics, (2) forming a sol or solution of the precursors, (3) performing gelation at the gel-point where shaping can be done according to application requirement, (4) sintering.

The sol-gel processes allow presently the production of many oxide compositions. The end products can be obtained very pure if the precursors are purified by distillatation, crystallization, electrolysis. Moreover the chemical process is always carried out at low temperature in its primary step, minimizing the chemical interactions with the container walls, per comparison with the high temperature synthesis of conventional ceramics[130].

Another advantage of sol-gel processes comes from the association of a colloidal state of the solid matter with a liquid, which allow to avoid pollution by dispersion of dust[130].

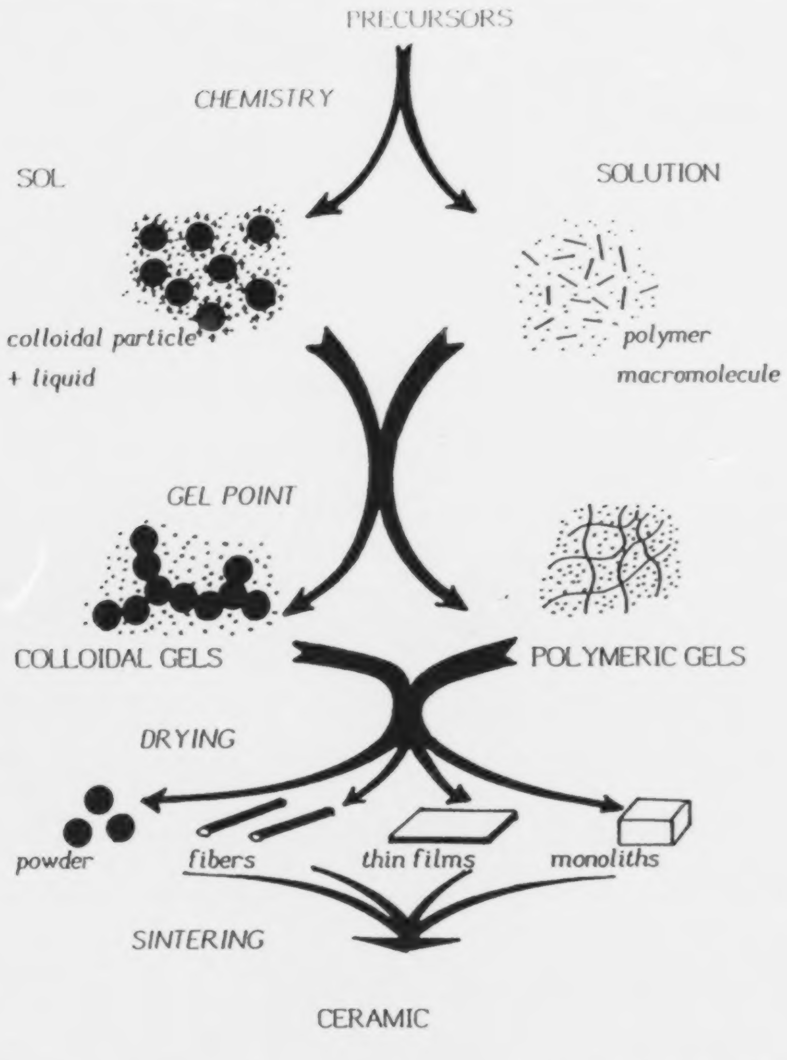
PRECURSORS
CHEMISTRY
SOL
SOLUTION
colloidal particle
+ liquid
polymer
macromolecule
GEL POINT
COLLOIDAL GELS
POLYMERIC GELS
DRYING
powder
fibers
thin films
monoliths
SINTERING
CERAMIC

Fig. 2.16 Simplified chart of sol-gel processing from A.C. Pierre[130].

More fundamental advantages come from the kinetics of the various chemical reactions which can be controlled, by reasons of the low processing temperature and often of the dilution conditions. The nucleation and growth of primary colloidal particles can also be selected to obtain a given shape, size, and size distribution, in a size domain which is largely submicronic. This, in return, results commonly in a lowering of the sintering temperature by several hundreds °C both for amorphous and for crystalline materials. Besides the energetic point of view, this may be critical for some applications, for instance in the case of ceramic-ceramic composites where the processing temperature must be lowered below the temperature of reaction with fiber-matrix[130].

Not only the size, but also the structure of the sol-gel ceramics can be controlled. The distribution of the various phases; crystalline or amorphous and pores; can be tailored in a large extent. Particularly, the phase present at grain boundaries can be controlled or eliminated[130].

A domain where the sol-gel processes offer outstanding advantages, is in the mixed oxide systems where chemical homogeneity of the various elements can be controlled down to the atomic level[130].

The main limitation of the ceramic sol-gel synthesis comes from the cost of the precursors, especially in the case of alkoxides which most of the time are expensive. The sol-gel processing will never be in a position to compete for the mass production of large scale materials[130].

Sol-gel processes have been successful in synthesizing advanced ceramics with ferroelectric, dielectic, piezoelectric, optical or electrooptical properties. Films, coatings, and fibers have also been synthesized by the sol-gel processing. Recently, the sol-gel processing have been applied for synthesizing ceramic high-T_c superconductors.

The precipitation or coprepitation techniques are very close to the sol-gel technique. They are gathered here under the name of liquid processings.

2.3.2) Case of ceramic superconductors

There are many methods to obtain high-T_c superconductor materials by a liquid or sol-gel processing. The selection of precursors to synthesize film, fiber, and bulk superconductors are based on the following desired properties: (1) Complexes of the different elements should be compatible; (2) precursors should be soluble in a suitable solvent; (3) precursor solutions should form homogeneous, continuous films if the deserved final products are films; (4) precursors should not let contaminants like residual carbon[131]. The various attempts described next according to precursors include: inorganic salts, organic salts, alkoxides and organometallics, and organic additives.

a) Inorganic salts

The inorganic salts the most often used in aqueous medium have been the nitrate salts because the Cu alkoxides are insoluble in water.

Nitrate mixed solutions can be prepared from reagent grade Bi_2O_3, $SrCO_3$, $CaCO_3$ and Cu, by dissolution in minimal amounts of nitric acid. Such solutions containing about 4 wt% nitrate have been used by Cooper, et al.[132] for spraying onto (100) MgO and (011) $SrTiO_3$ oriented substrates to form superconducting film. Gupta, et al.[132] used a similar route to get $Y_1Ba_2Cu_{7-\delta}$ thin film successfully. Bulk materials can also be synthesized in a similar way, except for the spraying step[62, 133].

For instance, Khurana, et al.[134] reported the coprecipitation of the Y, Ba, Cu hydroxides from high purity nitrates for preparing $YBa_2Cu_3O_7$ superconductors in aqueous medium. Sodium hydroxide was used to adjust the basicity. Normally, hydroxides of different metal ions precipitate at different PH values. However, coprecipitation of all the three hydroxides could be obtained with NaOH solutions at pH = 13 and 60°C while stirring solution continuously and vigorously. A change in color, from a transparent light blue to a blue-white, indicated the formation of colloidal precipitates of the hydroxides of Y, Ba and Cu. The hydroxide mixture was then converted into oxide by bubbling pure oxygen for 8-12 hours. The colour of the dispersion changed progressly to brown, then to black. The resulting dispersion was isolated by filtration, washed many times with deionized water and dried at 120°C for 10-12 hours. The Na^+ content in the precipitate after washing was found to be about 0.01 wt%.

Fujiki, et al.[135] hydrolyzed not only nitrates of Y, Ba, Cu but also halides and perchlorates ($M(ClO_4)_n$, where M is the cation). They used tetramethylammonium hydroxide as the base and a pH value between 7 and 8 at room temperature was found to be most appropriate. The colloidal blue-white precipitates obtained could be converted into oxides by treatment with tetramethylammonium hypobromite at room temperature or by raising the temperature of the tetramethylammonium hydroxide at 60-70°C. The dispersions turned to black. It was isolated by filtration or centrifugation, washed with water and ethanol, and dried under vacuum at 150°C. The stoichiometry of the sample was almost identical to the nominal composition. No precipitates formed during the process, in particular no water insoluble metal-carbonates.

Similar techniques could be used in the Bi-(Pb)-Sr-Ca-Cu-O system.

b) Organic salts

i) Acetates

In the Y-Ba-Cu-O system, P. Barboux, et al.[136] used a procedure in which Barium acetate $Ba(C_2H_3O_2)_2$ and copper acetate $Cu(C_2H_3O_2)_2{\cdot}H_2O$ were mixed with $Y(NO_3)_2$ in an aqueous solution. The pH was adjusted near 6.8 with ammonium hydroxide NH_4OH. After 30 min., a gel formed.

In the Bi-(Pb)-Sr-Ca-Cu-O system, Zhuang, et al.[27] used the acetates $BiOCH_3COO$, $Sr(CH_3COO)_2{\cdot}1/2H_2O$, $Pb(CH_3COO)_2$, $Ca(CH_3COO)_2{\cdot}H_2O$, $Cu(CH_3COO)_2$ as precursors. The pH of the Bi acetate solution was previously adjusted in the range 1 to 3 with HNO_3. After complexing the solution with a proportion of 0.43 mole of tartaric acid $HO_2CCH(OH)CH(OH)CO_2H$ per mole, a transparent viscous sol was obtained in 3 days. Gel fibers could be drawn from the viscous sol at 70°C. They also obtained bulk superconductors with a critical temperature above 100K[117].

Nitrates and acetates have been also both chosen as precursors in the Bi-(Pb)-Sr-Ca-Cu-O system[36, 137]. Bi, Sr nitrates and Pb, Ca, Cu acetates were mixed, and complexed with acetic acid then ammonia near pH = 5.5. The solution was heated at 60-70°C to get the gel.

ii) Citric and oxalic acids

Homogeneous liquid citrate precursors can be prepared from Bi_2O_3, $SrCO_3$, $CaCO_3$ and $CuCO_3 \cdot Cu(OH)_2$. They have been applied to make $Bi_4Sr_3Ca_3Cu_4O_{16+x}$ superconducting thin films[138]. $La_{2-x}Sr_xCuO_{4-y}$ and $YBa_2Cu_3O_{7-x}$ film and bulk samples have been also synthesized from citrates[139].

Nitrates can also be chosen as precursors , and complexed with citric acid ($HOC(CH_2CO_2H)_2CO_2H$) or oxalic acids (HO_2CCO_2H) to obtain real gel. This technique has been applied in the systems of Y-Ba-Cu-O[140, 141, 142, 150], and Bi-(Pb)-Sr-Ca-Cu-O[36, 92, 143, 144].

A typical procedure is the following:[140] Nitrates, chosen in proper proportions corresponding to the desired compound, are dissolved in water and complexed with citric acid and ethylene glycol CH_2OHCH_2OH or ammonia. A molar ratio of citric acid to total nitrate of 2 is usually chosen. This corresponds to the minimum amount of citric acid needed to bind all metal ions. After drying in the temperature range 60-90°C a viscous blue gel is obtained. These materials are very hygroscopic because of the free citric acid and metal nitrates. They must be further dehydrated above 120°C[145]. Other carboxylic acids, have also been used instead of citric acid in the sol-gel processing of both Y-Ba-Cu-O[146, 147, 149], and Bi-(Pb)-Sr-Ca-Cu-O systems[147, 148, 149].

iii) Hexanoates

The preparation of gels from Copper bis(2-ethylhexanoate) ($Cu(C_4H_9CH(C_2H_5)CO_2)_2$), Barium bis (2-ethyl hexanoate) ($Ba(C_4H_9CH(C_2H_5)CO_2)_2$), Yttrium tris (3-ethyl hexanoate ($Y(C_4H_9CH(C_2H_5)CO_2)_3$), has been reported[131]. These carboxylate precursors were dissolved in chloroform to give homogeneous solutions, where the viscosity could be adjusted by modifying the concentration. Such mixed carboxylate solutions have allowed to make films about 1.4 μm thick, on MgO or ZrO_2 subtrate by spin coating. There pyrolysis was done under oxygen.

iv) Neodecanoate [151, 152, 153]

Neodecanoates are carboxylates with formula $M[O_2C_2(CH_3)_2(CH_2)_5CH_3]_n$ (n = the oxidation state of metals). Copper neodecanoate can be formed by reaction of copper (II) acetate with tetramethylammonium neodecanoate. These carboxylate can be dissolved in a mixture of xylene (or toluene) with 5% pyridine, and have been applied to the syntheses of thin film of $YBa_2Cu_3O_y$, on $SrTiO_3$ and MgO substrates.

c) Alkoxides and organometallics

i) Metal alkoxide

Gels for synthesizing bulk superconductors in the Bi-(Pb)-Sr-Ca-Cu-O system have been prepared from triphenyl bismuth, Sr ethoxide, Ca ethoxide, and Cu(II) 2-ethyhexanoate[154].

We have mentioned that copper alkoxides are not soluble in the most common solvents which is the reason why nitrates and acetates have been usually chosen. However, their use has been reported in several studies.

Kramer[155, 156] used a copper(II) ethoxide/toluene suspension with Ba-methoxyethoxide and Y-methoxyethoxide to make bulk samples and thin (123) coating on

$SrTiO_3$ substrates [100]. Cu(II) ethoxide in toluene is "partially soluble", so that its hydrolysis was performed.

A recent conceptual innovation in the sol-gel method is the use of heterogeneity on a "nano" scale for applications and processing of ceramics. Ravindranathan, et al.[157, 158] applied the sol-gel route to the synthesis of triphasic nanocomposite gels to make $YBa_2Cu_3O_{7-x}$ superconductor at low temperature. A nonaqueous sol of copper oxide was prepared by dissolving anhydrous copper acetate, $Cu(CH_3COO)_2$, in methoxyethanol at 70°C, and refluxing the solution at 135°C for 15-20 hours. A brown solid separated out from the solution that was found to be fine-particle CuO. An yittrium acetate ethoxide solution can be prepared by a similar method and mixed with barium isopropoxide. The copper sol was then added to this mixture at room temperature, while stirring under argon. Hydrolysis was done with a 1:4 solution of water in methoxyethanol. A gel was obtained and calcined under oxygen.

The use of a complex Cu ethoxide solution has been reported[159]. These precursors could be used with other Bi, Sr and Ca ethoxide solutions to make thin coating by spraying on MgO (100) surface followed by rapid pyrolyzed at 600-700°C.

Hirano, et al.[160] prepared oriented $YBa_2Cu_3O_{7-8}$ thin films from Ba metal, $Y(CH_3COCHCOCH_3)_3$(Y(acac)$_3$), and $Cu(OC_2H_4OC_2H_5)_2$ (Cu ethoxide). Y(acac)$_3$ and Ba metal were dissolved in absolute 2-ethoxyethanol, and a $Cu(OC_2H_4OC_2H_5)_2$ dispersion in toluene was added slowly. The initial concentration of metal alkoxides was low (0.001 mol/L). The mixture was stirred under a dry N_2 atmosphere for 24 hours. Partial hydrolysis was done with CO_2-free distilled water diluted in 2-methoxyethanol. After concentration by vacuum evaporation, this solution was used for dip coating on MgO and $SrTiO_3$ substrates. After drying under nitrogen, the precursor thin films were heated treated directly in a furnace kept at a temperature between 550°C and 650°C for 10 min, in an ozone/oxygen atmosphere. This dipping-drying-heating process was repeated up to 25 times to increase the film thickness.

ii) Other Cu(II) or (I) organometallic precursors

Homogeneous tetrahydrofuran (THF) solutions containing $Y(OCHMe_2)_3$, $Ba(OCHMe_2)_3$, and a hydrolyzable copper organometallic compound such as $Cu(OCMe_3)$, Cu(mesityl), $Cu(NBu_2)$, $Cu(OCH_2CH_2NEt_2)$, or $Cu(OCH_2CH_2OBu)_2$ (Me = methyl, Et=ethyl, and Bu=butyl) can be used [161] to prepare the superconductor. The latter two Cu precursors are unusual examples of Cu(II) alkoxides solution. They can be prepared by alcohol exchange between $Cu(OMe)_2$, and N-diethyletha-nolamine in solution of toluene. A dark purple solution is obtained, giving a dark green solid, after solvent extraction. Electron spin resonance showed that after carbonization, it contained only monomeric Cu(II). An ethoxybutoxide comprising $Cu(OCH_2CH_2OBu)_2$ was prepared similarly by alcohol exchange of $Cu(OMe)_2$ with 2-butoxyethanol, and could be puriffied by recrystallization from toluene.

A typical Cu(I)-containing metal-oxide precursor was prepared as follows[161], a solution of $Y(OCHMe_2)_3$, $Ba(OCHMe_2)_2$ and $Cu(NBu_2)$ in THF was added drop wise to a solution of degassed water in THF. The mixture was refluxed under argon for 16 hours, and filtered to give an organic solid. A solid was obtained, washed with THF and pentane, and dried under 100°C in vacuum to give an orange powder with composition $YBaCu(I)_3$. To prevent the formation of $BaCO_3$, this precursor had to be stored in inert atmosphere prior to use.

d) Organic additives

These additives can be used to capture a homogeneous cation solution inside an organic gel and avoid segregation by precipitation. For instance, cellulose powder has been added to YBa_2Cu_3 solutions to make slurries with a high viscosity[162].

2.3.3) Sol-gel processing in the Bi-(Pb)-Sr-Ca-Cu-O system

In order to obtain high quality superconductors in the Bi-(Pb)-Sr-Ca-Cu-O system, many liquid or sol-gel processes have been applied. The products obtained, like gels, are usually calcined in a temperature range of 800 - 840°C for about 10 hours[137, 163]. According to Takana, et al.[137] the 2-2-1-2 phase is formed during the calcination stage, and the 2-2-2-3 phase must have nucleated in order to grow during further heat treatment.

Table. 2.11 shows the relationship between the sintering conditions and the critical temperatures achieved by liquid or sol-gel processes. The results are similar to those obtained by conventional ceramic processings, but the critical temperature is more sensitive to the processing. With a 1-1-1-2 initial composition without Pb, $T_{c,0}$ never goes above 85K. Addition of Pb is necessary to obtain high critical temperature.

With sol-gel processing, the optimum sintering temperature is in the range of 835-845°C[63, 117, 137, 144], which is a little lower than with conventional ceramic processing. The formation rate of the 2-2-2-3 phase is also enhanced[63, 147, 148]. For example, it takes only 48 hours of sintering at 845°C to obtain the superconductor with $T_{c,0} = 104K$, instead of over 100 hours by a conventional processing as shown in Table. 2.9 and 2.10. Contradictory results have been reported on the effect of extended heat treatment on the critical temperature of sol-gel materials. According to X-ray data by Tanaka et al.[63], the 2-2-2-3 phase proportion and $T_{c,0}$ decrease after 72 hour at 845°C. On the contrary, according to Heh. et al. a prolonged sintering would effectively increase $T_{c,0}$[144].

Table. 2.11 Relationship between sintering conditions and critical temperatures in sol-gel processes

Composition Bi:(Pb):Sr:Ca:Cu	Liquid Processing	Sintering Temp.(°C)	Time (h)	Phase	$T_{c,on}$ (K)	$T_{c,0}$ (K)	Ref
1.6:(0.4):2:2:3	Coprecipitation,(Sr,Ca carbonates Bi oxide and Cu, Pb acetates in acetic acid + oxalic acid)	810, air	100	2-2-2-3	125	106	[143]
1 : 1 : 1 : 2	Sol-gel, (Nitrates + Oxalic acid and ethylene glycol)	830, air	15	2-2-1-2+ 2-2-2-3	125	69	[148]
0.7:(0.3):1:1:1.8	Sol-gel, (Nitrates + citric acid and ethylene glycol)	835,Ar+ O_2	100	2-2-2-3		>100	[92]
1.85:(0.35):1.9: 2.0:3.1, or 2 : 2 : 2 : 3	Sol-gel, (Metal acetates + acetic acid + tartaric acid)	835, air	130	2-2-2-3	107-115	100-105	[117]
		845, air	40	2-2-1-2+ 2-2-2-3	110	78-80	
0.7:(0.3):1:1:1.8	Sol-gel, (Nitrates + citric acid and ethylene glycol)	845, air 845, air 845, air	10 20 80	2-2-1-2+ 2-2-2-3		90.8 95.6 98.3	[114]
2 : 2 : 1 : 2	Coprecipitation, (Nitrates in aqueous solution+ammonium acetate + 8-hydroxy quinoline in aceton)	840, air	24	2-2-1-2	>77		[164]
0.92:(0.17):0.96 :1.0:1.5	Sol-gel, (Bi,Sr nitrates, Ca,Cu,Pb acetates+acetic acid and ammonia)	845, air	24	2-2-1-2+ 2-2-2-3		90	[137]
0.92:(0.17):0.96 :1.0:1.5	Sol-gel, (Bi,Sr nitrates, Ca,Cu,Pb acetates+aceticacid and ammonia)	845, air	48	2-2-2-3		104	[63]
1 : 1 : 1 : 2	A liquid processing, (Metal l ethylenediamin-tetraacetic acid)	850, O_2	12	2-2-1-2			[165]
1.83:(0.34):1.88 : 1.92:3.23	Sol-gel(Oxide & carbonate in nitric acid + citricacid + ethylene glycol)	850,air	420	2-2-2-3		107	[36]
2 : 2 : 2 : 3	Sol-gel, (Triphenyl Bi in toluene, Cu(II)2 - ethyhexanoate, Sr ethoxide in ethoxyethanol, mixed)	865, air	cacid	2-2-1-2	~ 80	~ 65	[154]
2 : 2 : 1 : 2		865, air		2-2-1-2	~ 75	~ 40	
4 : 3 : 3 : 4		865, air		2-2-1-2	~ 75	~ 55	
2 : 2 : 1 : 2	Sol-gel, (Cu acetate, Bi nitrac in methoxyethanol, Sr,Ca in isopropanol, then mixed)	870, air	24	2-2-1-2		67	[158]
2 : 2 : 1 : 2	Coprecipation, (Nitrates + ammonium $Et_3N/H_2C_2O_4$)	870, air	12	2-2-1-2	~ 85	~ 82	[163]
1 : 1 : 1 : 2	Precipation, (Nitrates + ammonium Oxalate)	870,vac. 875, air	20 40	2-2-1-2+ 2-2-2-3	110	77	[166]
1 : 1 : 1 : 2	Sol-gel, (Nitrates + Oxalate acid)	890. air 880, air	0.4 60	2-2-1-2+ 2-2-2-3	110	~ 35	[147]

CHAPTER 3: EXPERIMENTAL RESEARCH

3.1) EXPERIMENTAL OBJECTIVE

As explained in Introduction (chapter 1), the present experimental research has been devoted to the synthesis of Bi-(Pb)-Sr-Ca-Cu-O superconductors by sol-gel processing.

Since copper alkoxides are not soluable in common solvents, we have chosen nitrates as the precursors and critic acid as the complexing agent. This choice follows previous studies on YBaCuO gels and Cu gels[150, 169.3]. We address here the complete sol-gel processing of Bi-(Pb)-Sr-Ca-Cu-O from gels to the ceramics.

The gelation process and the gels obtained have been studied first as indicated in the next section. In order to understand the chemical process of the gelation, ammonia titration experiments have been performed on Bi, Pb, Sr, Ca, Cu nitrates respectively as well as on complex solution with or without citric acid.

The solid state reactions (phase transformations) occuring in these gels during heat treatment are important to study and compare with those superconductors made by conventional process. The gels have therefore been submitted to heat treatments at different temperatures and analyzed by X-ray diffraction for their phase transformations.

Although the density, and microstructure influence largely the properties of materials, the sintering behavior of Bi-(Pb)-Sr-Ca-Cu-O superconductors made by a sol-gel processing has not been reported until now. In the present work, densities and pore size data have been measured to try to describe the sintering behavior better. The microstructures were examined by SEM and optical microscopy and data on the grain growth during heat treatment were obtained.

Finally the critical temperatures of the superconductors made were measured by a dc four probe method to try to find the relationship between superconducting properties and processing parameters.

Details on the experiments and equipment used are gathered in the next sections.

3.2) MATERIALS FABRICATION

3.2.1) Sample preparation

The main steps in the preparation of samples are summarized in Fig.3.1. They include dissolution, gelation, drying and calcination, finally synthesis of superconductors pellets. General informations are given below while the details on material behaviors are presented in chapter 4.

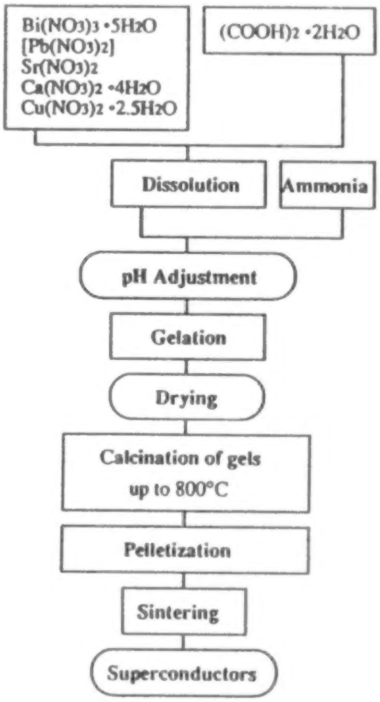

$Bi(NO_3)_3 \cdot 5H_2O$
$[Pb(NO_3)_2]$
$Sr(NO_3)_2$
$Ca(NO_3)_2 \cdot 4H_2O$
$Cu(NO_3)_2 \cdot 2.5H_2O$
$(COOH)_2 \cdot 2H_2O$
Dissolution
Ammonia
pH Adjustment
Gelation
Drying
Calcination of gels up to 800°C
Pelletization
Sintering
Superconductors

Fig. 3.1 Flow chart for the preparation of superconductors in the Bi-(Pb)-Sr-Ca-Cu-O system.

3.2.2) Choice of initial composition

As a result of the literature survey, 3 initial gel compositions have been selected. The first, gel(a) does not include any Pb. The 2 others, gel(b) and (c), were made with Pb. Their initial compositions are summarized in Table. 3.1. They have been reported to grow a high proportion of the 2-2-2-3 phase[35, 63, 137, 144]. Gel(b) is roughly a 1-1-1-2 like gel(a), except for the presence of Pb.

Table. 3.1 The initial compositions of gel(a), (b) and (c) in the present research.

gel	Bi - (Pb) - Sr - Ca - Cu initial molar composition
(a)	1.0 -(0.0)- 1.0 - 1.0 -2.0
(b)	0.75-(0.25)-1.0-1.0-2.0
(c)	1.84-(0.34)-1.92-2.0-3.0

3.2.3) Sol-gel processing

The precursors were all nitrates. They comprised over 99.5% pure $Bi(NO_3)_3{\bullet}5H_2O$, $Sr(NO_3)_2$ from Molycorp and Morton Thiokol, Inc., and $Pb(NO_3)_2$, $Ca(NO_3)_2{\bullet}4H_2O$, and $Cu(NO_3)_2{\bullet}2.5H_2O$ from BHD Chemicals. They were dissolved in water and mixed in a glass beaker in proportion according to the initial compositions of gel(a), (b) and (c). Citric acid (BHD Chemicals) was used as the complexation agent. Stirring was done magnetically on a hot plate. Aqueous ammonia was used to adjust the pH value of solutions. Titration experiments was done on each element and the mixtures, to choose an appropriate gelation pH. Drying was performed on a hot plate, or in an oven.

3.2.4) Calcination of the gels

All calcinations and heat-treatments were performed in a Linderberg's Moldtherm Box Furnace which could be programmed and controlled with a digital temperature controller. The most frequent heating and cooling rates used were 5°C per minute. Air was used as the furmace atmosphere.

The evolution of gels, during calcination, was studied after heat-treatment in an alumina crucible at 220, 400, 600, 700, 750, 800 °C for 12 hours. Samples of gel(a),(b), and (c) were heated at the same time in the same furnace for each set of condition. The materials were then analyzed by powder X-ray diffraction, and B.E.T. porosimetry.

In further heat treatment, calcination was always done at 800°C for 12 hours.

3.2.5) Superconductors transformation studies

After calcination at 800°C, the products were ground in a mortar to a very fine powder. The mass of materials were measured on a Mettler BB2400 balance with a precision of 0.01 gram. Pellets with 12.5 mm diameter and 1.5 mm thickness were produced by cold pressing under a pressure of 340 Mpa, with a specimen mount press from BUEHER, LTD. They were used to study the phase transformation, microstructure, sintering, and superconducting properties evolution of superconductors

Table 3.2 Summary of heat-treatment studies of superconductors from gel(a) (b) and (c)

	815°C	830°C	845°C	860°C
12 hours		gel(a), (b), (c)		
24 hours	gel(a), (b), (c)	gel(a), (b), (c)	gel(a), (b), (c)	gel(a), (b), (c)
48 hours	gel(a), (b), (c)	gel(a), (b), (c)	gel(a), (b), (c)	
96 hours			gel(a), (b), (c)	
144 hours	gel(a), (b), (c)	gel(a), (b), (c)	gel(a), (b), (c)	
288 hours		gel(a), (b), (c)	gel(a), (b), (c)	

In order to keep consistent experimental results, three gel(a), (b) and (c) pellets were heat- treated simultaneously in the same Lindberg's furnace, for a set of conditions.

The heating and cooling rates were fixed at 10°C per minute for all heat treatments. The pellets were heat treated at different temperatures for different times, as shown in Table 3.2. Then the heat treated pellets were analyzed by XRD, SEM, optical microscopy, BET, and superconducting critical temperatures by a dc four probe method.

3.3) CHARACTERIZATION OF MATERIALS AND EUIPMENT USED:

3.3.1) Titration experiment

The glass was used included a 50 ml stopcock buret with a reading mark every 0.1 mL. PH was measured with a Fisher Accumet Model 950 pH Meter at a precision of 0.01 and at a temperature fixed with a precision of 0.1°C.

An example of titration procedure is the following, 4.8500 g (0.01mole) bismuth nitrate $Bi(NO_3)_3 \cdot 5H_2O$, measured on a Sartorius balance with a precision of 0.0001gram, were poured into a flask, and dissolved in 40 ml water. Stirring with a magnetic bar was maintained for about 30 minutes at room temperature. The electrode and the thermometer connected with the pH meter were placed into the solution in the flask. The buret filled with 50 ml aqueous ammonia NH_4OH, and placed above the flask. Ammonia was added from the buret in increments of 1ml at the beginning, while controlling its flow with the stopcock. After 5 seconds, the pH and temperature were read. When nearing the equivalence point, ammonia was introduced in increments of 0.5ml.

3.3.2) X-ray diffraction

a) Equipment

A Rigaku-Denki X-ray diffractometer with a Philips goniometer was used to identify the phase in the heat-treated gels and pellets. The X-ray tube had a Cu target with a Ni filter and was operated under 35 KV and 15 mA. The X-ray diffractometer was connected with the PW1410 (Philips) detector, and a PM8000 flat-bed recorder (Philips) providing intensity vs. 2θ curve. The counting rate was fixed, depending on the samples, at $4x10^2$ c.p.s. or $1x10^3$ c.p.s., and the chart speed was set at 10mm per minute. In the present work, two kinds of X-ray diffraction patterns have been obtained: A first kind is by the standard X-ray powder diffraction method, and the other with the heat-treated pellets without grinding, to analyze preferred orientation.

b) Phase identification

Phase identification was accomplished mainly through data from the JCPDS Powder Diffraction Files[167] with the gels heat-treated at low temperatures. The X-ray data from Saggio, et al.[31], Srinivasan, et al.[34], and Koyama, et al.[35], which have been gathered in Table 2.5, 2.6, and 2.7 in the chapter 2, were also applied to identify the 2-2-0-1, 2-2-1-2, and 2-2-2-3 phases respectively.

3.3.3) Density measurement

The densities of the pellets were measured by the standard ASTM test method for bulk density of solid by wax coating and immersion[168]. In the experiment, a piece of the Parowax (ESSO) with density K= 0.8855 g/cm^3 and a wax melting container (an alumina crucible) were used. All masses were determined with a precision of 0.0001g on a Sartorius balance.

The experimental procedures were as follow: (1) the test pellet was dried between 105 and 110°C for 10 minutes to remove the entrapped moisture; (2) the initial weight, W, of each pellet, was determined; (3) the Parowax was melted in an alumina crucible at about 200°C and was used to coat the pellet by dipping. One half to two thirds of the pellet was immersed first, then the pellet was held by its waxed end and the unwaxed portion was dipped into the melted wax; (4) the weight of the wax-coated pellet, P, was determined; (5)

a very fine copper wire was tightened to the wax-coated pellet and suspended to the balance. The weight of the suspended pellet plus the fine copper wire, S', was determined after immersion in water; (6) the dry mass of the copper wire, S", and the dry mass of the suspended pellet, S=S'-S", were determined.

The density calculations are the following:

(1) the volume, V_1, of the test pellet (including the wax) in cubic centimeters is:

$$V_1 = P - S \qquad (3.1)$$

(2) the volume, V_2, of the wax coating on the test pellet in cubic centimeters is:

$$V_2 = (P - W)/K \qquad (3.2)$$

where K is the density of the wax in g/cm^3.

(3) the volume, V, of the test pellet alone in cubic centimeters is:

$$V = V_1 - V_2 \qquad (3.3)$$

(4) the bulk density, D, of the test pellet in grams per cubic centimeter is:

$$D = W/V \qquad (3.4)$$

In practice, for each pellet 3 measurements were made according to the above procedure, to obtain an average significant bulk density .

The measurement errors can be estimated as follows:

$$(\Delta D/D)^2 = (\Delta W/W)^2 + (\Delta V/V)^2 \qquad (3.5)$$

where $\Delta D = [\Sigma(D-D_{av})^2/(n-1)]^{1/2}$, $\Delta W = [\Sigma(W-W_{av})^2/(n-1)]^{1/2}$, and $\Delta V = [\Sigma(V-V_{av})^2/(n-1)]^{1/2}$, ($D_{av}$, W_{av} , V_{av} are average values for density, weight, and volume) and n is the number of measurements.

3.3.4) SEM and optical microscopy

a) Equipment

A SEM and an optical microscope have been used to observe the microstructures of superconductors.

The SEM used in this experiment was an International' Scientific Instrument-60 (ISI-60) operated under 30KV. The microstructures of the superconductors were observed by CRT, and photographies were taken when necessary. The elements were analyzed with an Princeton Gamma-Tech. System 4 Energy Dispersive X-Ray Spectroscope (PGT system 4 EDX) connected to the ISI-60 SEM.

The optical microscope was by Wild Heerbrugg Limited.

b) Sample preparation

A pellet to observe was cut by the middle. A half part was mounted with BUEHLER phenolic resin under a BUEHER specimen mount press. The pellet section was place parallel to the bottom of the die. The sample was polished on a wheel with alumina powder, then etched in hot diluted hydrochloric acid.

c) Estimation of grain growth

Polished samples were examined under the optical microscope. The average grain size was estimated by the lineal intercept method[169.1]. The experimental procedure in this work were as follows: (1) the polished sample was placed on the microscope at a magnification of 600X. The eyepiece included a calibration line, with a length L =

180 μm, comprising 100 subdivisions; (2) the line intercepted a number of grains randomly; this number was counted; (3) step (2) was repeated five times in five different directions on the surface of the test sample; (4) the average number of grains, N, was calculated; (5) the average grain size was calculated by D = L/N.

3.3.5) BET method

A QUANTA CHROME AUTOSORB-1 BET. equipment was used to analyze the sintering behaviors of the samples made in the present work. This piece of equipment measures the quantity of gas adsorbed onto, or desorbed from a solid surface at some given equilibrium vapor pressure. The pellet analyzed was broken into small pieces and placed in a glass cell for analysis. They were outgased before analyzsis, and their mass determined after outgasing. The gas adsorbed was nitrogen, and adsorption-desorption was carried out at 77K. The data were analyzed with an IBM microcomputer. The results included the BET surface area (single and/or multpoint), Langmuir surface area, adsorption and /or desorption isotherms (20 points), pore size and surface area distribution, micropore volume and surface area using t-plots.

3.3.6) The dc four-probe method[169.2]

The dc four-probe method was used to measure the resistance of a superconductor as a function of temperature down to 77K. The measuring equipment were made by ourselves. It included a current source driver, a controller (STRAWBERRY TREE COMPUTER, CORP.) connected to an IBM PS2 microcomputer, and a sample cell (Fig. 3.2). The current source driver could provide a stable continuous current through the sample, which was controlled automatically by the STRAWBERRY TREE controller. The controller transferred the measured data (voltage, resistance) to the IBM microcomputer, and the data was analyzed with the Lotus 123 software.

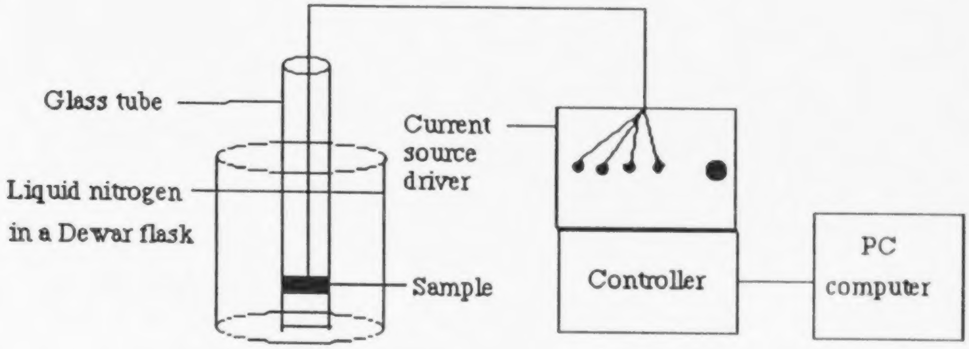

Fig. 3.2 Illustration of T_c measurement equipment set-up for a dc. four probe method.

The test sample was cut into rectangular pieces with dimensions of 10 x 4 x 0.8 mm^3 (as shown in Fig. 3.3). Four fine copper wires were used as probes. Each wire, with a length about 150mm, was connected with Indium at both ends. A small piece of Indium was pressed to attach it on the surface of the test samples. Four Indium points were placed along the length of the sample at spacing distances of about 2 mm. One end of each copper wire with Indium end was pressed into an Indium point on the sample surface. After the four wire's connections were established, the resistance between any two wires, measured with a volt meter, was not allowed to reach over 5Ω. Otherwise, new connections had to be made.

The sample with four copper probes was connected to the direct current source driver, and placed in the sample cell, in which a thermocouple was fixed near the sample.

A direct current was passed through the sample between outer probes and the resulting potential difference was measured between the inner probes. The current magnitude was chosen to be 10mA (because a large current would destroy the superconductivity in the test sample. The sample cell was placed into liquid nitrogen while the measurement were made. Both temperatures and resistance were read at intervals of 10 seconds.

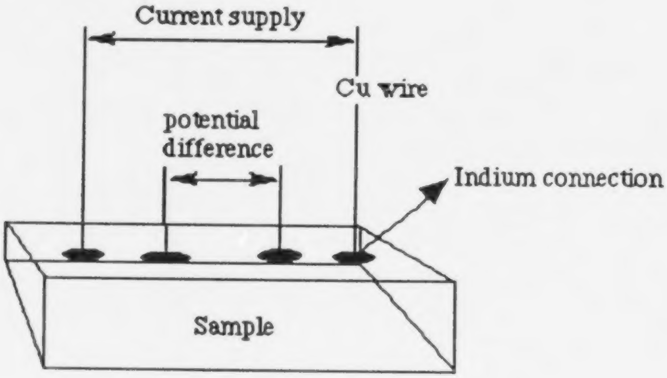
Current supply
Cu wire
potential
difference
Indium connection
Sample

Fig. 3.3 Illustration of a sample with Indium connections for T_c measurement.

CHAPTER 4: RESULTS

4.1) SOL-GEL PROCESSING

4.1.1) Gelation

Gels for superconductors in the Bi-(Pb)-Sr-Ca-Cu-O system could be obtained by complexation of the mixed nitrate solutions with citric acid and ammonia, as shown in Fig. 4.1(a), (b), (c) corresponding to gel(a), gel(b), (c) respectively. They are blue and transparent, and can be re-dissolved in water.

According to ammonia titration curves shown in Fig. 4.2, plateaus at pH values of about 0.5, 3.5, 5.0, 9.0 occur with nitrates of Bi, Cu, Pb, Sr/Ca analyzed separately (Fig.4.2(a)). As long as no critic acid is added a basic titration of a mixed nitrate solution shows a succession of equivalent points which can be attributed to each type of cations considered independently. The case of a solution corresponding to gel(c) is shown in Fig.4.2(b). When critic acid is added, these equivalence points are wiped out and replaced by a single new equivalence point. When the molar ratio of citric acid to cations is 1, precipitation occurs near at pH = 6 at 60°C. In order to complete complexation, a molar ratio of critic acid to cations equal to 2 has been found to be necessary. The gelation of these mixtures must be done by slow evaporation. A temperature of 70°C maintained on a hot plate has been found to perform the most effectively.

4.1.2) Gel structure and properties

The gels obtained are composed of a solid network with platelike layers as can be seen under the SEM (Fig. 4.3). Also, they formed essentially closed pores during gelation, which was confirmed by the very low specific area in the order of 1.0 m^2/g by the BET method. If gelation-drying is done in an oven, an impervious gel layer forms on the top of the sample. The gases resulting from the gels decomposition or drying during heat treatment (H_2O, N_2O_3, CO_2) cannot escape, and the gel samples bloat extensively, as shown in Fig. 4.4(a) and (b).

These bloated gels became black after they were heat treated above 100°C and below 250°C. The XRD analysis indicated they were amorphous up to 220°C (Fig.4.6). The bloated black gels could be redispersed in aqueous media. The black solutions obtained could be regelled at 70°C. The new gels were black and did not bloat again when they were heat treated. But they became more and more brittle. We believe that they could be optimized to design a more efficient sol-gel processing of superconductors. Fig. 4.5 shows pieces of the black gel(c) after heat-treatment at 180, 210, and 240°C for 2 hours. If the blue gels were heated above 250°C, the black products obtained could not be re-dissolved in water completely in relation with the beginning of crystallization.

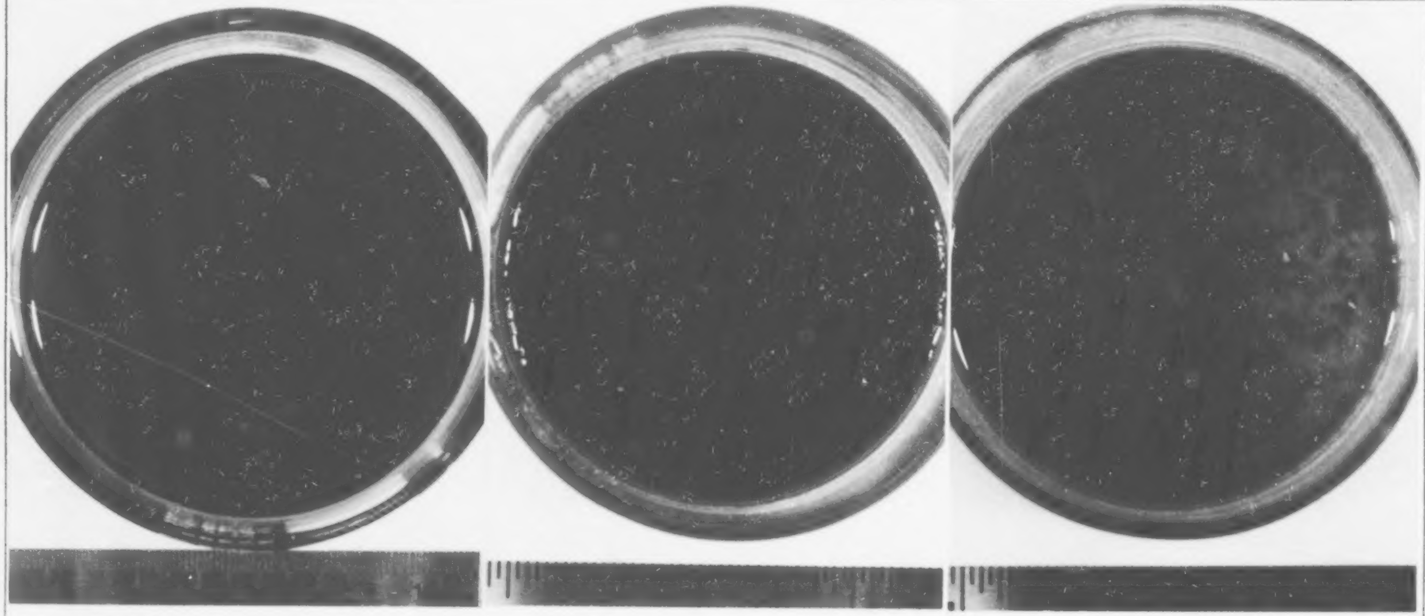

$Bi_1\ Sr_1\ Ca_1 Cu_2$

$Bi_{0.75}(Pb_{0.25})Sr_1\ Ca_1 Cu_2$

$Bi_{1.84}(Pb_{0.34})Sr_{1.92}Ca_2 Cu_3$

Fig. 4.1 Illustration of gel(a), (b) and (c)

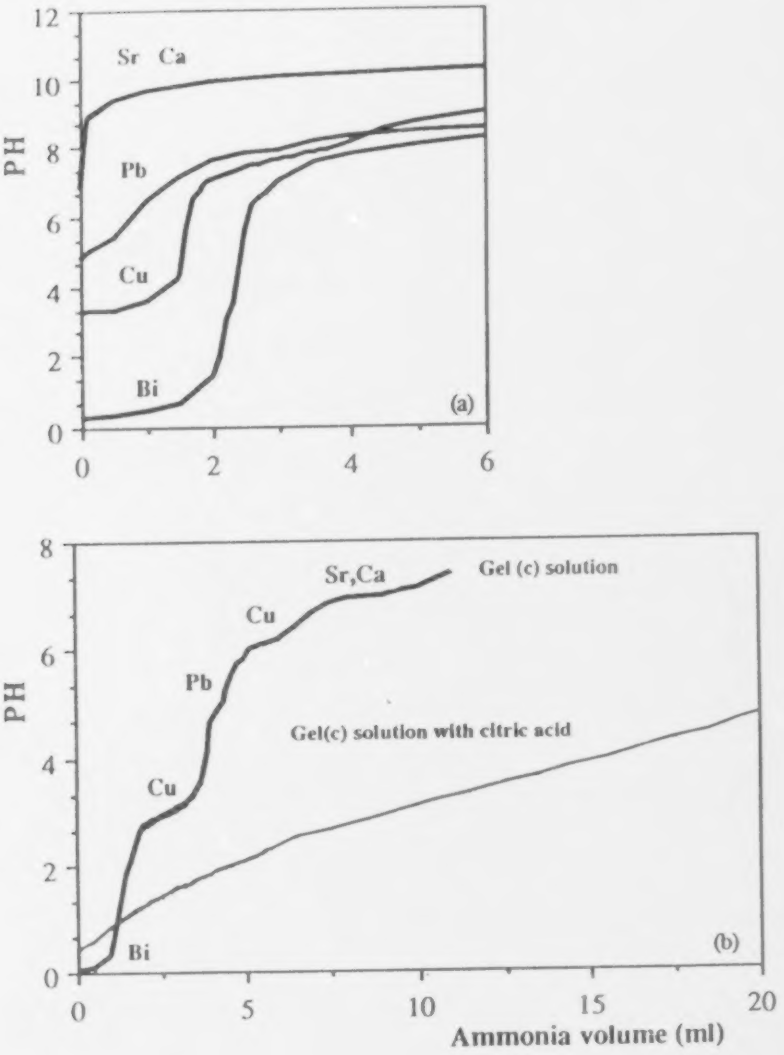

Fig. 4.2 Titration curves of nitrates with aqueous ammonia: (a) Bi, Pb, Sr, Ca, Cu nitrate titrated individually; (b) mixtures of Bi, Pb, Sr, Ca, and Cu nitrates with composition of gel(c) -titrated with or without citric acid.

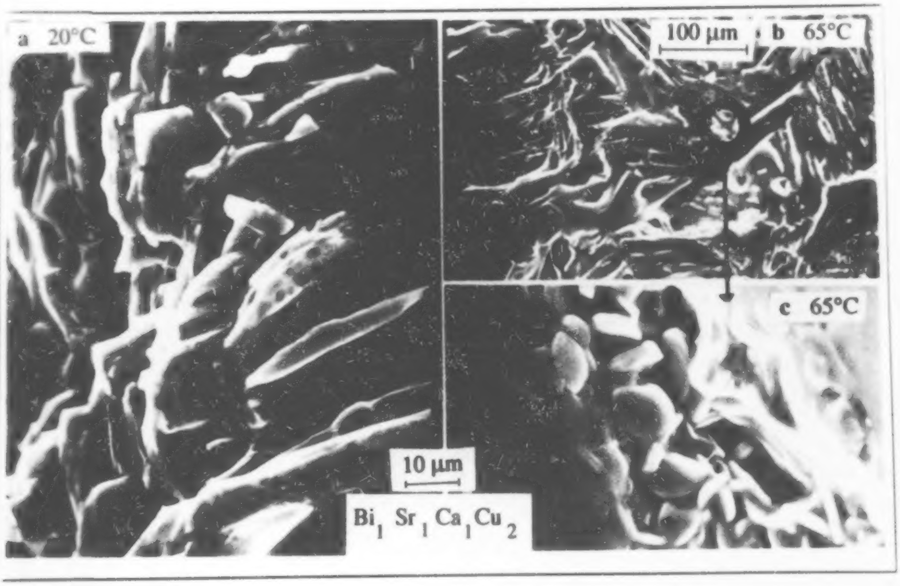
a 20°C
100 µm
b 65°C
c 65°C
10 µm
Bi1 Sr1 Ca1 Cu2

Fig. 4.3 Microstructures of gel(a) observed under a SEM. The Gel was dried (a) at 20°C; (b) and (c) at 65°C.

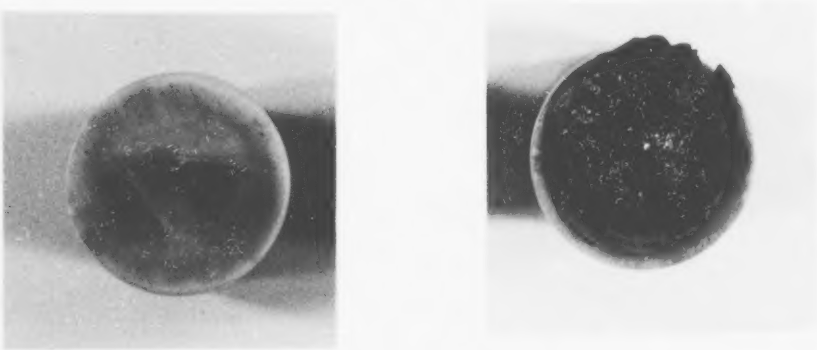

(a) (b)

Fig. 4.4 The appearance of the gel(c) (a) before heat-treatment; (b) after heat-treatment at 220°C for 2 hours.

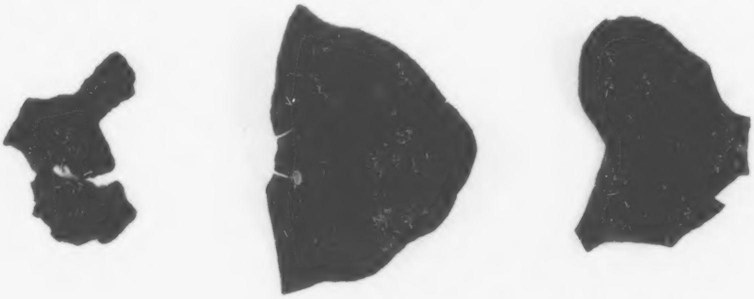

(a) 180°C (b) 210°C (C) 240°C

Fig. 4.5 Black gels obtained by redissolving the blue gels heat-treated at (a) 180°C; (b) 210°C, and (c) 240°C.

4.2) PHASE TRANSFORMATION

4.2.1) During calcination of the gels up to 800°C

Fig. 4.6 shows the X-ray powder diffraction patterns of gel(a) after heat treatment at 220, 400, 600, 700, 750, 800°C for 12 hours respectively. While it is still largely amorphous at 220°C, sharp diffraction lines corresponding to crystalline phases are observed above. Diffraction lines could be tentatively indexed according to the phases formed in the ternary systems Bi-Sr-Ca, Sr-Ca-Cu, Bi-Ca-Cu and Bi-Sr-Cu, according to Paz-Pujalt[69]. At 400°C the main lines correspond to $CuBi_2O_4$ with two quite strong CuO peaks very near the positions of the (0012) and (026) peaks in the 2-2-1-2 phase, they remain up to 750°C. At 600°C the main lines observed seem to belong to $Sr_{1-x}Ca_xCO_3$, CuO, and $CuBi_2O_4$. Some peaks could not be indexed. The black triangles in this figure indicate the peaks of the 2-2-0-1 phase which could be observed at 600, 700 and 750°C while the peaks of CuO and $Sr_{1-x}Ca_xCO_3$ are still present. The peak indensity of the 2-2-0-1 phase at 750°C is stronger than that at 700°C. The proportion of this phase increases therefore with the calcination temperature. Finally the 2-2-1-2 phase is really observable only at 800°C where it is the only one present. If Pb is added, the only difference in the X-ray diffraction patterns, is the formation of a Ca_2PbO_4 phase above 700°C as shown in Fig. 4.7(a) and (b).

4.2.2) In superconductors above 800°C

At 800°C, the calcined gels are too brittle and must be pressed into pellets. As reported above, this is also the temperature where the first high-Tc phase is formed in high proportion. Fig. 4.8, 4.9, and 4.10 show the X-ray diffraction patterns of heat treated pellets of gel(a), gel(b), and gel(c) respectively at 815°C, 830°C, 845°C, 860°C for 24 hours. The 2-2-1-2 phase is predominant in all pellets at all heat treatment temperatures. Weak peaks belonging to the 2-2-2-3 phase can be observed in gel(a) samples heat treated at 860°C (Fig.4.8), in gel(b) samples heat treated at 830 and 845°C (Fig.4.9), and in gel(c) at 830°C (Fig. 4.10). Preferred orientation is observable in relation with relative intensities of the (008), (0010) and (0012)peaks.

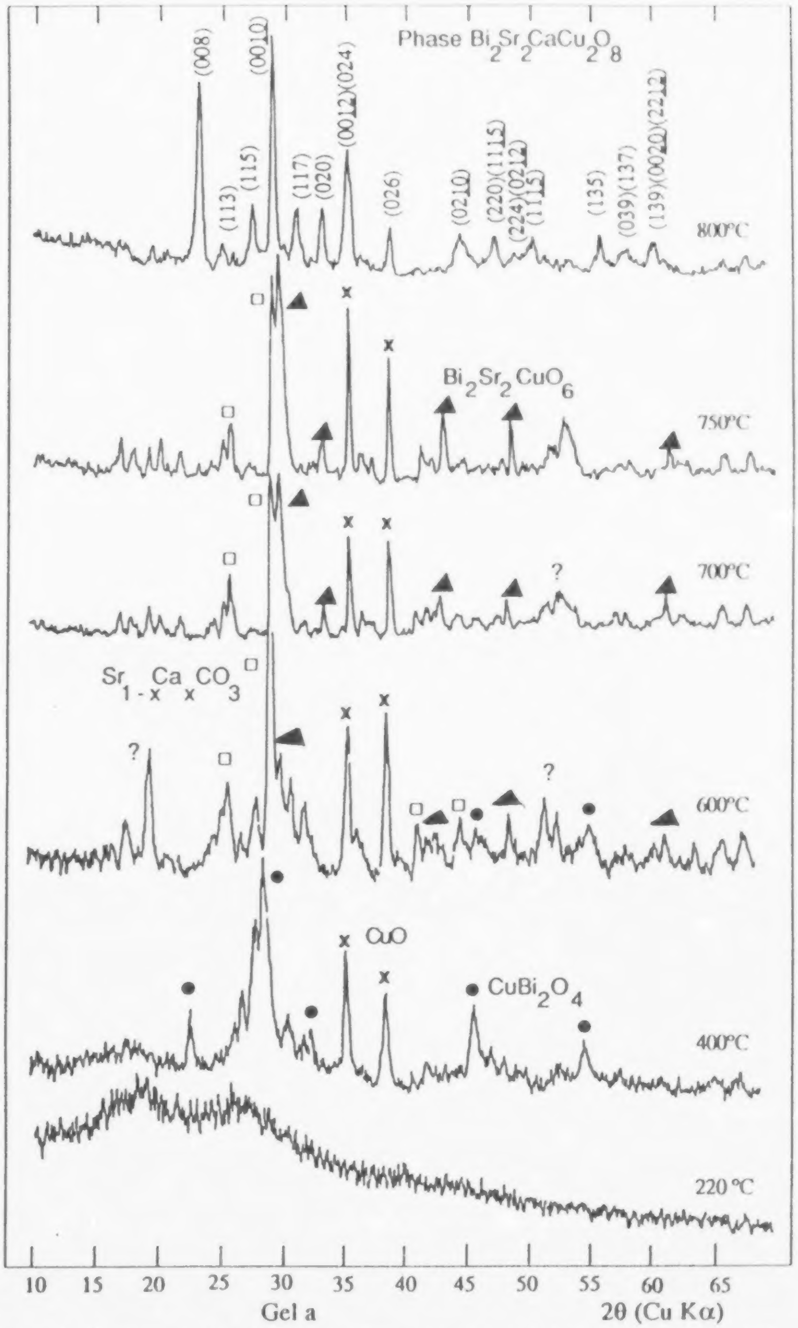

Fig. 4.6 X-ray powder diffraction patterns of gel(a) heat-treated at different temperature for 12 hours.

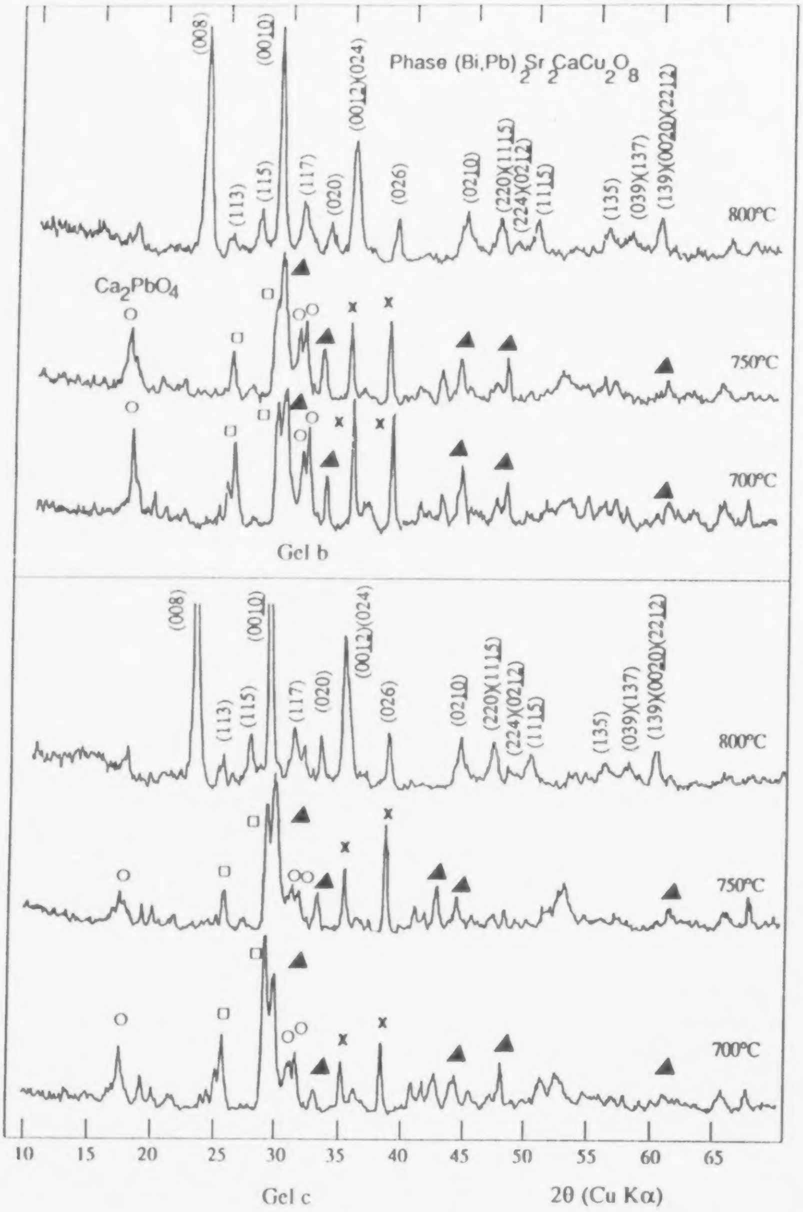

Fig. 4.7 X-ray powder diffraction patterns of gel(b) and (c) heat-treated at 700, 750, and 800°C for 12 hours.

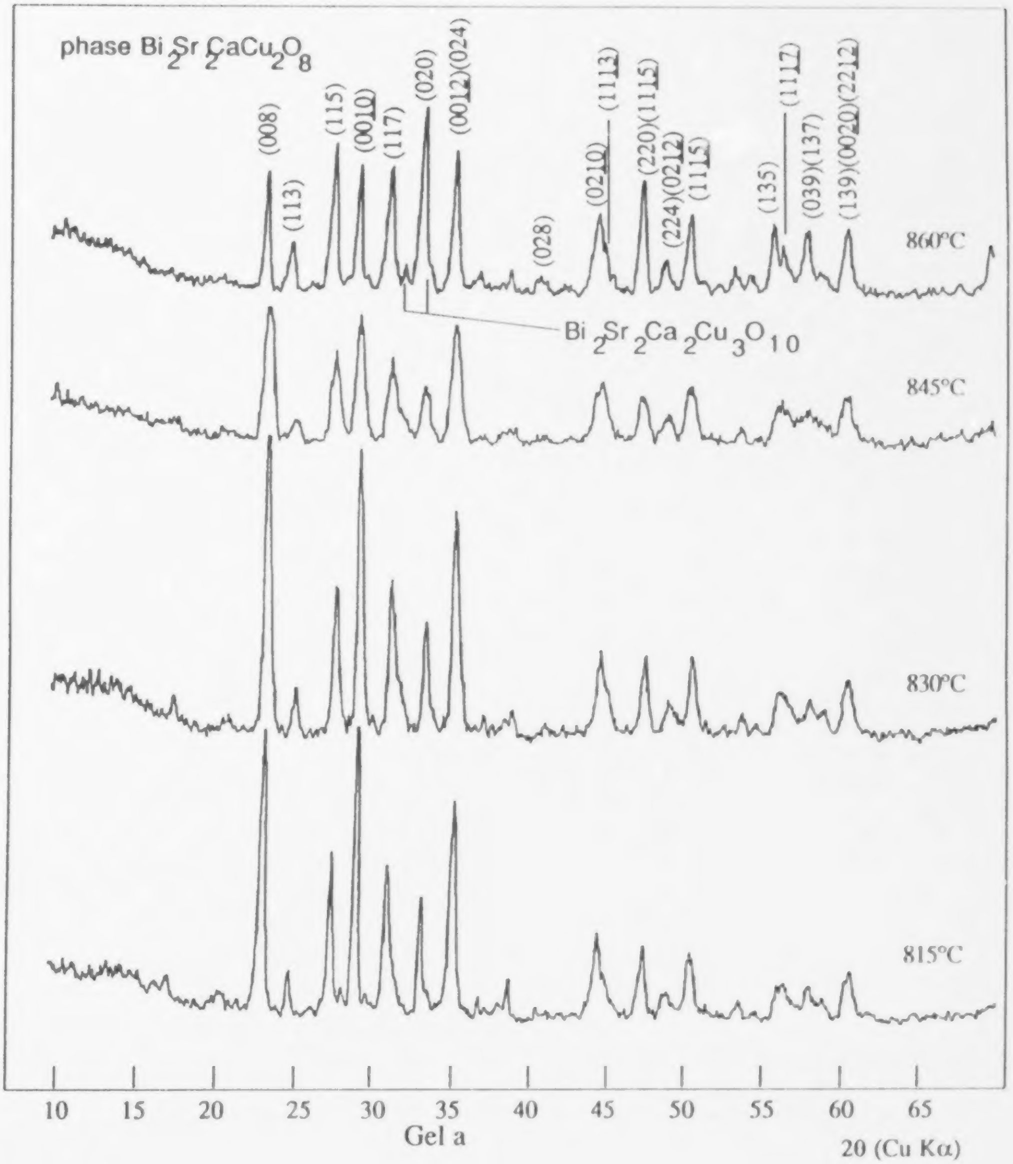

Fig. 4.8 X-ray diffraction patterns of gel(a) pellets heat treated at 815, 830, 845, and 860°C for 24 hours.

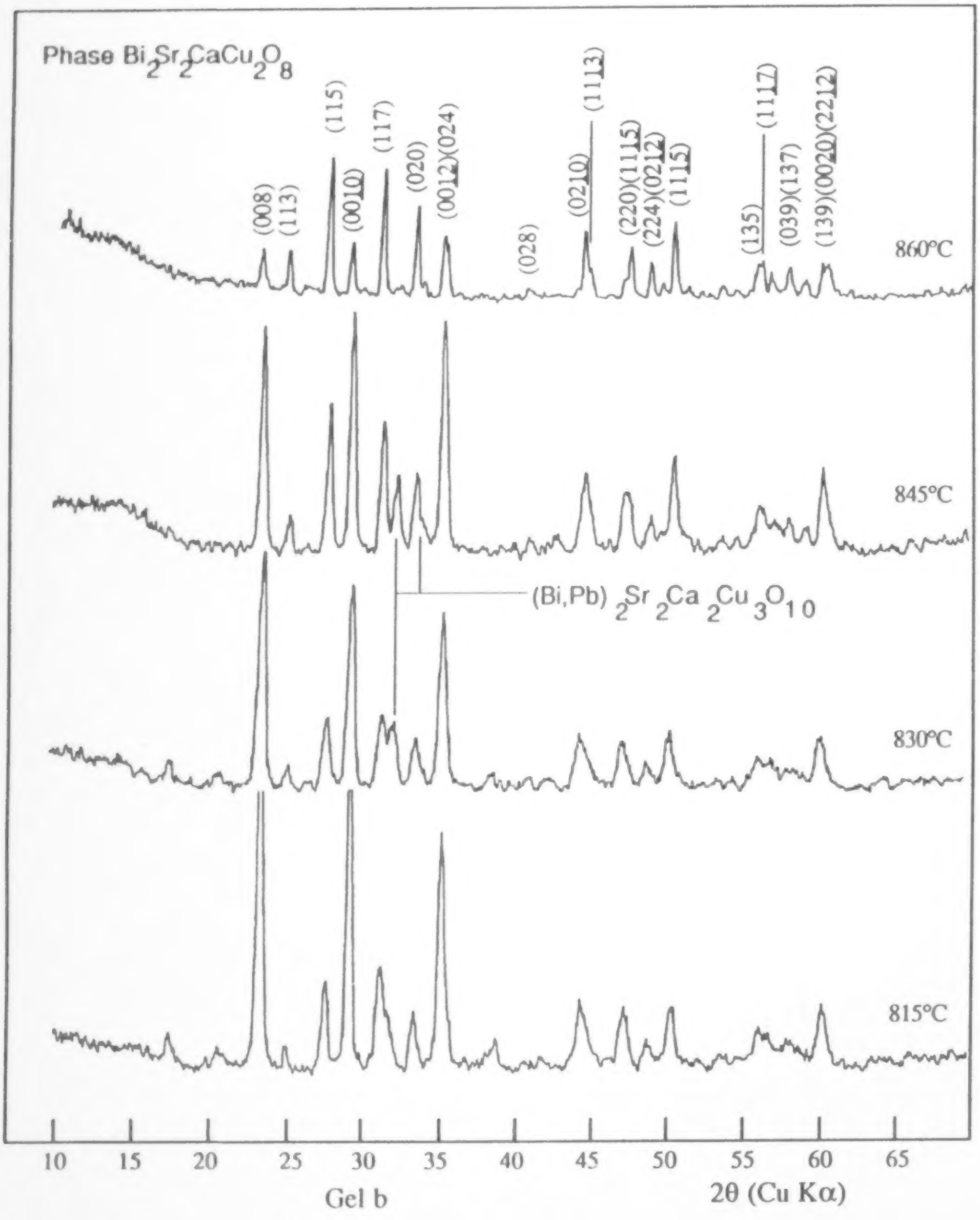

Fig. 4.9 X-ray diffraction patterns of gel(b) pellets heat treated at 815, 830, 845, and 860°C for 24 hours.

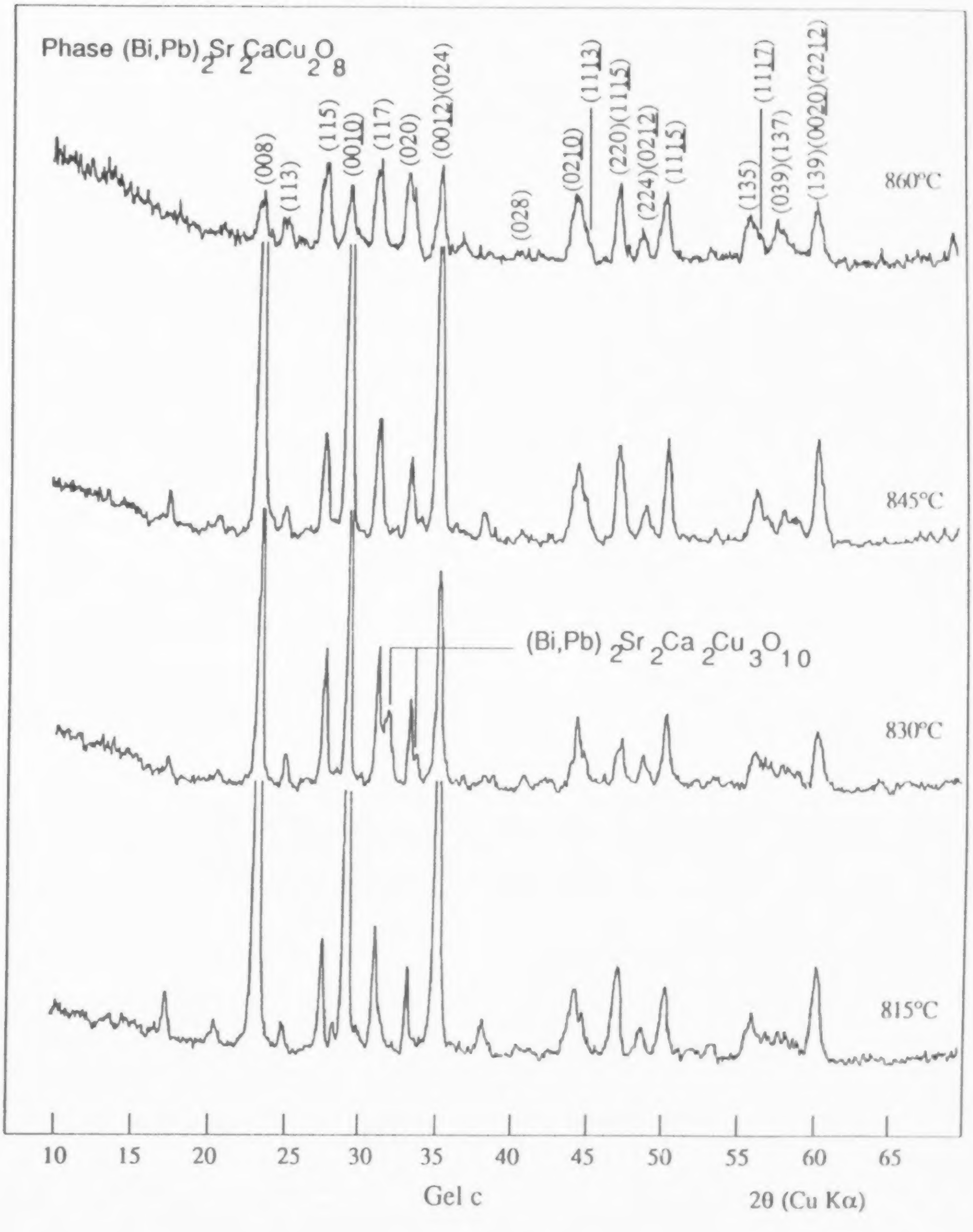

Fig. 4.10 X-ray diffraction patterns of gel(c) pellets heat treated at 815, 830, 845, and 860°C for 24 hours.

The X-ray patterns for increasing heat treatment times at 815, 830, and 845°C are reported from Fig.4.11 to Fig.4.19 for all gels.

Fig. 4.11, 4.12, and 4.13 are for gel(a),(b), and (c) heat treated at 815°C for 24, 48, and 144 hours respectively. The 2-2-1-2 phase is predominant, while the very weak peaks of the 2-2-2-3 phase could be detected in the gel(a) and (b) samples heat treated for 144 hours.

The results from the gel(a), (b), and (c) heat treated at 830°C are shown in Fig. 4.14, Fig.4.15, and Fig.4.16. In this group of diffraction patterns, the 2-2-1-2 phase is also predominant, but the intensity of some the 2-2-2-3 phase peaks is quite strong in gel(b), for instance, the (119) peak in the 2-2-2-3 phase could be detected when the samples were heat treated after 24 hours (Fig. 4.15).

The X-ray diffraction patterns of the sample which were heat treated at 845°C (Fig.4.17, 4.18, and 4.19) are remarkably different from that at 815 and 830°C. The peaks belonged to the 2-2-2-3 phase can be observed after 24 hour heat treatment in all three type samples. In the gel(a) samples, the intensity of the 2-2-2-3 phase peaks is the strongest after 48 hour heat treatment, but it decreases for longer time. On the contrary, the intensity of the 2-2-2-3 phase peaks continued to increase with heat treatment time in the gel(b) and (c) samples.

In order to estimate the volume fraction of the 2-2-2-3 phase, some samples were grinded into powder after heat treatment, before performing X-ray diffraction analysis. This allows to destroy the preferred orientation observed in pellets. The volume fraction of the 2-2-2-3 phase is estimated by the ratio of $\frac{I_h(0010)}{I_h(0010) + I_l(008)}$, where $I_h(0010)$ is the intensity of the (0010) peak of the 2-2-2-3 phase, and $I_l(008)$ the intensity of the (008) peak of the 2-2-1-2 phase. The result at 845°C is shown in Fig.4.20. The kinetics of appearance of this 2-2-2-3 phase, depends greatly on the initial compositions. The 2-2-2-3 phase proportion goes through a relative maximum of about 12% after 48 hours in the gel(a) samples. Its proportion in the gel(b) and (c) samples increases with heat treatment time. In gel(b) superconductors, the major phase is the 2-2-2-3 one (up to 76%) after 288 hours heat treatment. In the gel(c) samples, the formation kinetic behavior of the 2-2-2-3 phase is similar to that in the gel(b) samples, but the proportion remains lower.

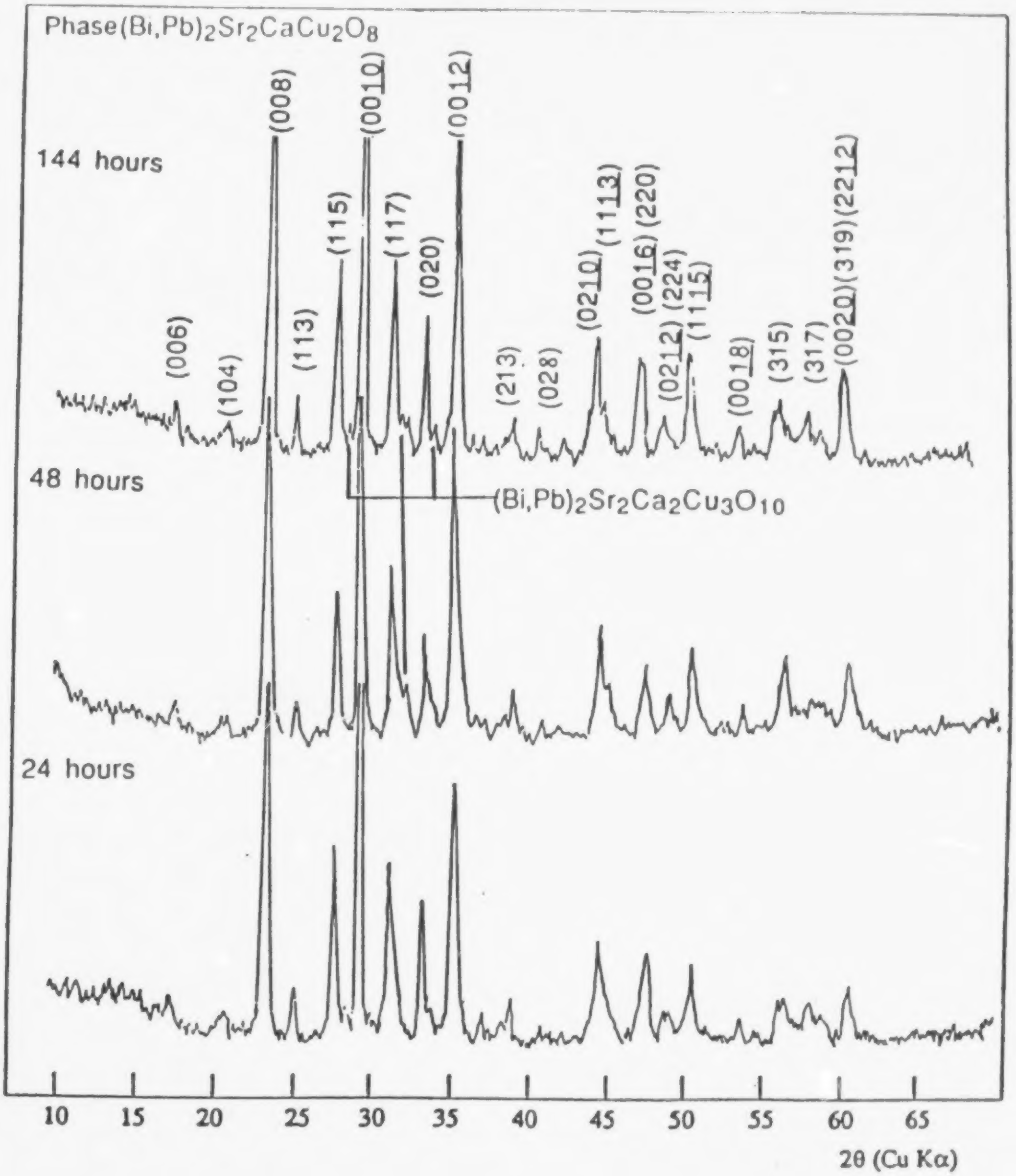

Fig. 4.11 X-ray diffraction patterns of gel(a) pellets heat-treated at 815°C for increasing times.

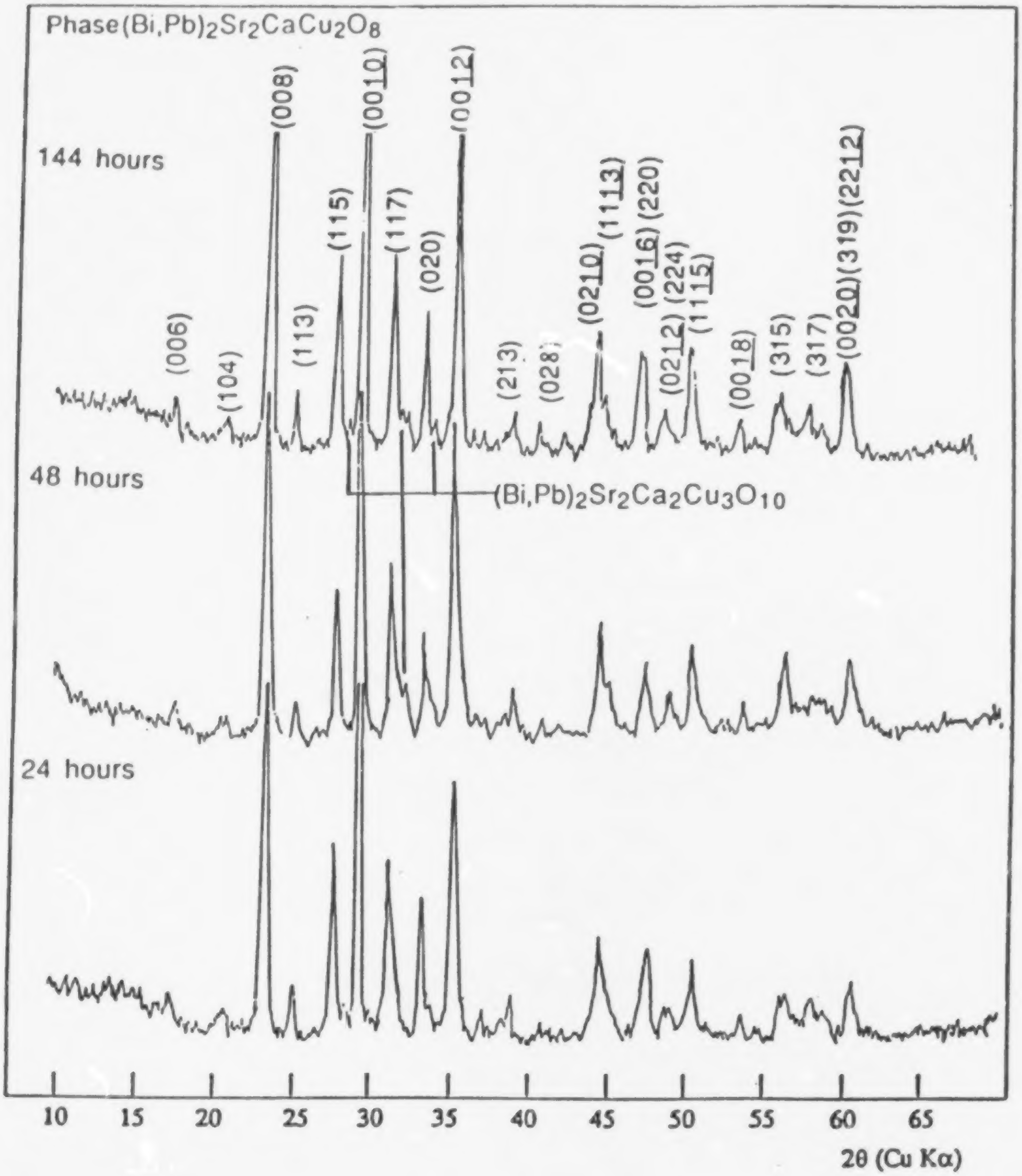

Fig. 4.12 X-ray diffraction patterns of gel(b) pellets heat-treated at 815°C for increasing times.

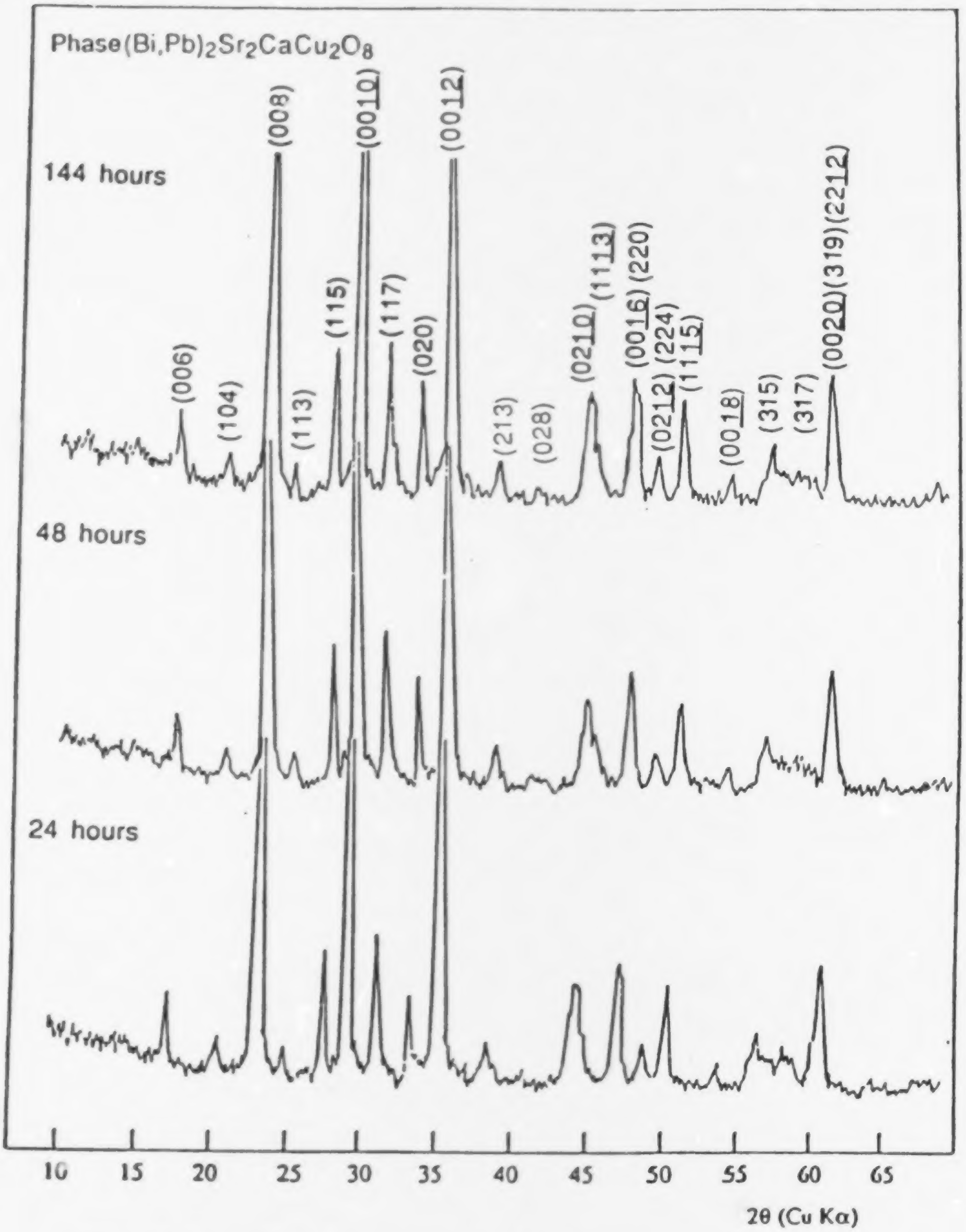

Fig. 4.13 X-ray diffraction patterns of gel(c) pellets heat-treated at 815°C for increasing times.

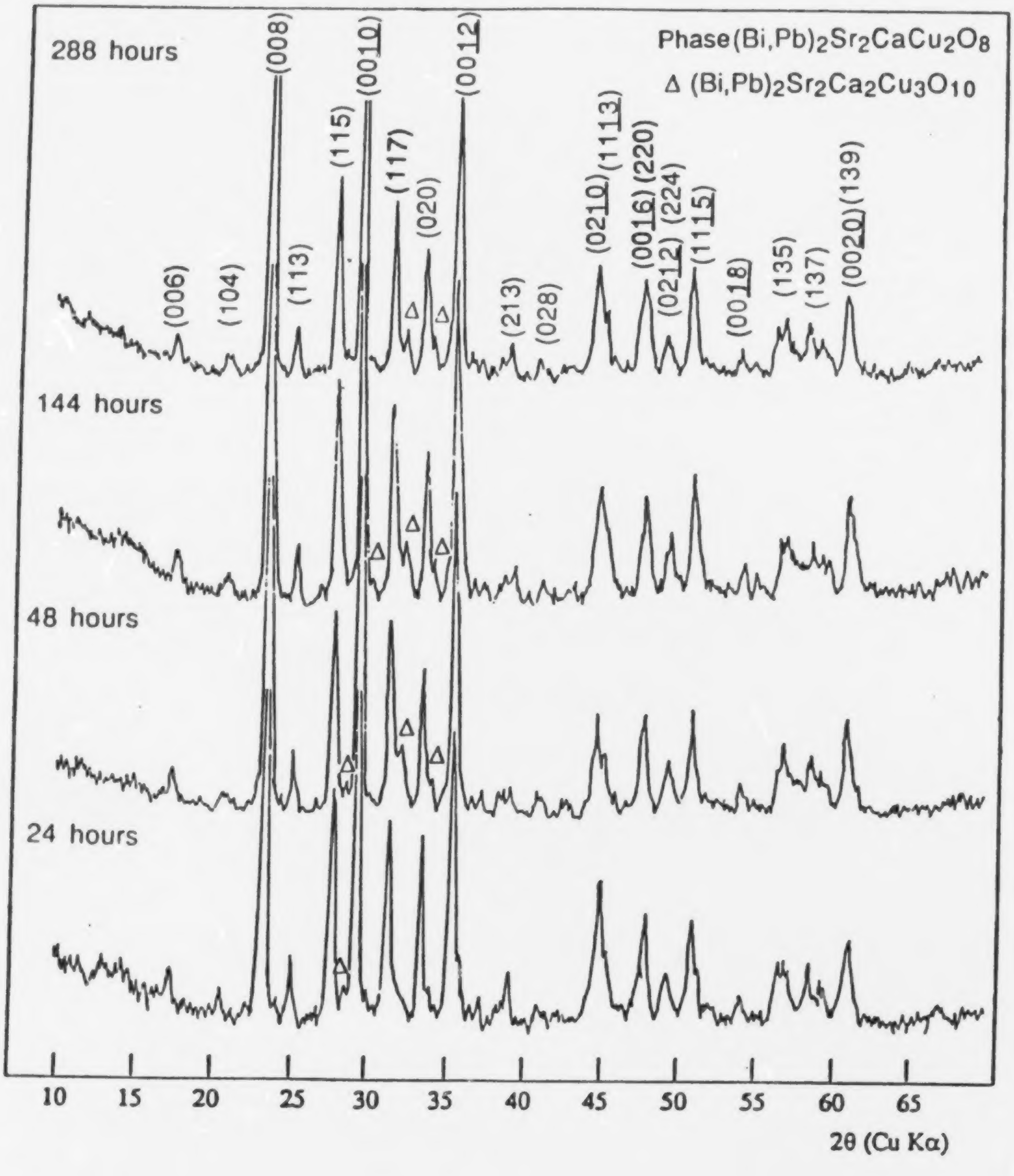

Fig. 4.14 X-ray diffraction patterns of gel(a) pellets heat-treated at 830°C for increasing times.

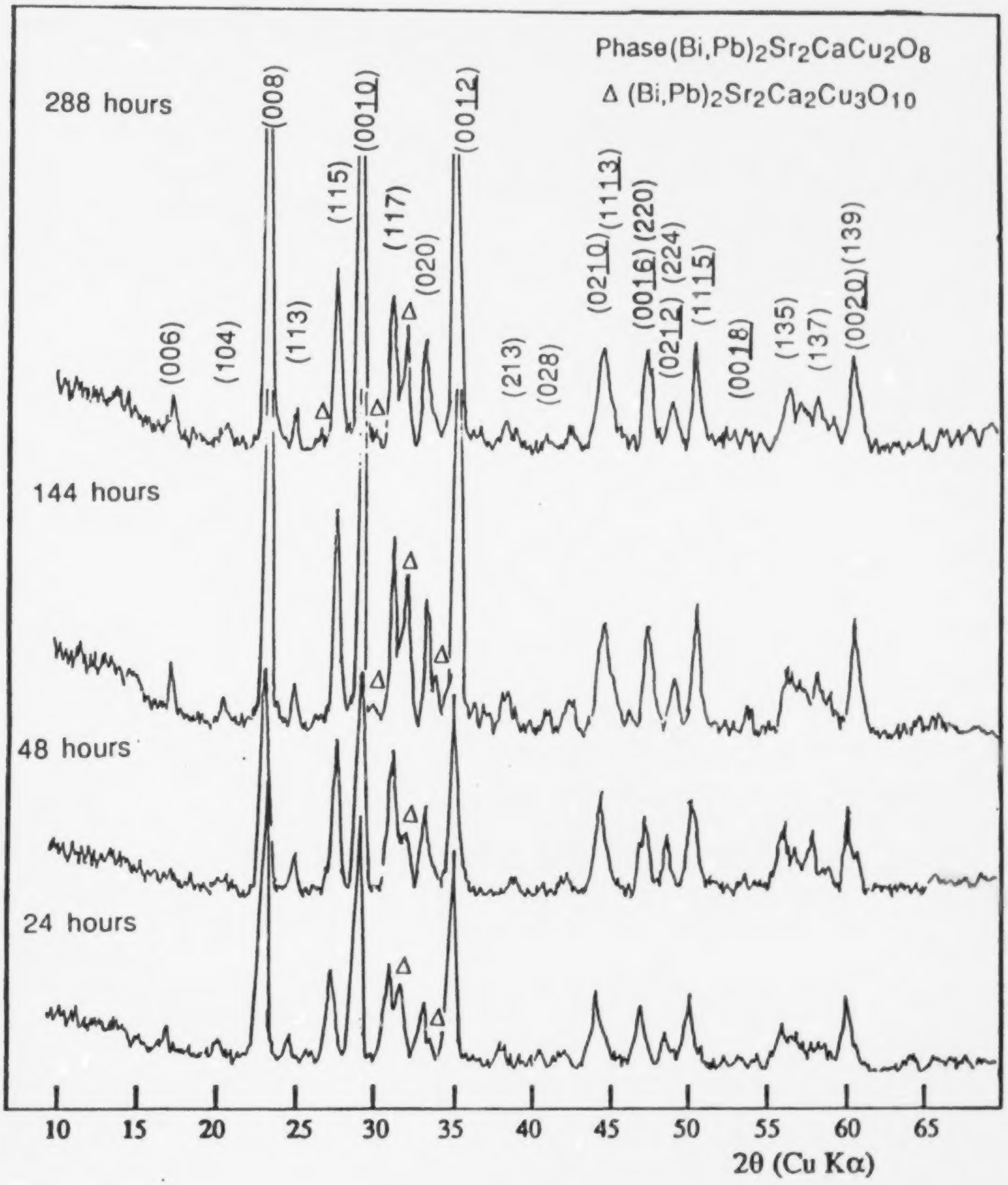

Fig. 4.15 X-ray diffraction patterns of gel(b) pellets heat-treated at 830°C for increasing times.

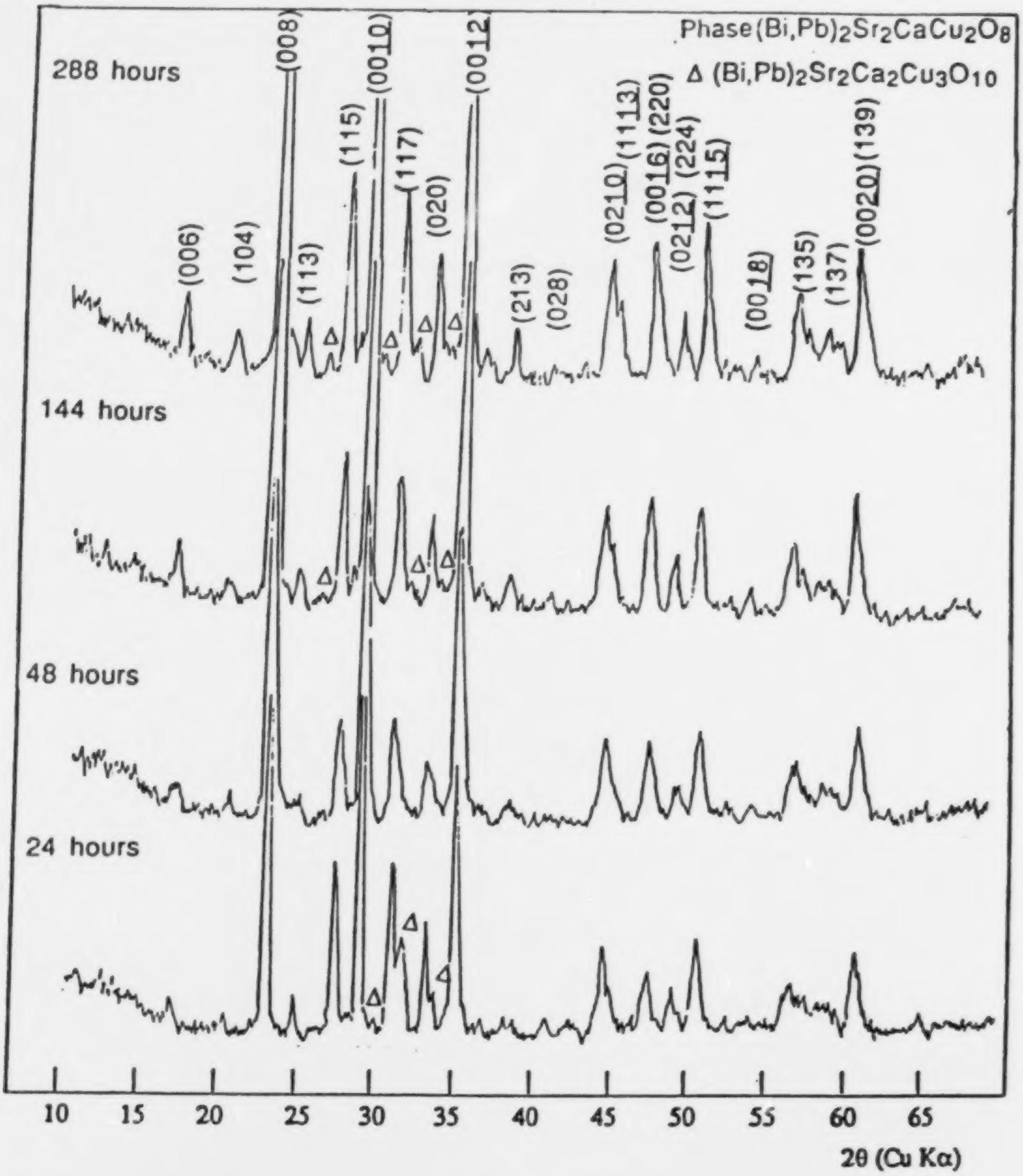

Fig. 4.16 X-ray diffraction patterns of gel(c) pellets heat-treated at 830°C for increasing times.

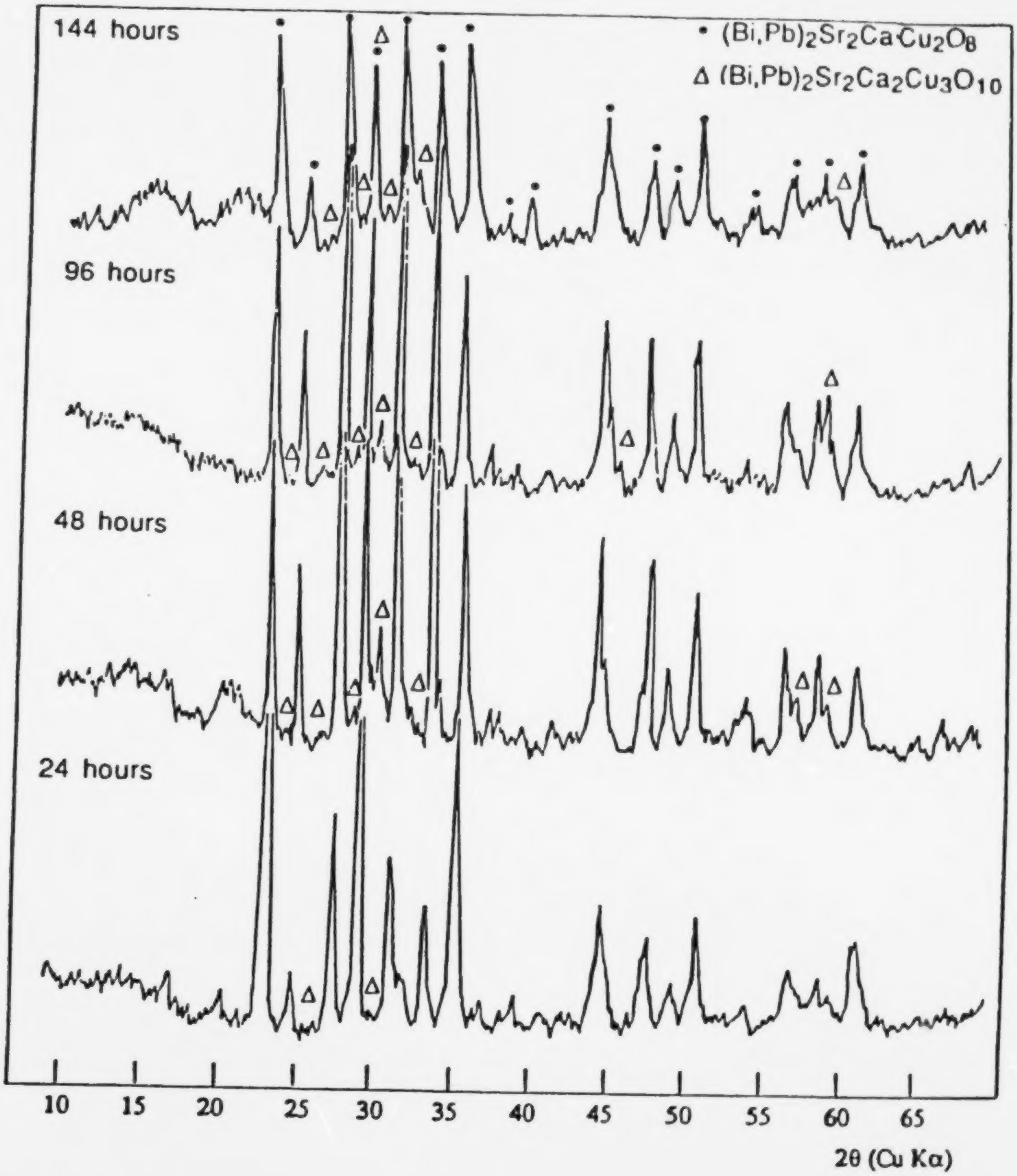

Fig. 4.17 X-ray diffraction patterns of gel(a) pellets heat-treated at 845°C for increasing times.

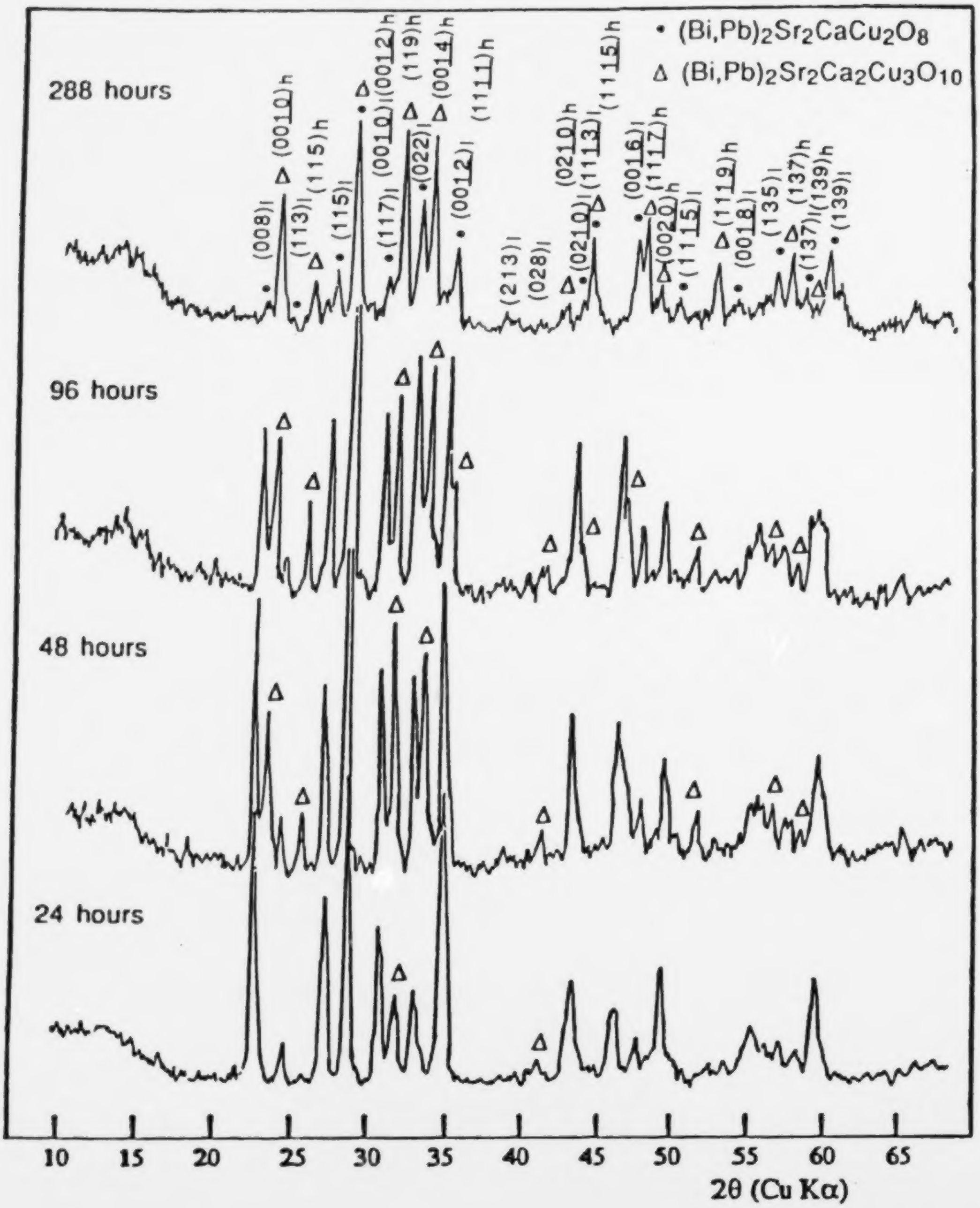

Fig. 4.18 X-ray diffraction patterns of gel(b) pellets heat-treated at 845°C for increasing times.

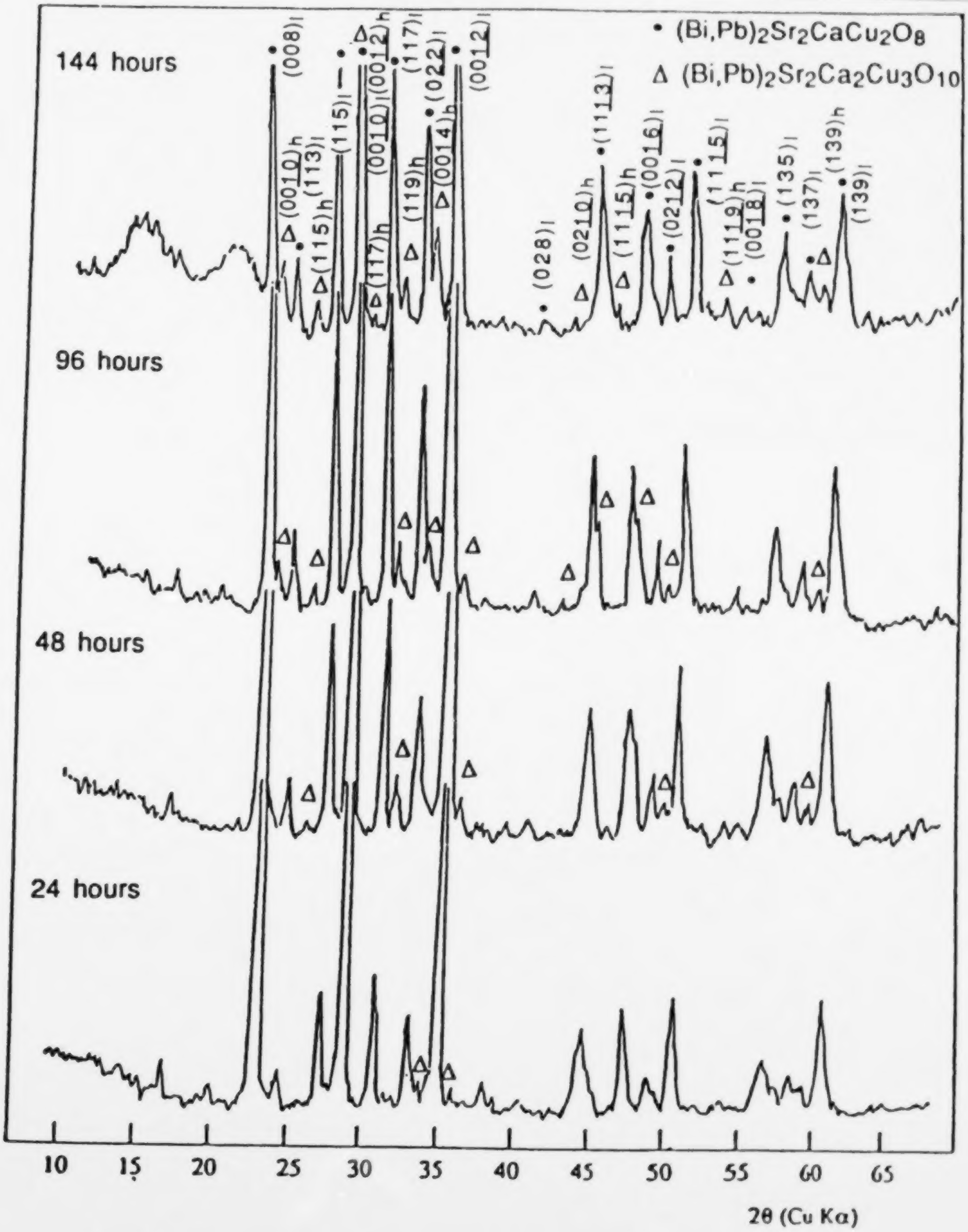

Fig. 4.19 X-ray diffraction patterns of gel(c) pellets heat-treated at 845°C for increasing times.

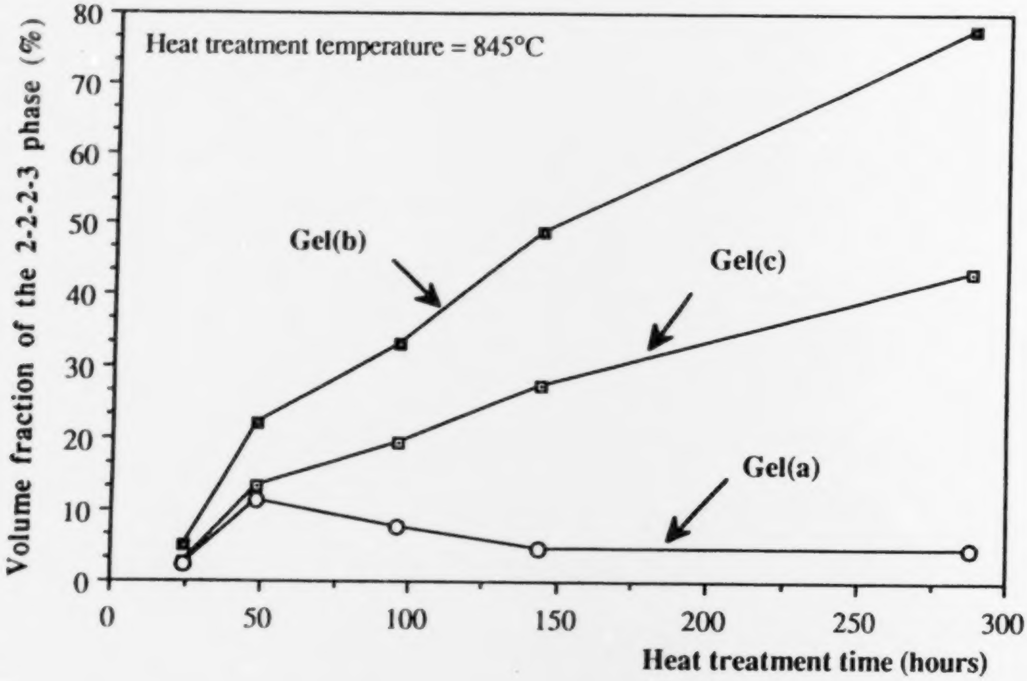

Fig. 4.20 Estimation of the 2-2-2-3 phase volume fraction at 845°C by the ratio of $I_h(0010)/I_h(0010)+I_l(008)$ from X-ray powder diffraction data.

4.3) SUPERCONDUCTOR PELLET'S MICROSTRUCTURE

4.3.1) Sintering behaviors

The bulk density evolution of the three superconductors, with time, is shown in Fig.4.21 for gel(a), (b) and (c) superconductors heat treated at 815, 830, and 845°C. The measurement errors were of the order of 5%. At 815°C, the trend is similar for all three materials. The density increases markedly during the first 24 hours, then it reaches a relatively stable value (Fig.4.21(a)).

At 845°C, the trend is also similar for all three superconductors. However, it differs drastically from what is observed at 815°C. After increasing during the first 24 hours, the density decreases steadily during further heat treatment (Fig.2.41(c)). The sample had swelled, and could even not keep the original shape after 288 hours heat treatment.

At 830°C, the superconductors show a densification behavior intermediate between what is observed at 815 and 845°C. While the gel(a) samples still show the same pattern of densification as at 815°C (increase to a stable density in the first 24 hours), the gel(b) and (c) samples with Pb already show an evolution similar to what was observed at 845°C (steady decrease after 24 hours).

At 860°C, with all materials, the shapes of the samples were rapidly distorted, and their density decreased rapidly with time while it became difficult to measure because of a lack in consistency.

In any case, a 24 hour heat treatment seems to be optimum. Fig.4.22 shows the relationship between the density after this time, and the heat treatment temperature. For the three materials, the densities attained are relatively stable, or falls moderately, up to 845°C. However, they drop drastically at higher temperature, for instance, at 860°C.

The evolution of pore structure with heat treatment time at 845°C, according to nitrogen adsorption by the BET method, are reported on Fig.4.23. The specific area increases with time (Fig.4.23(a)), while the average pore radius decreases (Fig.4.23(b)). This is an indication that a fine structure developed such as, for instance, fine platelike grains or fine slit like pores.

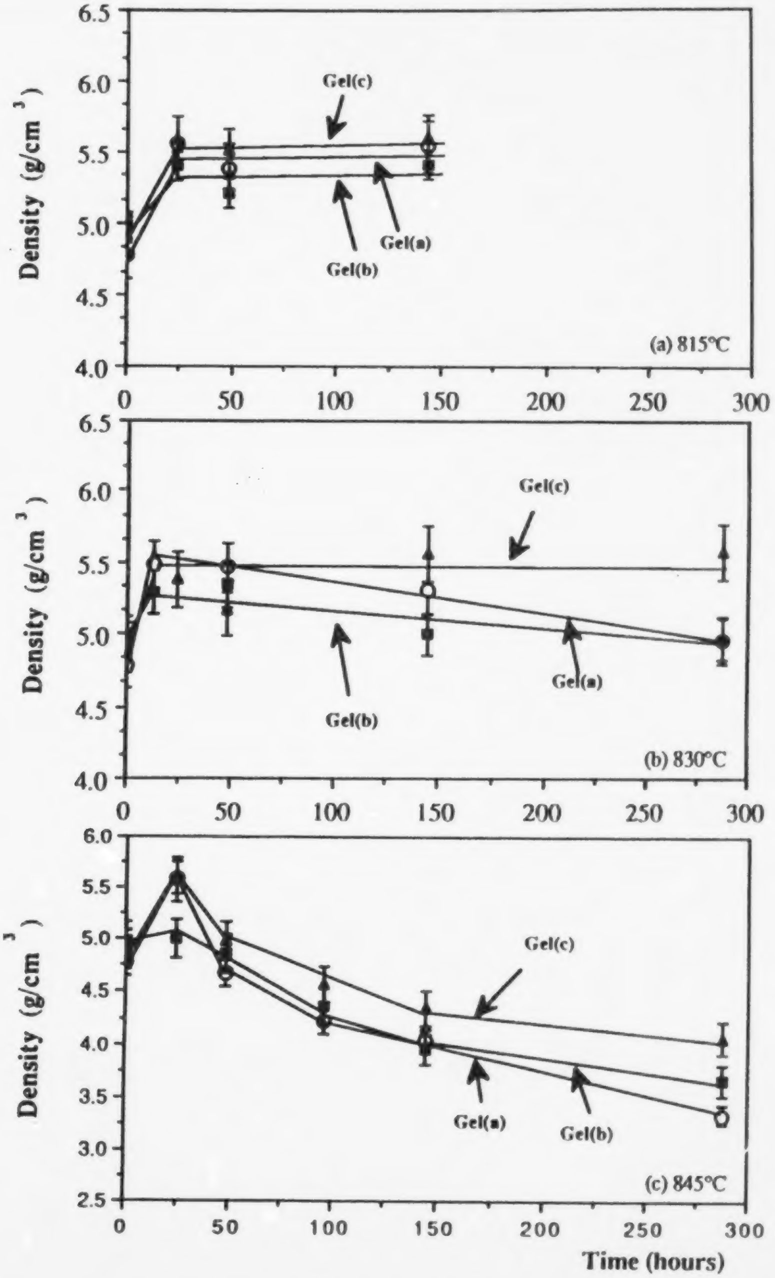

Fig. 4.21 Evolution of bulk density of samples with time at: (a) 815°C, (b) 830°C, (c) at 845°C

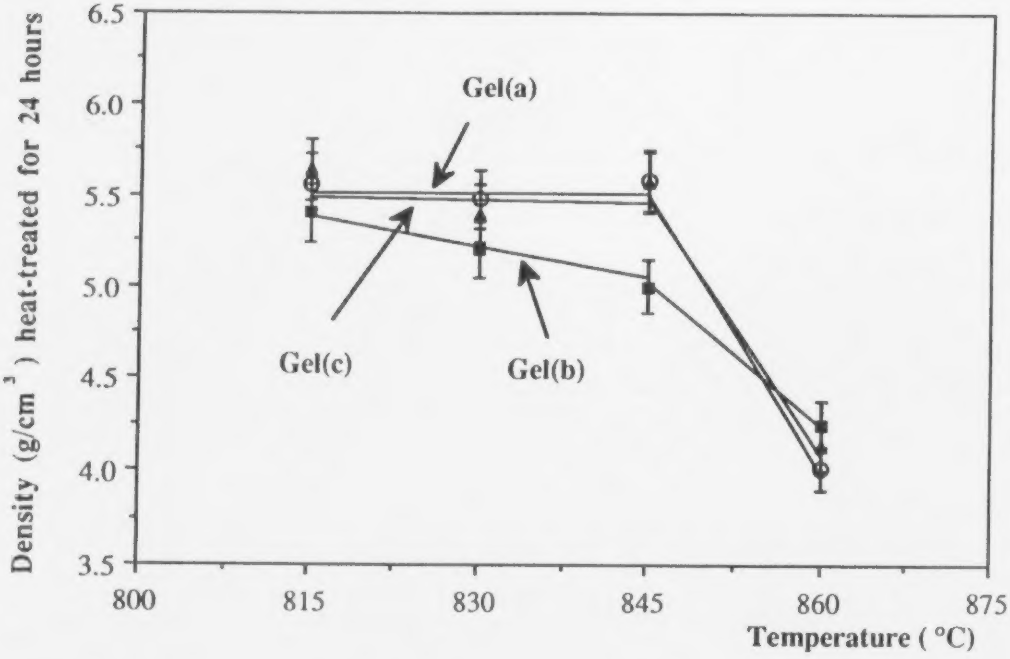

Fig. 4.22 Evolution, with temperature, of the bulk density attained after 24 hours heat treatments for the 3 superconductors.

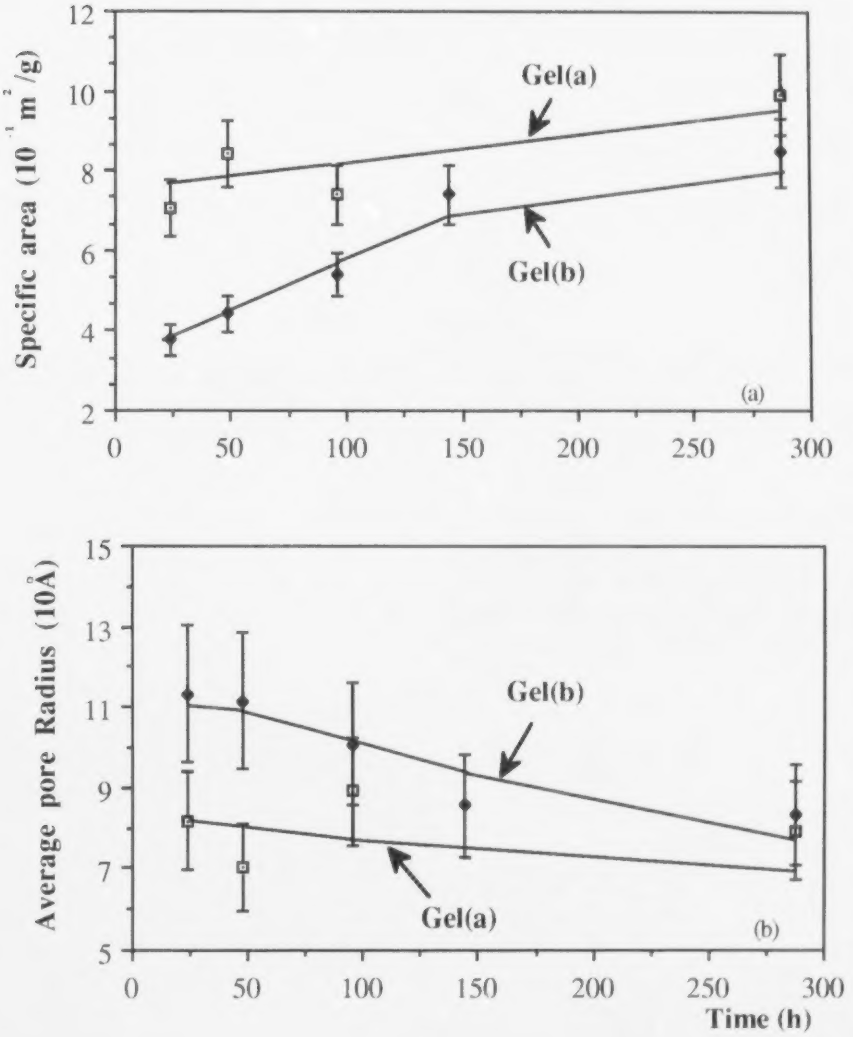

Fig. 4. 23 Pore structure evolution during heat treatment at 845°C, for gel (a) and (b) superconductors: (a) specific surface area; and (b) average pore radius.

4.3.2) Microstructure observation under the SEM

The mircostructural observations under the SEM show three types of different particularities, like on Fig.4.24 which concerns a gel(c) superconductor heat treated at 845°C for 144 hours. They comprise: (A) distorted platlike grains; (B) fine and straight platelike grains; (C) pores with heterogeneities. The EDAX spectrums (A), (B), (C), and (D) on Fig.4.24 correspond to the composition distributions of area (A), (B), (C), and average distribution from the complete sample surface, respectively. They indicate the distorted platelike grains A and straight platelike grains B can be considered to be the 2-2-1-2 and the 2-2-2-3 phase, which is in agreement with previous suggestions by Gao, et al.[76, 123]. Area C, on Fig. 4.24, is a pore with a coating very rich in calcium, and containing some copper. However it is almost devoid of lead and bismuth.

The straight platelike grains seem to form as a result of a cooperative cleavage inside bigger 2-2-1-2 domains. This cleavage proceeds on a finer and finer scale. It ends up providing straight grain nucleus as illustrated on Fig. 4.25. Then these nuclei undertake growth and become thicker and longer (Fig. 4.26). However, when both cleavage and growth proceeded concurrently, the particle distinction, between the "distorted" and "straight" platelike grains, was ambiguous in may instances. For identical after heat treatment at 845°C for 144 hour, the straight platelike grains are more abundant in gel(b) samples than that in gel(c) samples, while neither the straight nor the distorted platelike grains are still very developed in gel(a) superconductors (Fig. 4.26). These SEM observations are therefore in agreement with the X-ray diffraction data.

The following figures show the microstructure evolution depends largely on the sample composition. Fig. 4.27(a) and (b) show the microstructures of gel(b) superconductors heat treated at 815°C for 24 and 144 hours respectively, in which only the distorted platelike grains are present. Fig. 4.28 and 4.29 show microstructures of gel(b) and (c) heat treated at 830°C for increasing times respectively. The major phase is 2-2-1-2 in Fig. 4.29 for all cases, while the fine straight platelike grains are quite abundant in Fig. 4.28(c) and (d) which is from gel(b) samples heat treated for 144 and 288 hours. The microstructure evolutions with time, in gel(a), (b), and (c) superconductors at 845°C, are illustrated on Fig. 4.30, 4.31, and 4.32, respectively. The grains in gel(a) samples are quite small and platelike are not well developed even after 288 hour heat treatment (Fig. 4.30). On the contrary, the platelike grains have developed extensively in gel(b) and (c) samples (Fig. 4.31 and 4.32).

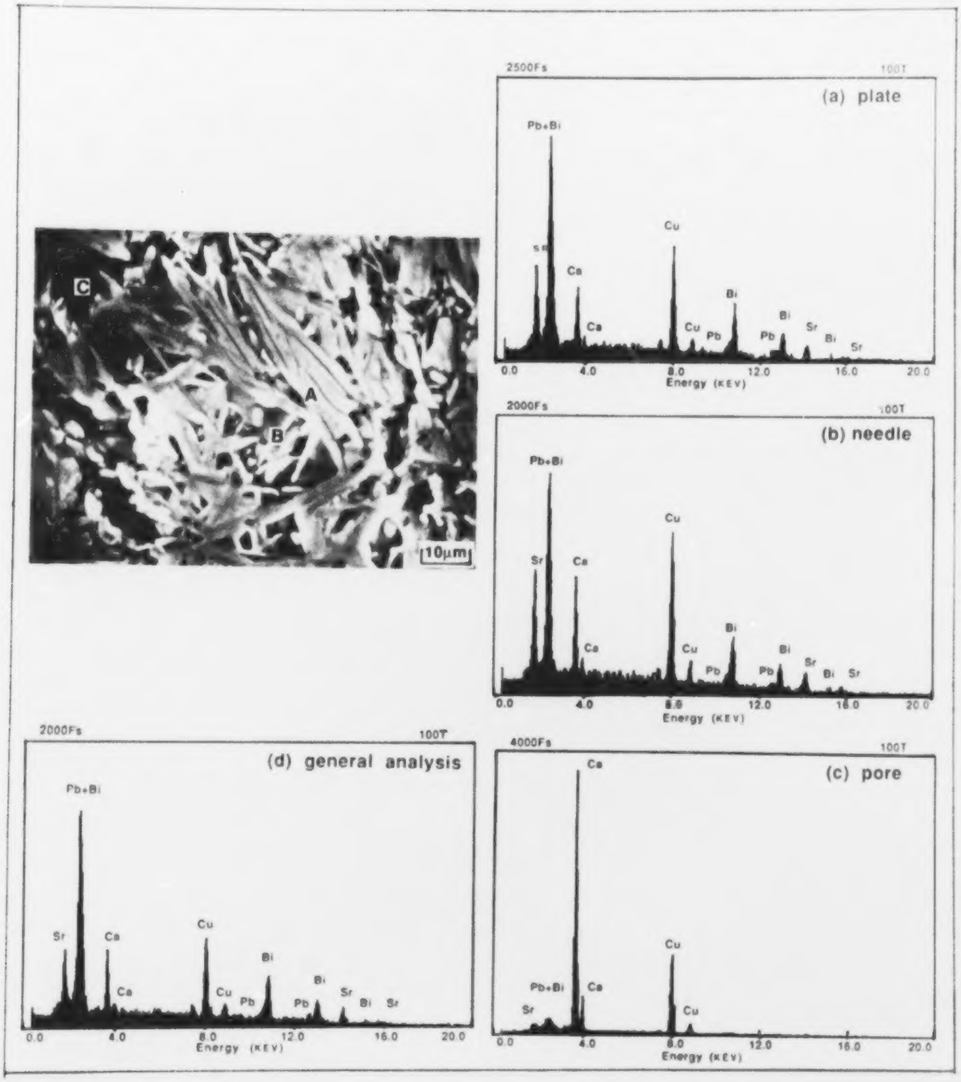

Fig. 4.24 Scanning electron micrograph and semi-quantitative EDAX analysis of a gel(b) superconductor heat-treated at 845°C for 144 hours.

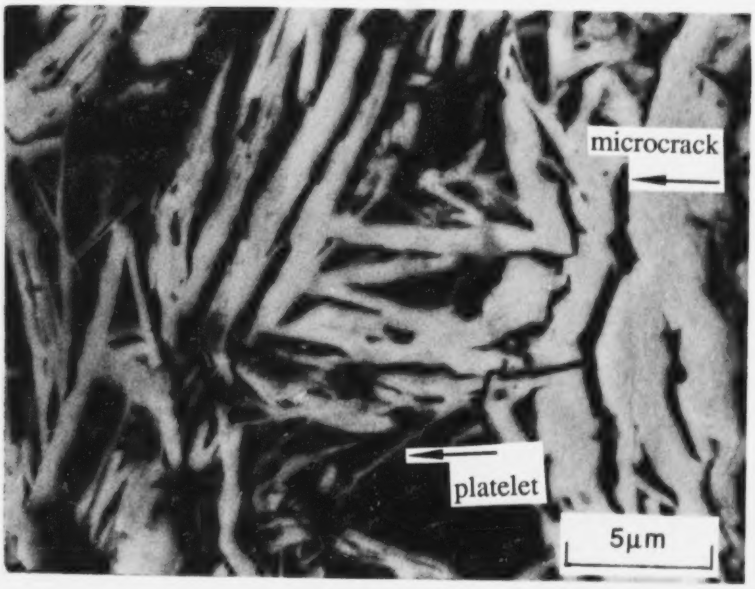
microcrack
platelet
5μm

Fig. 4.25 Formation of slit shaped microcracks inside a gel(c) superconductor heat treated at 830°C.

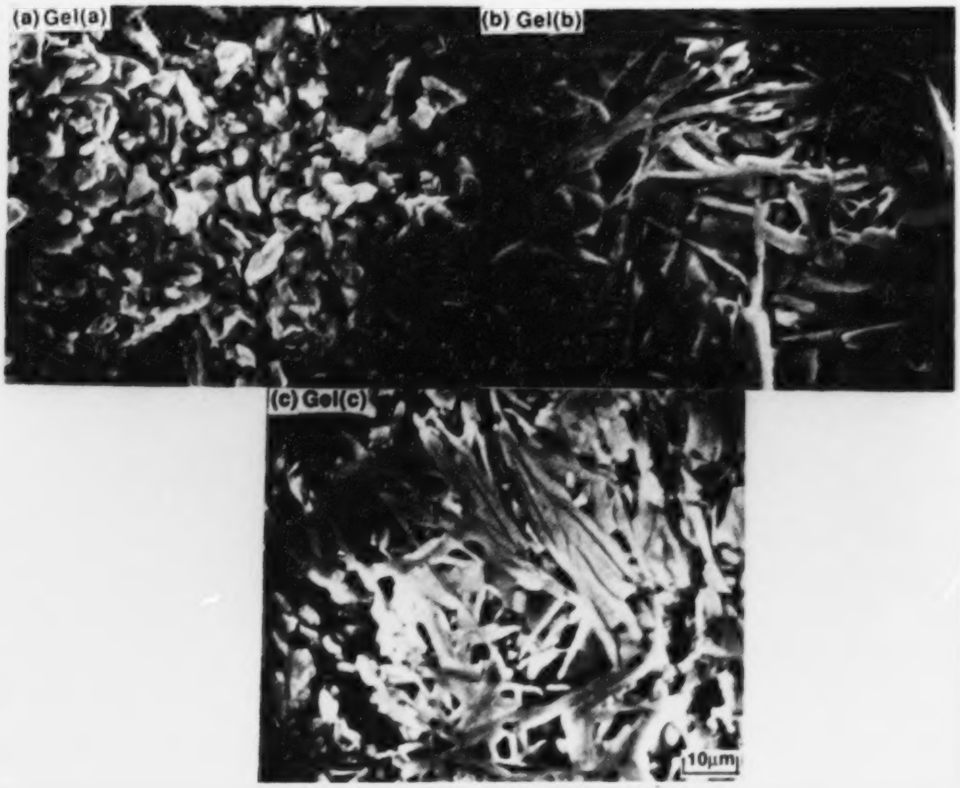
(a) Gel(a)
(b) Gel(b)
(c) Gel(c)
10μm

Fig. 4.26 SEM micrographs of gel(a), (b) and (c) superconductor pellets after 144 hours heat-treatment at 845°C.

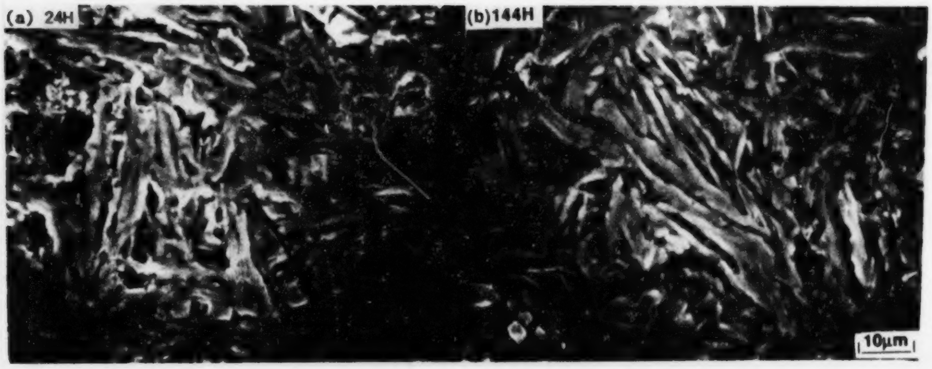

Fig. 4.27 Evolution of the microstructure under the SEM, for gel(b) superconductor pellets heat treated at 815°C for: (a) 24 h; (b) 144 h.

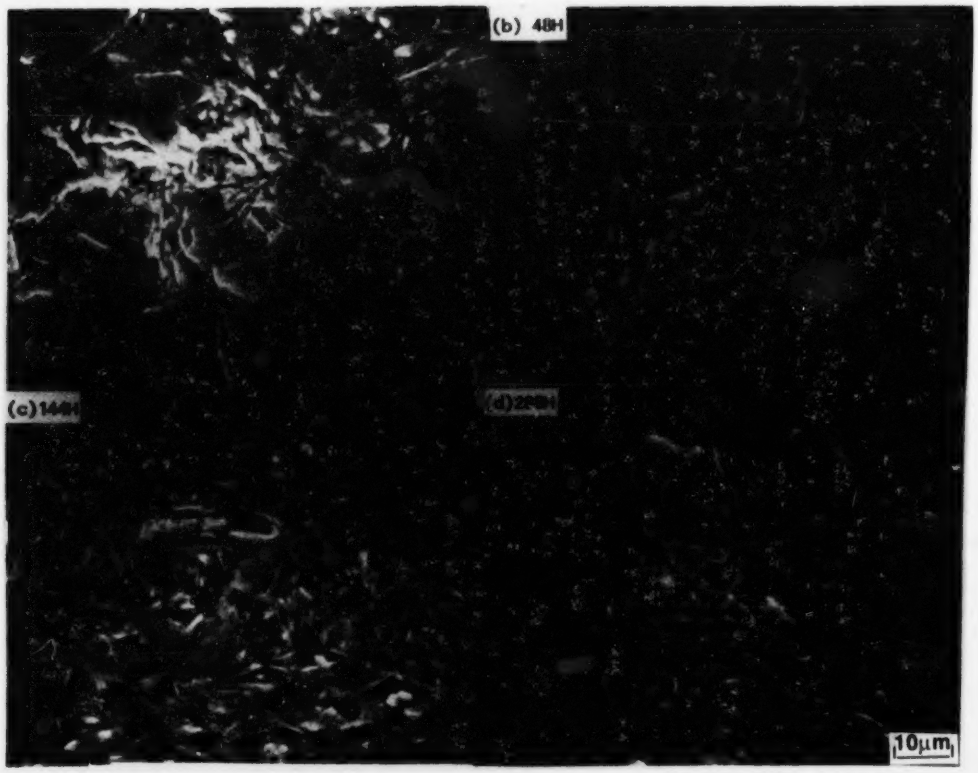
(b) 48H
(c)144H
(d)288H
10μm

Fig. 4.28 Evolution of the microstructure under the SEM, for gel(b) superconductor pellets heat treated at 830°C for: (a) 24 h; (b) 48 h; (c) 144 h; (d) 288 h.

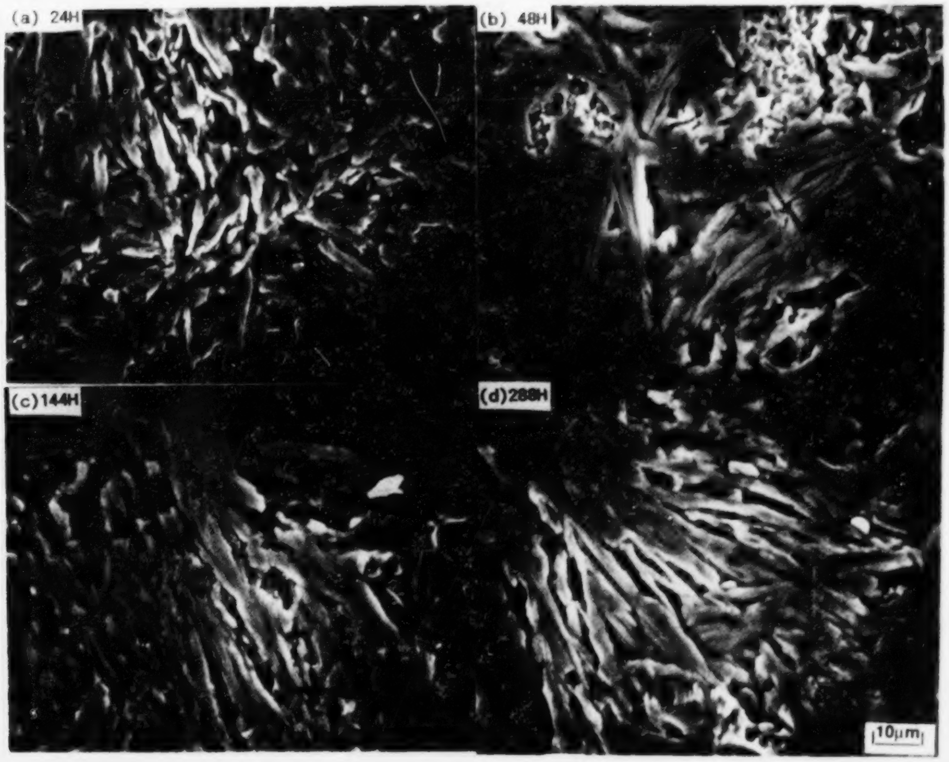
(a) 24H
(b) 48H
(c)144H
(d)288H
10μm

Fig. 4.29 Evolution of the microstructure under the SEM, for gel(c) superconductor pellets heat treated at 830°C for: (a) 24 h; (b) 48 h; (c) 144 h; (d) 288 h.

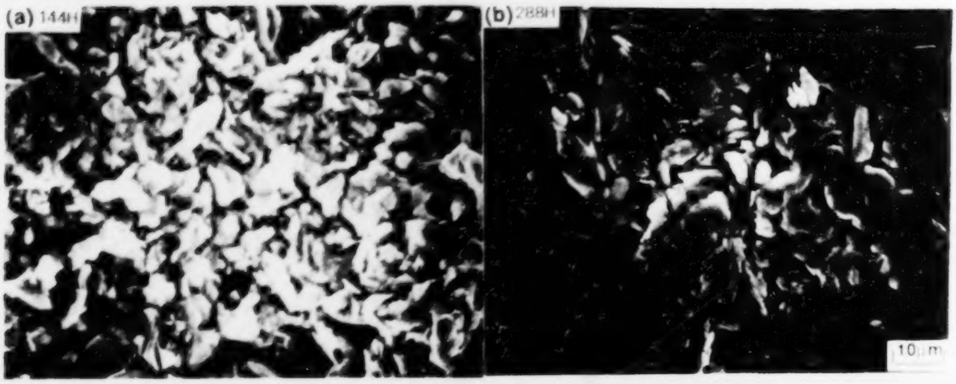
(a) 144H
(b) 288H
10μm

Fig. 4.30 Evolution of the microstructure under the SEM, for a gel(a) superconductor pellets heat treated at 845°C for: (a) 144 h; (b) 288 h.

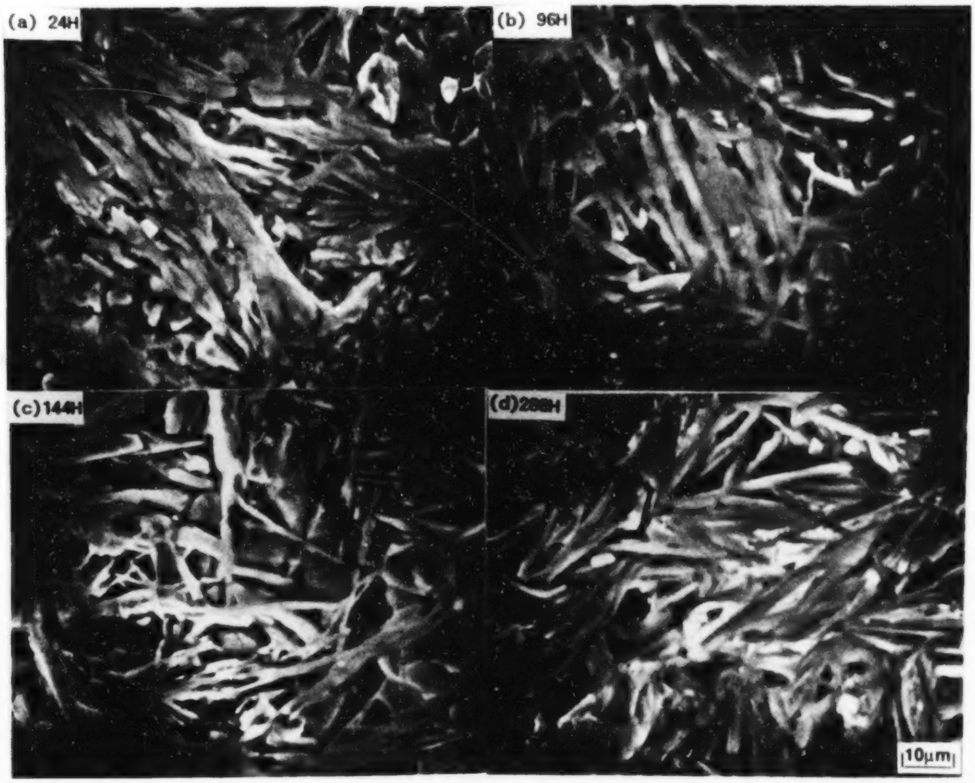
(a) 24H
(b) 96H
(c)144H
(d)288H
10μm

Fig. 4.31 Evolution of the microstructure under the SEM, for a gel(b) superconductor pellets heat treated at 845°C for: (a) 24 h; (b) 96 h; (c) 144 h; (d) 288 h.

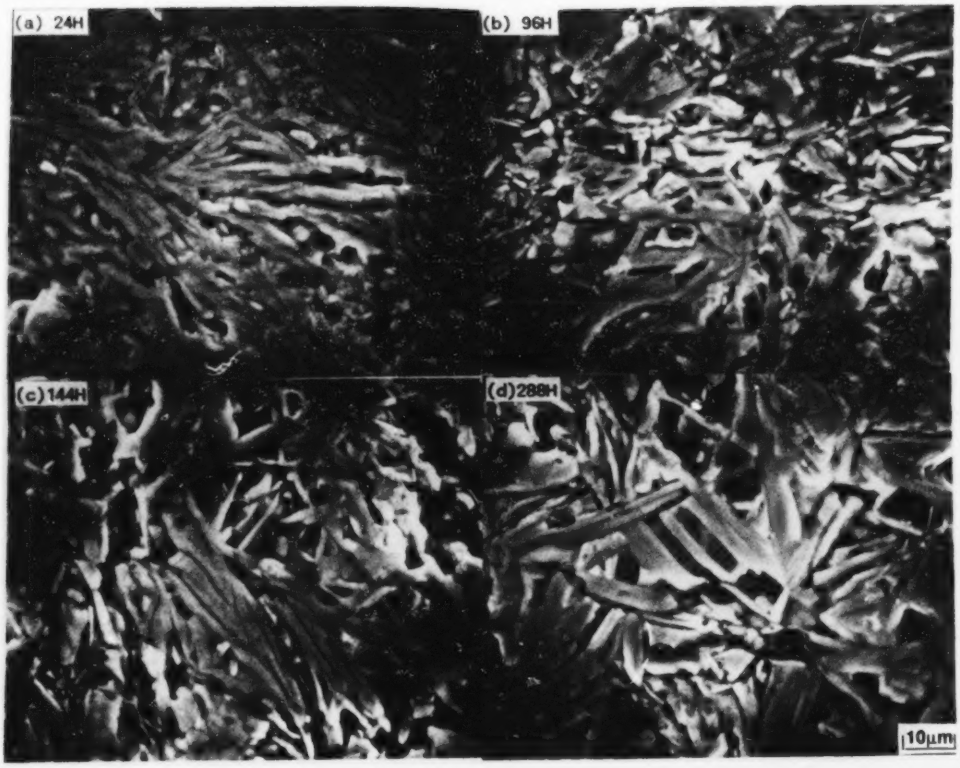
(a) 24H
(b) 96H
(c)144H
(d)288H
10μm

Fig. 4.32 Evolution of the microstructure under the SEM, for a gel(c) superconductor pellets heat treated at 845°C for: (a) 24 h; (b) 96 h; (c)144 h; (d) 288 h.

4.3.3) Grain growth and Oriented microstructure

In cases where the 2-2-1-2 phase was by far the major, it is possible to estimate an average grain size simply. The average grain size grows both with time and temperature, as shown on Fig. 4.33(a) for gel(c). The average grain sizes of gel(a), (b) and (c) samples at the initial point of heat treatment (heat treatment time = 0) were estimated from the B.E.T. specific area data of powders after calcined at 800°C, using the theoretical density $\rho = 6.11 g/cm^3$ of the 2-2-1-2 phase.

With gel(a) superconductors at 815°C, the grain size is too small to be measured. In gel(b) at 830 and 845°C, the 2-2-2-3 phase is no longer negligible after long heat treatment times. However, due to difficulty in discriminating with a certitude between the 2-2-1-2 and 2-2-2-3 phases, the average grain sizes have been measured as if only one phase was present (Fig. 4.33). Interestingly, the growth kinetics remain quite similar with superconductors containing Pb. The grains are noticeably bigger with the gel(b) and (c) superconductors, which contain some lead, than that with the gel(a), without lead.

The average grain sizes vs time data have been plotted on a Log-Log scale, on Fig. 4.34. They fit quite well with a simple law of the type

$$D^n = Kt \qquad (4.1)$$

where D is the average grain size at time t, n is a dimensionless exponent and K is a rate constant. The values of n, determined by a regression results are listed in Table. 4.1. It turns out that for gel(b) and (c) superconductors, the data seem to fit a grain growth mechanism for which $n \approx 2.9$ at all temperatures(from 815 to 845°C). The gel(a) superconductors seem somewhat different , the value of n are higher, up to 7.73, at 830°C.

It has been mentioned before that the major diffraction lines could be indexed according to the 2-2-1-2 phase. A marked enhancement of the (00l) peaks of the 2-2-1-2 phase indicated a preferred orientation of the Cu-O layers in the plane of the pellets occurred during heat treatment. The degree of the preferred orientation, Q, was estimated by (2.16).

$$Q = 1 - \frac{I(115)}{I(0010)} \Big/ \frac{I_0(115)}{I_0(0010)} \qquad (2.16)$$

The results are shown in Fig.4.35. The gel(a) samples shows no preferred orientation. But the orientation degrees of the gel(b) and (c) samples increase markedly, up to 35%, after the first 48 hours heat treatment at 815°C. Then it remains relatively constant during further heat treatment (Fig.4.35(a)). The orientation degree increases almost linearly, up to over 35%, for the gel(c) samples heat treated at 830°C (Fig.4.35(b)).

Table. 4.1 Estimate of n, from the data on grain growth

Sample No#	Temperature (°C)	n	K
gel(b)	815	2.95	1.23
gel(b)	845	2.68	4.38
gel(c)	815	2.86	0.93
gel(c)	830	2.97	1.14
gel(c)	845	2.74	4.38
gel(a)	830	7.73	69.4
gel(a)	845	4.53	3.70

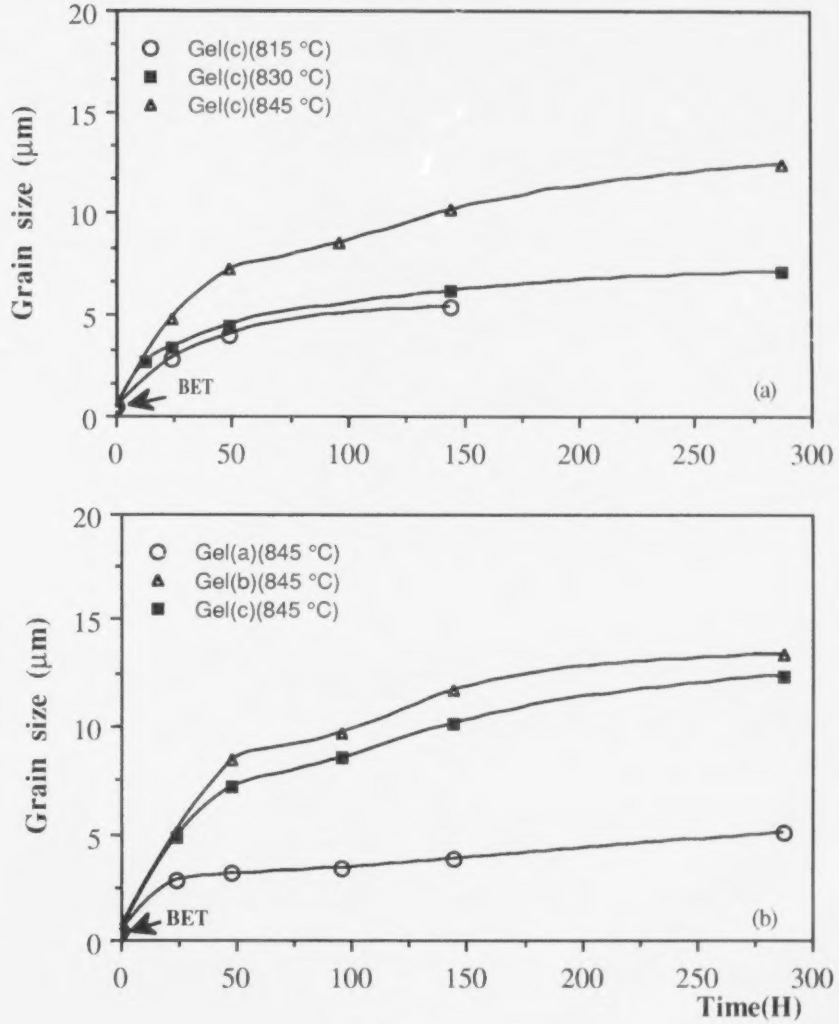

Fig. 4.33 Grain growth kinetics in superconductors: (a) gel(c) superconductors at different temperature; (b) gel(a), (b), and (c) superconductors at 845°C.

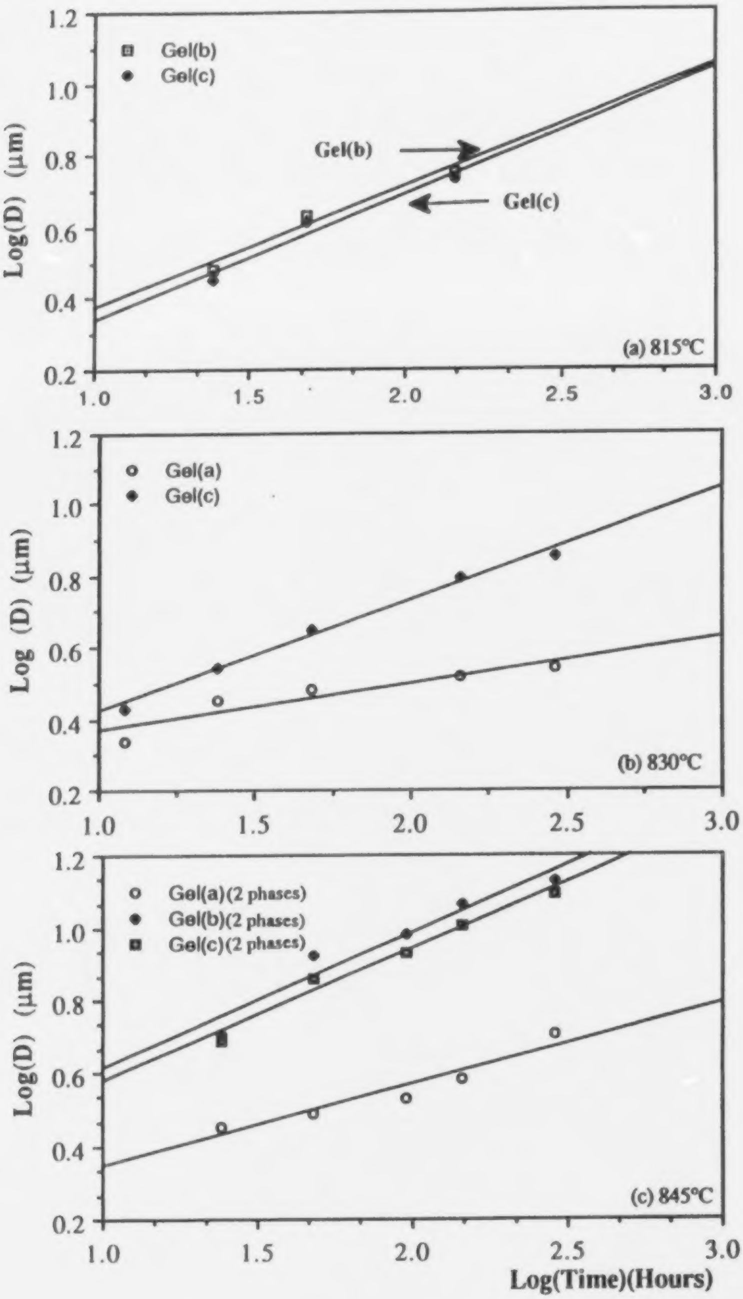

Fig. 4.34 Grain growth data plotted with log(D) as a function of log(t).

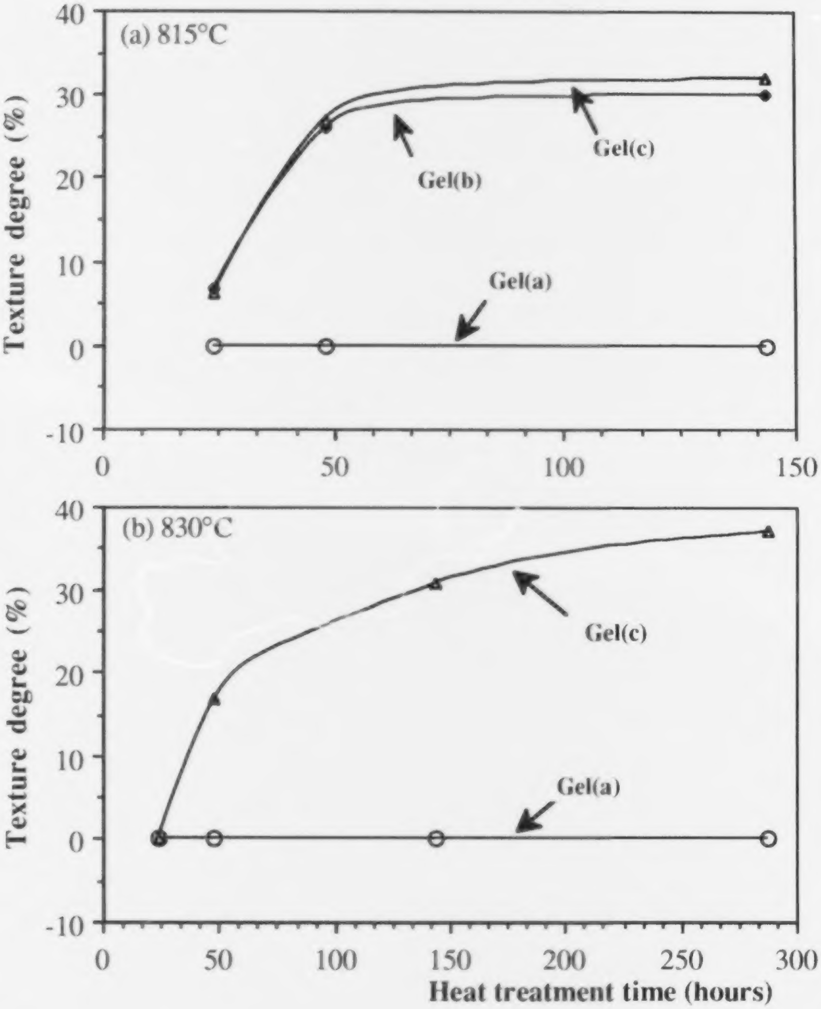

Fig. 4.35 Estimate of the orientation degree of superconductor pellets from by X-ray diffraction pattern; (a) at 815°C; (b) at 830°C.

4.4) CRITICAL TEMPERATURE, $T_{c,0}$

The data on resistance versus temperature, down to liquid nitrogen temperature, are reported on Fig. 4.36 to Fig. 4.41. The critical temperatures of different samples are listed on Table.4.2. It is above 100K for all samples where the 2-2-2-3 phase was in sufficient proportion, that is to say the superconductors containing some lead and heat treated at 845°C for more than 96 hours.

Table. 4.2 Critical temperature ($T_{c,0}$) where the resistivity cancels, for gel(a), (b), and (c) superconductors

sample No#	Heat treatment Temperature (°C)	Heat treatment time (hours)	$T_{c,0}$ (K)
gel(a)	845	144	89
gel(b)	845	96	106
gel(b)	845	144	107.6
gel(c)	830	144	79.8
gel(c)	845	144	103.2
gel(c)	845	288	106.8

$T_{c,0}$ improves also with the heat-treatment time, that is to say the 2-2-2-3 phase proportion. And it is slightly higher in gel(b) with initial composition 1-1-1-2, where a higher proportion of the 2-2-2-3 phase has formed than in gel(c) with initial composition 2-2-2-3.

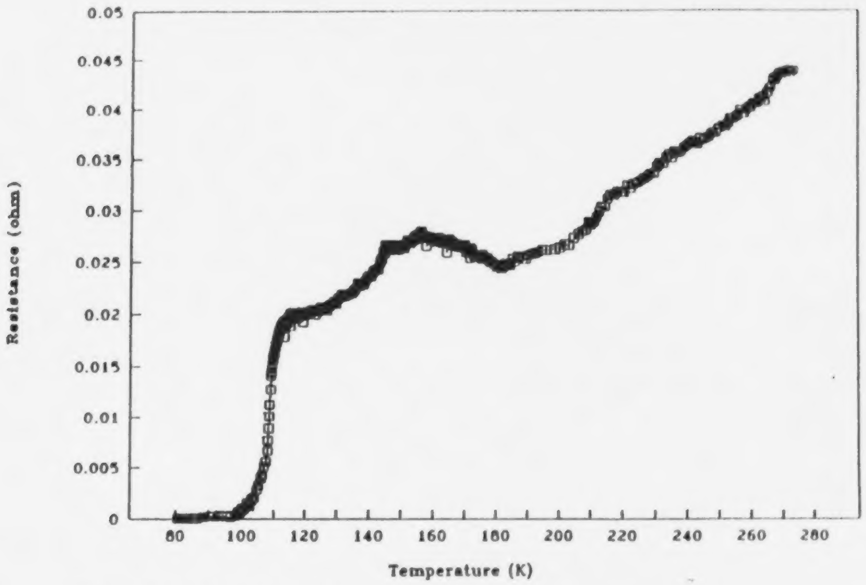

Fig. 4.36 Variation of the resistance with temperature for the gel(a) sample sintered at 845°C for 144 hours

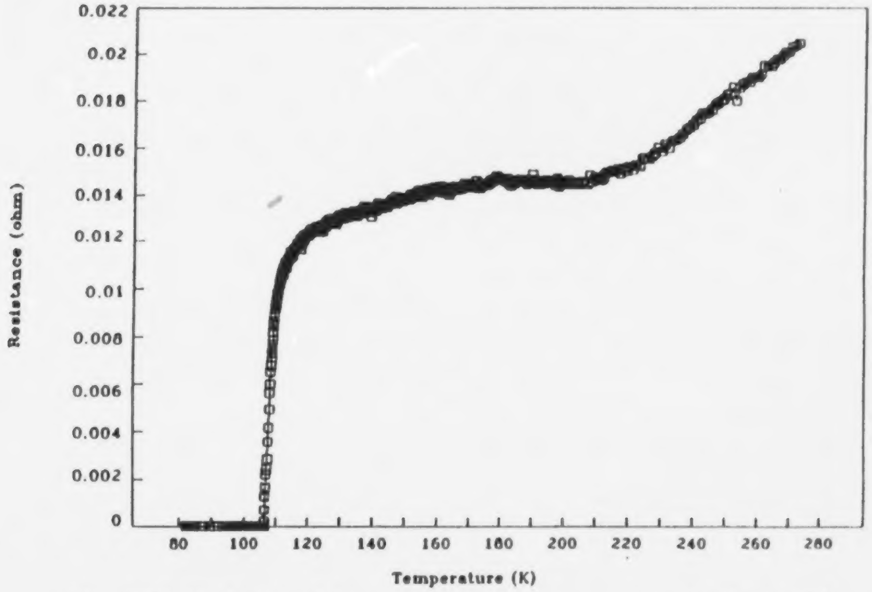

Fig. 4.37 Variation of the resistance with temperature for the gel(b) sample sintered at 845°C for 96 hours

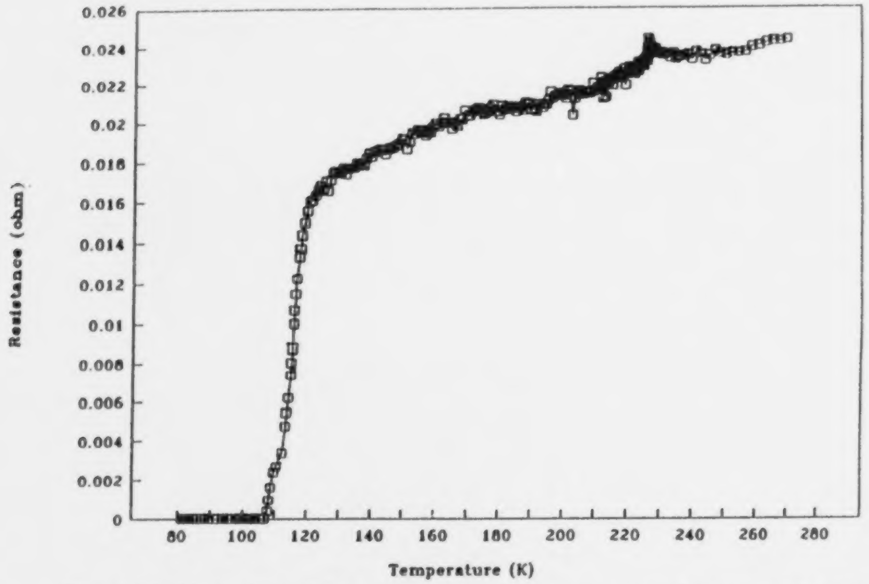

Fig. 4.38 Variation of the resistance with temperature for the gel(b) sample sintered at 845°C for 144 hours

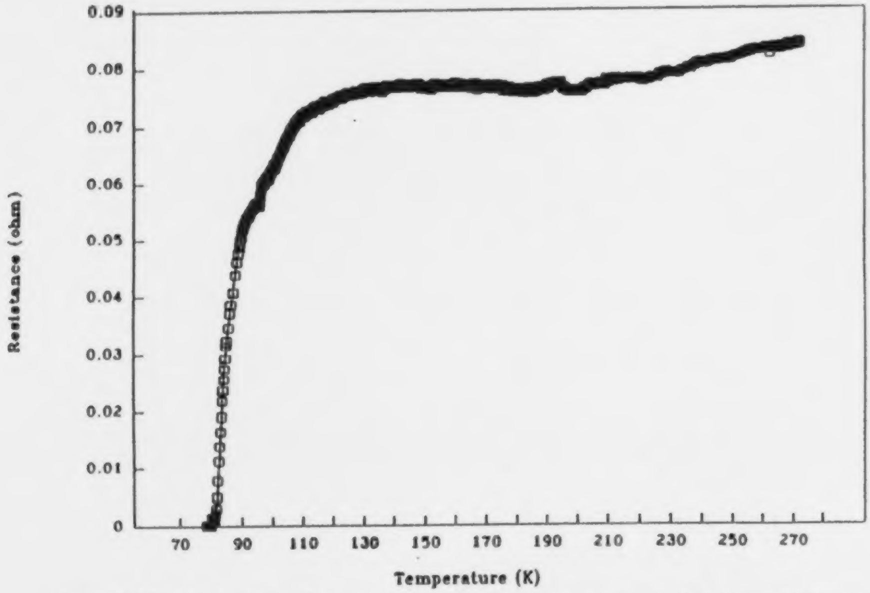

Fig. 4.39 Variation of the resistance with temperature for the gel(c) sample sintered at 830°C for 144 hours

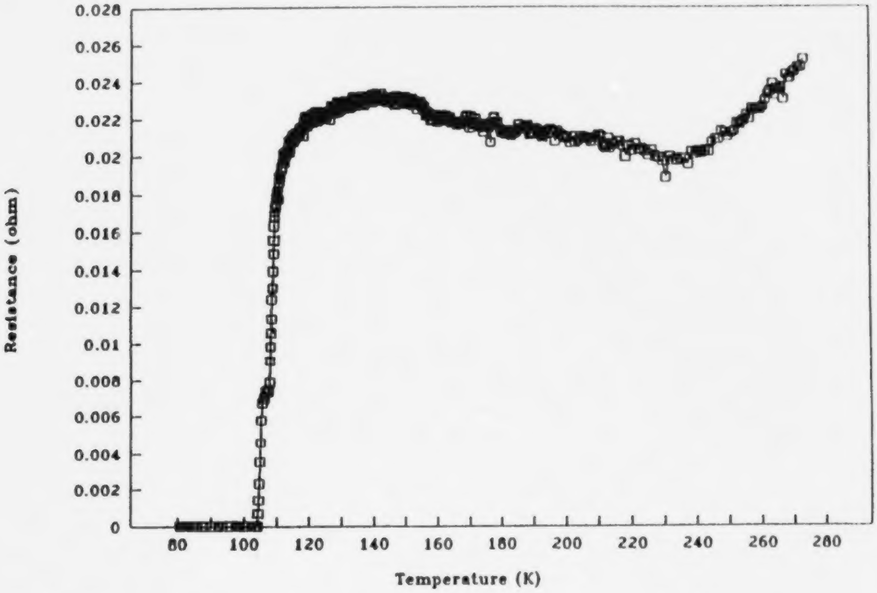

Fig. 4.40 Variation of the resistance with temperature for the gel(c) sample sintered at 845°C for 144 hours

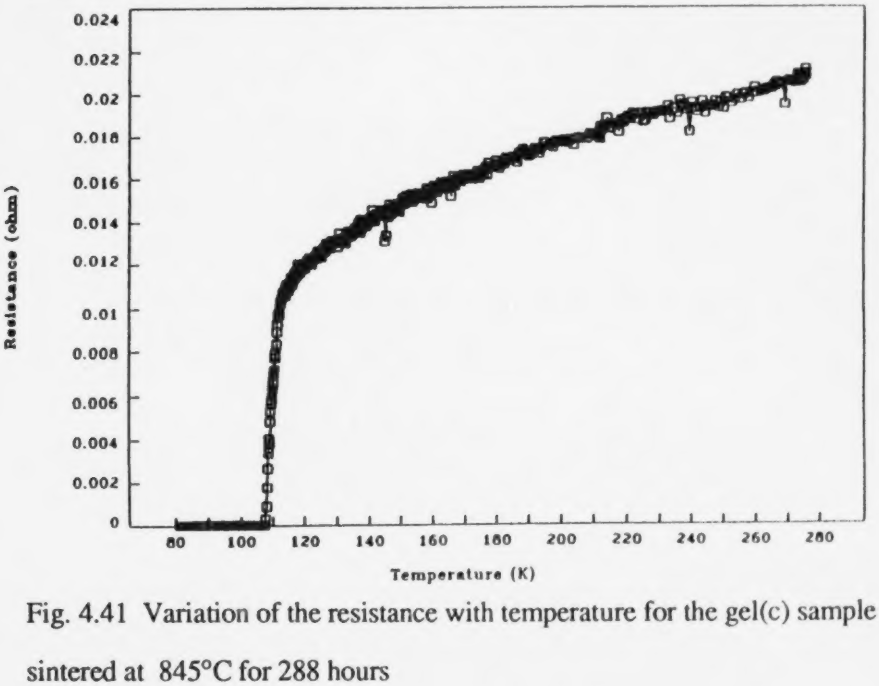

Fig. 4.41 Variation of the resistance with temperature for the gel(c) sample sintered at 845°C for 288 hours

CHAPTER 5: DISCUSSION

5.1) GELATION AND ULTRASTRUCTURE OF GELS

It is basic requirement for sol-gel processing that precursors should be soluble in a suitable solvent. This is not the case with Cu alkoxides. Other soluble inorganic or organic copper compounds have therefore to be chosen. However, the nature of precursors is known to play an important role in the nature of phases formed and properties of materials. Previous researches in this group, have been achieved copper oxide gels from two types of precursors, the cupric nitrate and the cupric acetate[169.3]. It is not surprising that the Bi-(Pb)-Sr-Ca-Cu-O gels, which have been synthesized successfully in this experiment by complexation of mixtures of nitrates by critic acid and ammonia, show common properties with hydrous copper oxide gels in the previous work[150, 169.3].

During the sol-gel processing of superconductors in the Bi-(Pb)-Sr-Ca-Cu-O system, the Bi, Pb, Sr, Ca, Cu cations build independent solvated mononuclear complexes with p water molecules, according to reaction of the type

$$M^{n+} + pH_2O \rightarrow [M(H_2O)_p]^{2+} \qquad (5.1)$$

where M represents the different cations.

These mononuclear species condense in polynuclear complexes with structures and properties depending on the ligands, cation, pH, temperature, and more generally on all the chemical processing parameters. With water molecules and anions, A, the classical mechanism described by Baes and Mesmer[170] rests on a succession of bimolecular reactions including deprotonation (reaction (5.2)) and polymerization, which can be summarized by the reaction (5.3):

$$[M(H_2O)_p]^{n+} \rightarrow M(H_2O)_{p-1}(OH)^{(n-1)+} + H^+ \qquad (5.2)$$

$$xM(H_2O)_n^{z+} + yOH^- + aA^- \leftrightarrow$$
$$M_xO_u(OH)_{y-2u}(H_2O)_wA_a^{(xz-y-a)+} + (xn + u - w)H_2O \qquad (5.3)$$

A key question is to know if mixed condensation, that is to say the building of polynuclear complexes including the 5 cations in the Bi system superconductors, can be achieved. According to the titration curves shown in Fig. 4.2, complexation reactions occur when citric acid is added into the cation aqueous solutions, leading to a process of gelation instead of precipitation when drying is performed. Because the equivalence point of each cation is replaced by a simple equivalence point, we can assume that polynuclear complexes of different elements have linked together. In other words, all precursors have made a single gel. The importance of citric acid in this gelation process is confirmed by the fact a molar ratio of citric acid at at least 2 must be added. If the ratio is too low, for example, 1, a precipitation occurs during drying at pH near 6. Ammonia also helps complexation, and the pH value around 7, selected for gelation corresponds to the new equivalence point. If the pH value is too high above or too low below 7, even with a citric acid to cations of 2, a precipitation also occurs. It is probable that mixing is not achieved at the atomic scale but at the scale of polynuclear complexes. However it shows that precursors as simple as the nitrates, with the help of carboxylic acids, offer quite interesting sol-gel routes.

One of the most distinctive characteristics of the gels made in this research, is similar to the results found in the copper oxides gels. They are composed of a solid network with non porous layers (Fig. 4.3). Consequently, once a layer of a gel has formed on the top of a sample by evaporation, water cannot leave any more and the underlying solution stops drying and gelling. If the temperature is increased, the tendency of water to vaporize increases and the gels swell, and can even explode. When the temperature is too high, for example, above 90°C, the gels starts also to melt and become black, which is in agreement with the formation of a black viscous cupric oxide[169.3].

Considering the high temperature superconducting phases in this system are extremely anisotropic and composed of platelike grains it would be interesting to maintain the lamellar appearance of these gels during further heat treatment. This could provide a preferred orientation of platelike grains in a sample, which could lead to the obtaining of superconductors with a high critical current density.

Like with the Cu gels, the main results of the heat treatment study up to 250°C of the complex blue gels are that: (1) their chemical composition changes progressively; (2) they undertake a progressive bloating destroying the lamellar structure; and (3) they can still redissolved in aqueous media after calcination below 250°C.

The first two results are well illustrated in Figs. 4.3 and 4.4. The main chemical transformations below 250°C consist in a progressive loss of water and nitrates. The departure of nitrates shows up by a change in color from blue to the black aspect of the superconductors, which coincides with the appearance of the CuO layers which will be so important for superconducting properties. The bloating behavior is a consequence of the gels lamellaes which are impervious, as indicated by a low specific surface ($0.69 m^2/g$ at 200°C). The gases resulting from the gels decomposition during heat treatment (H_2O, N_2O_3,CO_2) can not escape, and hence, bloating of the samples occurs. This bloating behavior during heat treatment is responsible for losing the main potential advantage of this sol-gel route: the lamellar structure. An original calcination treatment needs therefore to be designed.

Maybe the most important result in this respect, is the bloated black gels can be redispersed in an aqueous media. At 180°C, the residual nitric ions are sufficient to allow complete redissolution. With a temperature increasing progressively up to 250°C, the residual amount of nitrates decreases and the black solution is mixed with an increasing proportion of black particles of increasing size. These particles are crystalline while the remaining black solutions still dry to amorphous products. A very progressive nucleation and growth of a crystalline phase occurs therefore inside these gels. This is consistent with a complex gel not homogeneous at the atomic scale, but at the scale of polynuclear complexes. Above 250°C, the bloating black gels are no longer soluble, which is consistent with an extensive crystallization according to X-ray data, and coincides also with a very exothermic decomposition of the carbonated groups according to DTA data[163].

With respect to a tailoring of the grain configuration in superconducting materials, these black dispersions offer a broad range of possibilities. With the help of electrolytes and /or organic additives like ethylene glycol, they can themselves be gelled in colloidal gels which do not bloat anymore during further heat treatment. Hence, by studying this phenomenon in more detail, they might directly give superconductors with a much better aspect than the products obtained directly from the nitrates without redissolution.

5.2) PHASE TRANSFORMATIONS

It has been mentioned that the black gels are still quite amorphous after heat treatment at 220°C for 12 hours. In the light of the dissolution study, the polynuclear species of each cation linked by the citrate anions provide crystallization nuclei dispersed in an amorphous matrix.

At higher temperatures, the phase transformation requires diffusion. It has to proceed on short distances, but depends on the mobility of each cation and stability of polynuclear species. Our results show similarities with Paz-Pujalt's study in the ternary systems Bi-Sr-Ca, Sr-Ca-Cu, Bi-Ca-Cu, and Bi-Sr-Cu, and in the Bi-Sr-Ca-Cu-O system[69]. His results show that Bi_2O_3 and CuO should be formed at the initial stage. Then these two phases start to transform into $CuBi_2O_4$ at about 500°C. The phase diagram for system CuO-Bi_2O_3 indicates that the only two phases present are CuO and $CuBi_2O_4$ for the composition $2CuO\text{-}Bi_2O_3$ at 600°C[171]. In this sol-gel process, Bi_2O_3 was actually not detected and the main peaks correspond to $CuBi_2O_4$ and CuO at 400°C. Our sol-gel processing lowered therefore the formation temperature of $CuBi_2O_4$ by at least 100°C compared to conventional processing. The formation of this bimetallic oxide provides certain advantages; it diminishes the losses in bismuth which tends to evaporate after Bi_2O_3 melts (817°C). Also, it provides enhanced contact between the remaining reactants by becoming a liquid at 840°C.

$CuBi_2O_4$ disappears at 600°C while an $Sr_{1-x}Ca_xCO_3$ compound forms. The 2-2-0-1 low T_c phase starts to form at this temperature and continues to develop up to 750°C. Ca incorporates therefore progressively in $CuBi_2O_4$ while $Sr_{1-x}Ca_xCO_3$ disappears. At 750°C, $Bi_2Ca_2CuO_6$ is compatible with its symbiotic phase $Bi_2Sr_2CuO_6$ (the 2-2-0-1 phase). Mackrodt [172] has examined the stability of $Bi_2Ca_2CuO_6$ relative to that of the 2-2-0-1 phase. His results indicate that $Bi_2Ca_2CuO_6$ is less stable than the 2-2-0-1 phase with a difference of formation heat of 100KJ/mole. Therefore, it is not likely to remain. At this temperature, calcium is still present as a carbonate. The formation temperature of the 2-2-0-1 phase is reduced by more than 100°C in our sol-gel processing compared to conventional processing where this phase forms usually around 700°C. Actually , the 2-2-1-2 high critical temperature phase (80K) was not detectable at 750°C, but the phase transformation of the 2-2-0-1 phase to the 2-2-1-2 phase was completed at 800°C in our process, where it was the only one detectable. The 2-2-0-1 and 2-2-1-2 phases coexist at this temperature in conventional processing in agreement with the quaternary oxide phase diagram in the Br-Sr-Ca-Cu quaternary oxide system in air[47]. The only difference between the gels without Pb and the gels with Pb is the formation of a Ca_2PbO_4 compound which influences favorably the formation of the 2-2-2-3 phase at higher temperature(Fig.4.7).

The overall process, compared with Paz-Pujalt's work[69], may be represented as follows:

$$Cu + Bi_2O_3 \xrightarrow{<400°C} CuBi_2O_4 \tag{5.4}$$

$$SrO2 + CaO + CO_2 \xrightarrow{<600°C} Sr_{1-x}Ca_xCO_3 \tag{5.5}$$

$$Sr_{1-x}\,Ca_xCO_3 \xrightarrow{<600°C} SrCO_3 + CaO \tag{5.6}$$

$$2SrCO_3 + CuBi_2O_4 \xrightarrow{\sim 600°C} Bi_2Sr_2CuO_6(2\text{-}2\text{-}0\text{-}1) + 2CO_2 \tag{5.7}$$

$$Bi_2Sr_2CuO_6 + CaO + CuO \xrightarrow{<800°C} Bi_2Sr_2CaCu_2O_8(2\text{-}2\text{-}1\text{-}2) \tag{5.8}$$

Nonetheless, up to 750°C, a few diffraction peaks remain unidentified and the above crystallization sequence cannot be considered as definitive. A progressive transformation of topotactic nature, similar to that occurring in the transformation of boehmite gels into transition aluminas, cannot be rejected[173]. This is particularly true when considering that the main peaks of the 2-2-1-2 phase, at 800°C, seem to derive directly from main diffraction peaks observed at lower temperatures. For instance, 2 main peaks of the 2-2-1-2 phase have exactly the same positions as 2 important CuO peaks, so that they could be attributed to both phases.

Above 800°C, and up to 860°C, the X-ray patterns of the 3 types of gel(a), (b), and (c) after 24 hour heat treatment are quite similar (Fig.4.8-4.9). The complete diffraction patterns of the 2-2-1-2 phase can be observed. According to Hettich, et al.'s phase diagrams[49], 5 phases exist at 850°C, they are the 2-2-0-1, 2-2-1-2, 2-2-2-3 phases, $Bi_2Sr_2CaO_6$, and Ca_2CuO. Since the 2-2-0-1, $Bi_2Sr_2CaO_6$, and Ca_2CuO are less stable than the 2-2-1-2 and 2-2-2-3 phase at this temperature, the two high T_c phases should therefore be the major ones in the final products after heat treatment at 850°C. However the 3 other phases may be present residually at grain boundaries, and explain lower T_c. Because the 2-2-2-3 phase has the highest critical temperature in the Bi-system, the final products are expected to have as much of the 2-2-2-3 phase as possible. Actually, a critical proportion of the 2-2-2-3 phase in a sample is necessary to establish a percolative path with the highest critical temperature T_c (110K). It has been mentioned in chapter 2 that the successful synthesis of the 2-2-2-3 phase typically requires a heat treatment above the partial melting temperature but below the temperature of complete melting and decomposition of this system. The processing of the Bi-Sr-Ca-Cu-O compound outside this processing window usually results predominately in the 2-2-1-2 phase with intergrowth structure and various second-phase particles such as CuO, CaO, and the 2-2-0-1 phase. In air, by conventional processing, the temperature window is about 10°C near 850°C[92].

Peaks belonging to the 2-2-2-3 phase, in our X-ray diffraction patterns, are present at 830°C and 845°C in gel(b) samples, and only at 830°C in gel(c) samples, and they are hardly detected at 860°C in gel(a) samples, after 24 hour heat treatment. The shape of samples distorted rapidly, and some dark yellow residuals remained in the crucible when the samples were heat treated at 860°C. This indicates the samples have been melt and decomposed completely at 860°C. Further studies shown that at 815°C the 2-2-2-3 phase was not detectable, even for 144 hour heat treatment in air for all three types of samples (Fig. 4.11-13). At 830°C it started to form but the formation rate was slow (Fig. 4.14-16), the suitable temperature for the formation of this phase is at 845°C (Fig. 4.17-19). In our sol-gel processing like in conventional processing, the 2-2-2-3 phase can only be formed in a very narrow temperature window near 845°C under air, and it requires long heating times.

With multicomponent oxides, the mechanisms of phase formations at temperature lower than 1000°C, are well known to depend largely on the processing technique. An ideal sol-gel processing technique should provide a true homogeneous distribution of all cation at atomic level. In turn, this might allow the formation of the 2-2-0-1, 2-2-1-2, and 2-2-2-3 phase at lower temperature than in a conventional processing. The present sol-gel processing technique has allowed to lower the formation temperatures of the $CuBi_2O_4$ and 2-2-0-1 phases by over 100°C, but could not decrease the formation temperatures of the 2-2-1-2 and 2-2-2-3 phases significantly. This can be related to the fact that the 2-2-1-2 and 2-2-2-3 phases have to be formed from intermediate phases such as Bi_2O_3, CuO, $CuBi_2O_4$, CaO, $SrCO_3$, and the 2-2-0-1superconductor. The initial homogeneous polynuclear distribution has therefore been destroyed completely. The presence of heterogeneities rich in calcium, and containing some copper, in gel(c) samples heat treated at 845°C for 144 hours, (Fig. 4.24), confirms the destruction of the initial homogeneity as achieved by the present sol-gel processing.

Overall, whatever the initial compositions being studied here and independently of the presence or absence of lead, the formation of two superconducting phases, 2-2-1-2 and 2-2-2-3, is confirmed. In the present study, the most noticeable difference between gels with different initial compositions concerns the formation rate of the 2-2-2-3 phase and its final proportion. The most drastic experimental fact, shown in Fig. 4.20, is that the 2-2-2-3 phase is more abundant in samples with Pb, and with an initial composition 1-1-1-2 instead of 2-2-2-3.

The initial composition of the gel(c) has been known to be the optimum one to produce the high-T_c phase[35, 63]. The solid state reactions are similar in gel(b) and gel(c) samples. The difference is that the excess of Cu in gel(b) results in a greater amount of CuO than in gel(c) samples. Since CuO helps the formation of Ca_2PbO_4 below 750°C, the volume fraction of this phase is greater in gel(b) than in gel(c), as shown in Fig. 4.7. According to Huang's result[53, 64], the formation of the 2-2-2-3 phase depends on the amount of the Ca_2PbO_4 and CuO phases. It is therefore not surprising if the formation rate of the 2-2-2-3 phase is faster in gel(b) than that in gel(c) samples. For instance, the volume fractions of the 2-2-2-3 phase are respectively about 50% and 25% in gel(b) and in gel(c) samples after 144 hour heat treatment at 845°C.

The advantage of an excess of copper on the kinetics of phase transformation in sol-gel processing is quite clear. However, on the other hand, when the transformation of the 2-2-1-2 to 2-2-2-3 phase should reach completion, the excess copper will be left as a second-phase influencing the superconducting properties, especially the critical current density.

The development of a network of fine slit shaped pores, has been observed in samples heat treated above 815°C (Fig. 4.25). This fact, together with the progressive intercalation of the other cations in between the Cu-O layers of the copper oxide, supports a topotactic formation of the 2-2-1-2 phase. As the network of fine slit shaped pores forms, uniform cluster of the 2-2-1-2 phase take on the appearance of aggregates of distorted platelike grains at higher temperatures. This cleavage takes place along the (**a**,**b**)-plane, and probably along the Bi-O layers[85]. These slit shape pores do also contribute, for a sizeable proportion, to the increase in specific surface area observed under the BET (Fig. 4.23)

On the contrary, the well defined shapes of the 2-2-2-3 phase suggest a formation mechanism by nucleation and growth. Then they undertake growth and become thicker and longer (Fig.4.24).

Although the highest-T_c phase in the Bi-Sr-Ca-Cu system has a 2-2-2-3 stoichiometry with respect to Bi-Sr-Ca-Cu, the 2-2-2-3 phase can not be obtained easily if the initial composition is exactly 2-2-2-3 with respect to Bi-Sr-Ca-Cu. Furthermore, the density of the 2-2-1-2 phase is 6.11 g/cm^3 whilst that of the 2-2-2-3 is 6.02 g/cm^3. This is bound to introduce a strain-energy term into the free energy balance for its formation. The increase in Gribbs free energy ΔG associated with this strain energy will retard the transformation until a liquid phase can appear. In this study, copper was chosen to be in excess in the initial compositions of gel(a) and gel(b) samples because the excess of Ca or Cu can lower the partial melting temperature of a compound with a composition near 2-2-2-3, hence, reduce the strain-energy, enhance the diffusion rate, and facilitate the formation of the 2-2-2-3 phase. After calcination of gel(a) samples at 800°C, copper is present in the 2-2-1-2 phase, CuO, and Ca_2CuO_3. even if these phases cannot be detected by X-ray diffraction. These compounds transforms into the 2-2-2-3 phase at a temperature near 845°C, according to the following reaction;

$$Bi_2Sr_2CaCu_2O_8 \text{ (2-2-1-2)} + CaO + CuO \rightarrow Bi_2Sr_2Ca_2Cu_3O_{10} \text{ (2-2-2-3)} \qquad (5.9)$$

On Fig. 4.20 concerning gel(a) samples, the volume fraction of the 2-2-2-3 phase goes through a maximum after 48 hour heat treatment at 845°C. This is in agreement with Hatano's result[55]. In his study on superconductors from carbonates and oxides, with an initial composition similar to that of gel(a), the 2-2-1-2 and 2-2-2-3 phases are reported to transform from each other according to the sequence:

$$\text{2-2-1-2} \rightarrow \text{2-2-2-3} \rightarrow \text{2-2-1-2} \qquad (5.10)$$

The instability of the 2-2-2-3 phase in gel(a) samples is due to the cleavage of this phase near the BiO planes perpendicular to the c-axis. Because of this cleavage, the 2-2-2-3 phase which starts to form at the initial heat treatment stage at 845°C, is destroyed to give the 2-2-1-2 phase back. This last phase has crystal structure similar with the 2-2-2-3 phase and is more stable at this temperature. The addition of Pb enhances the inter-layer bonding of BiO planes, and stabilizes the 2-2-2-3 phase. Not only does the addition of lead stabilize this phase, but it also promotes its formation. The Ca_2PbO_4 phase formed at about 700°C plays an important role in the formation of the 2-2-2-3 phase. The partial melting in the Bi-Pb-Sr-Ca-Cu-O system is the result of the coexistence of the 2-2-1-2 , Ca_2PbO_4, and CuO phases. In the equation (5.10), the CaO, which must be involved in the transition of the 2-2-1-2 to 2-2-2-3 phase, is caused by the decomposition of Ca_2PbO_4. It occurrs above 822°C in conventional processing[174] while the CuO and the 2-2-1-2 phases form below 800°C. Also, Shiloh, et al.[175] indicate Pb react with SrO_2 or $SrCO_3$ to form a Sr_2PbO_4 phase

5.3) MICROSTRUCTURE AND SINTERING BEHAVIORS

The sintering behavior of samples in this sol-gel processing appears to be largely in competition with grain growth. This is consistent with a recent research on density and microstructure of calcium titanate, which has also a perovskite structure[176].

With all samples at all temperatures, sintering occurred only during the first 24 hours. The density reached was about 5.5 g/cm^3, that is to say about 90% of theoretical density. Sintering at temperature at 830°C resulted in a reduction of the final density with gel(a) and gel(b) samples while the density of gel(c) samples maintained at about 5.5 g/cm^3. The retrograde densification is outstanding at 845°C with all three different type samples after the initial sintering process (Fig. 4.21(c)). Its occurrence has been reported at a higher temperature on similar superconductors made from oxides and carbonates[71]. Such a reduction in density might be expected if significant sample volatilization was occurring. The volatilization of Bi and Pb at high temperature has been proven by Karbarz, et al.[73]. However the sample weight loss was moderate and did not increase with increased heat treatment times. Rather, the reduction in density correlates closely with increasing grain growth, and might therefore be explained by grain growth predominating over densification after an induction period. The sample sintered at 830°C for 144 hours shows the microcracks in the 2-2-1-2 grain (Fig. 4.25). The formation of microcracks is tightly connected to the reduction in density. It corresponds to a partial melting which helps the growth of the 2-2-2-3 phase. Reverse densification is therefore related to the growth of the 2-2-2-3 straight platelike grains pushing the structure apart. The formation of a liquid phase is consistent with the distortion of samples. On samples heat treated at 860°C, the shape of the samples was distorted totally, and the weight had decreased quickly. Also, the 2-2-2-3 phase is less dense than the 2-2-1-2 phase by about 2%, which creates a strain-stress in the grain. If the stress build-up becomes too high to be supported by the materials, the sample yields and swells while microcrack appear.

This conflict between grain growth and densification in the Bi-system is a challenge to obtain high-quality superconductors. A way to solve this problem may consist in regrinding the heat treated samples with a high proportion of the 2-2-2-3 phase, pressing and heat-treating again[72].

According to the Herring's scaling laws[177], grain growth can be described by an equation of the type (4.3);

$$D^n = Kt$$

This equation comprises a constant K, related to the activation energy of the transport process and an exponent n depending on the transport path. In the most simple grain growth model (i.e. normal grain growth)[178], n = 2. However , in many ceramic systems, the grain growth exponent, n, is usually higher than 2 due to the existence of pores, second phases, grain segregation, and nonstoichiometry. It depends on the mechanism involved in the matter transport process. In theoretical models, the grain growth exponent, n, can vary from 3 to 5. A cubic law corresponds to transport through a liquid phase. Grain growth kinetics in the presence of a liquid phase were shown by Lay [179] to follow a cubic relation, and it is important to note that only a small amount of liquid between particles is necessary. The cubic grain growth mechanism has been observed in other ceramic systems that contain a liquid phase including Al_2O_3 doped UO_2 and MoO_3 doped manganese zinc ferrite[140]. German[180] also indicates that the exponent, n = 3, is a quite common value in a grain growth by a liquid phase. However, it is difficult to determine experimentally with accuracy[140].

In this study, most grain growth data are characterized by a value of n close to 3. It seems therefore the grain growth mechanism is by transport through a liquid phase. In the Saggio's CuO-1/2 Bi_2O_3-SrO phase diagram[31], melting occurs at even 800°C for Bi-rich composition. Bismuth oxide melts at 817°C[69]. In the last section, we have discussed the fact that the homogeneous distribution of cations is destroyed during heat treatment. So, the existence of Bi-rich composition at local areas cannot be rejected, which might form a liquid phase in local areas. Uzumaki, et al.[174] have confirmed that a liquid phase is formed by the decomposition of Ca_2PbO_4 at 822°C when Pb is added to the Bi-Sr-Ca-Cu-O system. The formation of the liquid phase at this temperature is an important reason for grain growth to follow a cubic law in samples containing Pb. Several reports have mentioned that a liquid phase forms and promotes the phase transformation from 2-2-1-2 to 2-2-2-3[52, 53, 64]. According to Aota's study [91], the 2-2-2-3 phase starts to decompose partially at 850°C. The addition of Pb and the excess of Cu in this sol-gel processing have decreased the partial melting temperature effectively[53, 64].

In the superconductors from gel(a) without lead n is higher, from 4.53 to 7.73. Simultaneously, the grain growth occurs therefore very probably not through liquid phase transport. Lead modifies therefore signficantly the grain growth mechanism. The transport mechanisms responsible for so high exponent are not well understood. Chu, et al.[140] suggests that a grain boundary diffusion mechanism control the grain growth with the exponent n = 5. A definitive research work is necessary to establish a more precise grain growth mechanism for this oxide superconductor.

5.4) SUPERCONDUCTIVITY

The critical temperatures data in Table 4.2, and the data on the 2-2-2-3 phase volume indicate they increase altogether. $T_{c,0}$ = 106K in the gel(b) sample with a 32% 2-2-2-3 volume fraction while $T_{c,0}$ = 107.6K in the sample with 50% volume fraction. This may be due to residual phases at grain boundaries, which disappear as the 2-2-2-3 phase forms. Even the 2-2-0-1 phase may not transform into the high-T_c superconducting phase completely. A small amount not detectable by X-ray diffraction, may remain at grain boundaries and influence the critical temperature [181]. Further investigation on this problem is needed. However, the density, the average grain size, the pore volume and the average pore radius (Fig. 4.23 and 4.33) have relatively little effect on the critical temperature. Furthermore, as discussed above, the formation of the 2-2-2-3 phase depends largely on the presence of lead in the composition and processing parameters such as heat treatment temperature and time. The critical temperature depends therefore first on the composition as usually admitted. Generally speaking, all methods, which help to form the 2-2-2-3 superconducting phase, can help to increase the critical temperature to 110K.

The critical temperature is more sensitive to addition of lead in materials made by sol-gel than that in materials made by conventional processing. For example, the critical temperature of gel(a) without any lead, after heat treatment at 845°C for 144 hours, remains below 90K in this work. On the contrary, a sample with the same initial composition as that of gel(a) made by conventional processing has been reported with a $T_{c,0}$ above 100K[119].

The very short coherence length below 40Å of the 2-2-1-2 and 2-2-2-3 superconductors in the Bi-(Pb)-Sr-Ca-Cu-O system may very easily result in the low critical current density. The average pore radius of gel(a) and gel(b) samples heat treated at 845°C is over 70Å . These pores and grain boundaries acting like "weak-link" have therefore probably an important effect. Because the Bi-(Pb)-Sr-Ca-Cu-O superconductors are strongly anisotropic with a critical current density, J_c, at least two orders of magnitude higher in the (**a,b**)-plane than that along the **c**-axis[182], it is expected that the achievement of a high critical current density require a highly oriented microstructure. In the present research, oriented microstructures have been obtained in samples with lead, and the orientation degree increases with the heat treatment time. The origin of the oriented microstructure is due to the rapid and oriented growth of the 2-2-1-2 phase, possibly due to pressing[85]. Such extended platelike grains did not form a oriented microstructure in gel(a) samples without Pb (Fig. 4.30, and 4.35). The addition of lead not only help to form and stabilize the 2-2-2-3 superconducting phase but also promote the grain growth and the formation of an oriented microstructure. The partially oriented microstructure, obtained in this study, is nonetheless insufficient. The achievement of a high critical current density will require further studies.

CHAPTER 6: CONCLUSIONS

Gels for superconducting materials in the Bi-(Pb)-Sr-Ca-Cu-O system could be made from nitrate precursors by complexation with citric acid, and ammonia. Heat treatment between 180°C and 250°C eliminates progressively, the color of gels changes from blue to black while they swell. However they can be redispersed in aqueous media.

The three different superconducting phases in this system could be be obtained. The lowest $T_{c,0}$ phase (2-2-0-1) starts to form at 600°C. The phase with critical temperature $T_{c,0} = 80K$ (2-2-1-2) forms at 800°C. Finally the highest $T_{c,0}$ phase (2-2-2-3) forms in a very nerrow temperature range 830-850°C.

The 2-2-2-3 high-T_c superconducting phase is more abundant in samples containing lead and for an initial composition of 1-1-1-2 with respect to Bi-Sr-Ca-Cu.

The 2-2-1-2 phase forms by progressive intercalation of the other cations between the CuO layers of the copper oxide. This 2-2-1-2 phase transforms to the 2-2-2-3 phase by the cleavage, and formation of a liquid phase helping the nucleation and growth of the 2-2-2-3 phase. The formation temperatures of the 2-2-1-2 and 2-2-2-3 superconducting phase was not be lowered in this sol-gel processing compared with conventional processing. This is due to the destruction of an initial distribution of all cations achieved which is not homogeneous at the atomic level, but at the level of polynuclear species in the present gels. This favors the appearance of many intermediate phases.

Sintering and grain growth compete largely during heat-treatment between 800 and 845°C. Sintering process predominates during an induction period shorter than 24 hours, while grain growth of the 2-2-2-3 phase by liquid transport stops sintering. Grain growth predominates during further heat treatment.

The critical temperature, $T_{c,0}$, depends first on the proportion of the 2-2-2-3 superconducting phase in a sample, and to a lower extent depends on the initial composition and processing parameters. Critical temperature above 100K have been obtained with Pb addition in the Bi-Sr-Ca-Cu system.

CHAPTER 7: FURTHER WORK

In this research, black gels have been obtained successfully through heat treatment of blue gels at below 250°C and redissolution in an aqueous medium. They do not bloat again during further heat treatment. This provides a new sol-gel route which may possibly lead to better superconductors with a more uniform microstostructure and better properties such as high critical curent density J_c. The properties of these black gels reserve therefore to be studied.

Our microstructures studied have shown the superconductors were composed of the platelike grains. Techniques to produce better-oriented microstructure should be studied. Several methods mentioned in the chapter 2 have been used to obtain the high-oriented microstructure but other ways such as a magnetic induced method may be applied. Addition of silver by conventional procsessing in this system has also proved to be a good way to improve the critical current density. If Ag is added in this sol-gel processsing, what will be happen? Intensive research is needed on this issue.

Because the main obstacles to the application of high temperature superconductors is the low critical current density, the effect of processing parameters, such as heat treatment temperature and time, and microstructure on this property could also be studied for long times and more temperatures, than has been done here.

In this experiment, it is proposed that the 2-2-1-2 phase is formed by progressive intercalation of other cations between the CuO layers. More experiments are needed to determine with certitude phase transformation mechanism. It is important to know if the fabrication temperature could be lowered. In this aim TEM observation would be interesting.

REFERENCE

[1] H.K. Onnes, *Akad. van Wetenschappen (Amsterdam)*, (1911)**14**, pp113; H.K. Onnes, *Communs. Phys. Lab. Univ. Leiden Supplement* (1913)**35**

[2] J.R. Christman, *"Fundamentals of Solid State Physics "*, John Wiley & Sons, c.1988

[3] S. Chubbs, *"High Temperature Superconductors in the BSCCO System"* , project report in University of Alberta, 1990

[4] T.R. Radhakrishnan, *"Introduction to Superconductivity "*, *High Temperature Superconductors,* Ed. S.V.Subramanyam and E.S.Raja Gopal, Wiley Eastern Ltd. New Delhi, India, c.1989, pp1-8

[5] V.L.Ginzburg, "High Temperature Superconductivity", *Progress in High Temperature Superconductivity-vol.1*, Proceedings of the Adriatico Research Conference on High Temperature Superconductors, ICTP,Trieste, Italy, 5-8 July, 1987, Ed. S.Lundqvist, E.Tosatti, M.P. Tosi, and Y. Lu, World Scienfic Publishing Co. Pte. Ltd., Singapore, c.1987, pp3-32

[6] W.Meissner and R. Ochsenfeld, *Naturwissenschaften,* (1933)**21**, pp787

[7] F. London and H. London, *Physica* (1935)**2**, pp34; *Proc. Roy. Soc. (London))*. (1935) **A149**, pp71

[8] V.L. Ginzburg and L.D. Landau, *JETP* . (1950)**20**, pp1064

[9] J. Bardeen, L.Cooper, and J.Schrieffer, *Phys. Rev.* (1957)**108**, pp1175

[10] A.A. Abrovskove, *J. Phys. Chem. Solids*, (1957)**2**, pp199

[11] B.D. Josephson, *Phys. Letts.* (1962)**1**, pp251

[12] Z. Fang and D. Lu, *"Solid State Physics"* in Chinese, published in Shanghai, P.R.China, c.1981, pp296-348

[13] J.G.Bednorz and K.A.Müller, *Z. Phys.* (1986)**64**, pp189

[14] M.K. Wu, J.R. Ashburn, C.J. Trong, P.H. Meng, L. Gao, Z.J. Huang, Y.Q. Wang and C.W. Chu, *Phys. Rev. Lett.* (1987)**58**, pp908

[15] H. Meada, Y.Tanaka, and M. Fukutomi, *Jpn. J. Appl. Phys.*, (1988)**27**, pp.L1209

[16] Z.Z. Sheng, K. Kiehl, J. Bennett, A. El Ali, D. Marsh, G. D. Mooney, F. Arammash, J. Smith, D. Viar, and A.M. Hermann, *Appl. Phys. Lett.*, (1988)**52**, pp1738; Z.Z. Sheng and A.M. Hermann, *Nature*, (1988)**332**, pp138

[17] C.J. Gorter and H.B.G. Casimir, *Z. Phys.* (1934)**35**, pp963

[18] C. Kittel,*"Introduction to Solid State Physics"*, 6th edition, John Wiley & Sons, Inc. c.1986

[19] J.D. Doss, *"Engineer's Guide to High-Temperature Superconductivity"*, John Wiley & Sons, Inc. c.1989

[20] A.C. Roos-innes and E.H.Rhoderick, *"Introduction to Superconductivity"*, second edition, Pergamon Press Ltd. c.1978

[21] L.N. Cooper, *Phys. Rev.* (1956)**104**, pp1189

[22] S. Jin and J.E. Graebner, *Mater. Sci. & Eng. B*, (1991)**7**, pp243,

[23] H. Itozaki, K. Higaki, K. Harada, S. Tanaka, N. Fujimori and S. Yazu, *"Advance in Superconductivity"*, Ed. K. Kitazawa and T. Ishiguro, c.1989, pp599

[24] R.G. Humphreys, J.S. Satchell, N.G. Chew, J.A. Edwards, S.W. Goodyear, S.E. Blenkinsop, O.D. Dosser and A.G. Gullis, *Supercond. Sci. Tch.*, (1990)**1**, pp1

[25] D.W. Johnson Jr. and G.S. Grader, *J. Am. Ceram. Soc.*, (1988)**71**, pp.c-291

[26.1] J. Tabuchi, and K. Utsumi, *Appl. Phys. Lett.*, (1988)**53**, pp606

[26.2] K. Tachikawa, I. Watana and S. Kosuge, M. Kabasawa, T. Suzuki, Y. Matsuda and Y. Shinbo, *Appl. Phys. Lett.*, (1988)**52**, pp1011

[27] H. Zhuang, H. Kozuka, and S. Sakka, *Jpn. J. Appl. Phys.*, (1989)**28**, pp.L1805

[28] J.M. Brenner, R.S. Feigelson, D. Gazit, and P.N. Peszkin, *Materials Science and Engineering, B* (1990)**5**, pp351

[29] K. Matsuzaki, S. Torri, and T. Masumoto, *Mater. Lett.*, (1991)**10**, pp485

[30] O. Eibl, *Physica C*, (1990)**168**, pp215

[31] J.A. Saggio, K. Sujata, J. hahn, S.J. Hwu, K.R. Poeppelmeier, and T.O. Mason, *J. Am. Ceram. Soc.* (1989)**72**, pp849

[32] A.H. Carim, A. P. M. Kentgens and J.H.T. Hengst, *J. Mater. Rev.* (1988)**3**, pp1317

[33] J.B. Torrance, Y. Tokura, and S.J. Laplaca, *Solid State Communication*, (1988)**66**, pp703

[34] R. Srinivasan, M. Saum, R.J. De Angelis, J.O. Deasy, J.W. Brill, C.E. Hamrin Jr., *J. Mater. Sci. Lett.* (1989)**8**, pp196

[35] S. Koyama, U. Endo, and T. Kawai, *Jpn. J. Appl. Phys.*, (1988)**27**, pp.L1861

[36] N. Kijima, H. Endo, J. Tsuchija, A. Sumiyama, M. Mizuno, and Y.Oguri, *Jpn. J. Appl. Phys.* (1989)**28**, pp.L787

[37] C.K. Rhee, C.J. Kim, H.G. Lee, I.H. Kuk, J.M. Lee, I.S. Chang, P.S. Han, S.I. Pyun, and D.Y. Wun, *Jap. J. Appl. Phys.* (1989)**28**, pp.L1137

[38] L. Pierre, J. Schneck, D. Morin, J.C. Tolèdano, J. Primot, C. Daguet and H. Savary, *J. Appl. Phys.*, (1990)**68**, pp2296

[39] Y. Gao, P. Coppens, M.A. Subramanian, A.W. Sleight, *Science* (1988)**241**, pp954

[40] Y. Gao, P. Lee, J. Ye, P. Bush, V. Petricek, P. Coppens, *Physica C* (1989)**160**, pp431

[41] H.W. Zendbergen, W.A. Groen, F.C. Mijihoff, G.van Tendeloo, S. Amelinckx, *Physica C,* (1988)**156**, pp325

[42] B.C. Chakoumakos, P.S. Ebey, B.C. Sales, and E.Sonder, *J. Mater. Res.* (1989)**4**, pp767

[43] L. Pierre, J. Schneck, J.C. Toledano, C. Daguet, *Phys. Rev. B.* (1990)**41**, pp766

[44] M.J. Casanove, P. Baules, E. Snoeck, C. Roucau, *Physica C* (1989)**159**, pp461

[45] P.H.M. van Loosdrecht and A. Janner, "*Electronic Properties of High-Tc Superconductors and Related Compounds*", Springer-Verlag,c.1990, pp29

[46] Y. Ikeda, H. Ito, S. Shimomura, Y oue, K. Inaba, Z.Hiroi, and M.Takano, *Physica C* (1989)**159**, pp93

[47] B.Hong, J. Hahn, and T.O. Mason, *J. Am. Ceram. Soc.* (1990)**73**, pp1965

[48] R. Roth, C.J. Rawn, J.J. Ritter, and B.P. Burton, *J. Am. Ceram. Soc.* (1989)**72**, pp1545

[49] B. Hettich, M. Schwarz and H. Sixl, "*Electronic Properties of High-Tc Superconductors and Related Compounds* ", Springer-Verlag, c.1990, pp12

[50] H. Kitaguchi, J. Takada, K. Oda and Y. Miura, *J. Mater. Res.*, (1990)**5**, pp929

[51] N.M. Hwang, R. S. Roth, and C.J. Rawn, *J. Am. Ceram. Soc.* (1990)**73**, pp2531

[52] A. Ono, *Jpn. J. Appl. Phys.* (1988)**27**, pp.L2276

[53] Y.T. Huang, W.N. Wang, S.F. Wu, C.Y. She, W.M. Hurng, W.H.Lee, and P.T. Wu , *J. Am. Ceram. Soc.* (1990)73, pp3507

[54] W.J. Lin, L.C. Wang, H.B. Hu, I.N. Lin, C.C. Young, W.Y. Lin, S.J. Yang, and S.E. Hsu, *Jpn. J. Appl. Phys.* (1990)**29**, pp846

[55] T. Hatano, K. Aota, S. Ikeda, K. Makamura, and K. Ogawa, *Jpn. J. Appl. Phys.* (1988)**27**, pp.L2055

[56] J. Tsuchiya, H. Endo, N. Kijima, A. Sumiyama, M. Mizuno and Y. Oguri, *Jpn. J. Appl. Phys.* (1989)**28**, pp.L1918

[57] R. B. Tripathi, D.W. Johnson, Jr., and D.A. Fleming, *J. Mater. Res.*, (1991)**6**, pp455

[58] D. Shi, M. Tang, K. Vandervoort, and H. Claus, *Phys. Rev. B* (1989)**39** , pp9091

[59] S. Horiuchi, K. Shoda, X.J. Wu, H. Nozaki and M. Tsutsumi, *Physica C* (1990)**168**, pp205

[60] B. Stadlober, P. Knoll, H. Jodlbauer, W. Lang, N. Brnčević, R. Abt, E. Schweiger, G. Leising, and H. Kahlert, "*Electronic Properties of High-Tc Superconductors and Related Compounds*", Springer-Verlag, c.1990, pp46

[61] R. Gross, J. Bosch, H. G. Wener,, J. Fisher, and R.P. Hübener, *Cryogenics* (1989)**29**, pp716

[62] U. Endo, S. Koyama and T. Kawai, *Jpn. J. Appl. Phys.* (1989)**28**, pp.L190

[63] K. Tanaka, A. Nozue, and K. Kamiya, *J. Mater. Sci.* (1990)**25**, pp3551

[64] Y.T. Huang, C.Y. She, W.N. Wang, C.K. Chiang, and W.H. Lee, *Physica C* (1990)**169**, pp76

[65] Y. Matsui, H. Meada, Y. Tanaka, and S. Horiuchi, *Jpn. J. Appl. Phys.* (1989)**28**, pp. L946

[66] H. Jang, H.J. Shin, J.H. Moon, *J. Mater. Rev.* (1991)**6**, pp916

[67] W. Liu, private communation, Nov. 1989

[68] R.S. Liu, J.J. Chu, C.T. Chang, *Mater. Lett.* (1989)**8**, pp293

[69] G.R. Paz-Pujalt, *Physica C* (1990)**166**, pp177

[70] K. Ma and A.C. Pierre, 5th International Conference on Ultrastructure Processing, February 17-21, 1991, Orlando, Florida

[71] D.W. Johnson Jr. and W.W. Rhodes, *J. Am. Ceram. Soc.* (1989)**72**, pp2346

[72] K. Jain, D.K. Suri, K.C. Nagpal, S.U.M. Rao, and B.K. Das, *Mat. Res. Bull.* (1990)**25**, pp1057

[73] F.A. Karbarz, O. D. Lacy, K.C. Goretta, U. Balachandran, D. Shi, J.G., Chen, M. Xu, and M.C. Hash, *Mat. Res. Bull.* (1990)**25**, pp251

[74] M. Reissner, R. Ambrosch, W. Steiner, H. Kuzmany, P. Schaffarich, R. Stroh, and W. Wruss, *Electronic Properties of High-Tc Superconductors and Related Compounds*", Springer-Verlag, c.1990, pp65

[75] H.A. Hoff and C.S. Pande, *JOM.*, (1990)**June**, pp10

[76] W. Gao, S. Li, R. Parrella, D.A. Rudman, and J.B. Vander Sande, *J. Mater. Rev.* (1990)**5**, pp2633

[77] J.W. Ekin, *Adv. Ceram. Mater.* (1987)**2**, 586

[78] D.Dimos, P. Chaudhari and J. Mannhart, *Phys. Rev. B* (1990)**41**, pp4038

[79] S.E. Babcock, X.Y. Cai, D.L. Kaiser, and D.C. Larbalstier, *Nature*, (1990)**347**, pp167

[80] S.E. Babcock, and D.C. Larbalstier, *J. Mater. Rev.* (1990)**5**, pp919

[81] O. Eibl, *Physica C* (1990)**168**, pp239

[82] O. Eibl, *Physica C* (1990)**168**, pp249

[83] R. Ramesh, B.G. Bagley, J.M. Tarascon, S.M. Green, M.L. Rudee, and H.L. Luo, *J. Appl. Phys.* (1990)**67**, pp379

[84] C.J. Kim, C.K. Rhee, C.T. Lee, G.W. Hong, Y.H. Herr, H.G. Lee, and D.Y. Won, *J. Mater. Sci. Lett.* (1990)**9**, pp774

[85] K. Kugimya, S. Kawashima, O. Inoue, and S. Adachi, *Mater. Lett.* (1988)**6**, pp277

[86] K. Jain, D.K. Suri, K.C. Nagpal, S.U.M. Rao, and B.K. Das, *Jpn. J. Appl. Phys.*, (1990)**29**, pp.L576

[87] H. Meguro, T. Komatsu, R. Sato and K. Matusita, *J. Mater. Sci. Lett.* (1990)**9**, pp1359

[88] W. Wang, M. Zhou, T. Zuo, J. Huang, J. Cai, X. Zhou, and Q. Wei, *Physica C* (1990)**68**, pp5939

[89] Y. Mastumoto, J. Hombo, Y. Yamaguchi, and T. Mistunaga, *Mat. Res. Bull.* (1989)**24**, pp1469

[90] A. Perrin, A. Dinia, O. Peña, C. Perrin, and M. Sergent, *Mater. Lett.* (1989)**8**, pp165

[91] K. Aota, H. Hattori, T. Hatana, K. Nakamura, and K. Ogawa, *Jpn. J. Appl. Phys.* (1989)**27**, pp.L2196

[92] A. Aoki, *Jpn. J. Appl. Phys.* (1990)**29**, pp.L270

[93] S.X. Dou, K.H. Song, H.K. Liu, C.C. Sorrel, M.H. Apperley, and N. Savvides, *Appl. Phys. Lett.* (1990)**56**, pp493

[94] D. Kijrillov, I. Bozovic, T.H. Geballe, A. Kapitulnik and D.Z. Mitzi, *Phys. Rev. B* (1988)**38**, pp11955

[95] A. Yamanaka, F. Kinami, and K. Inoue, *Physica C* (1989)**162-164**, pp1099

[96] M. Lee, D.B. Mitizi, A. Kapitulnik and M.R. Beasly, *Phys. Rev. B* (1989)**39**, pp801

[97] G. Briceno and A. Zettl, *Solid State Commun.* (1989)**70**, pp1055

[98] Y. Petroff, "*Electronic Properties of High-Tc Superconductors and Related Compounds*", Springer-Verlag, c.1990, pp114

[99] C.G. Olsen, R. Liu, D.W. Lynch, R.S. List, A.J. Arko, B.W. Veal, Y.C. Chang, P.Z. Jiang and A.P. Paulikas, *Solid State Commun.* (1990)**76**, pp411

[100] A.M. Rao, P.C. Eklund, G.W. Lehman, D.W. Face, G.L. Doll, G.Dresselhaus and M.S. Dresselhaus, *Phys. Rev. B* (1990)**42**, pp193

[101] M. Boekholt, M. Hoffmann and G. Güntherodt, *Physica C* (1991)**175**, pp127

[102] R.B. Tripathi and D.W. Johnson Jr. *Mat. Res. Bull.* (1990)**25**, pp1307

[103] T.T.M. Palstra, B.Batlogg, L.F. Schneemeyer, R.B. van Dover, and J.V. Waszczak, *Phys. Rev. B* (1988)**38**, pp5102

[104] G. Deutscher, *Physic C* (1988)**153-155**, pp15

[105] R. Job and M. Rosenberg, *Physica C* (1991)**172**, pp361

[106] B. Batlogg, T.T.M. Pastra, L.F. Schneemeyer, R.B. Van Dover and R.J. Cava, *Physica C* (1988)**153-155**, pp1062

[107] S.H. Han, Z. Hergedüs, µ. Andersson, M. Nygren, Ö. Rapp, Y.F. Yan, Q.Chen, T.N. Wei, and R.M. Hazen, *Scientific Ameracan* (1988)**258**, pp74

[108] Y. Ikeda, M. Takano, Z. Hiroi, K. Oda, H. Kitaguchi, J. Takada, Y. Miura, Y. Takeda, O. Yamamoto, and H. Mazaki, *Jpn. J. Appl. Phys.* (1988)**27**, pp.L2067

[109] B.Raveau, C.Michel, and M.Herviru, *J. of Solid State Chemistry* (1990)**85**, pp181

[110] J.P. Franck J. Jung, W.A. Miner, and M.A.-K. Mohamed, *Phys. Rev. B* (1988)**38**, pp754

[111] H. Sato, and W. Zhu, *J. of Solid State Chem.* (1988)**75**, pp207

[112] Y. Takeda, R. Kanno, and F.Tanigawa, *Physica C* (1989)**159**, pp789

[113] J.M. Tarascon, P. Barboux and L.H. Greene, *Physica C* (1988)**153-155**, pp566

[114] J. Akimitsu, A. Yamazaki, and H. Sawa, *Jpn. J. Appl. Phys.* (1989) **28**, pp.L2080

[115] I. Nedkov, Z. Ivanov, and M. Taslakov, *Mater. Lett.* (1989)**8**, pp87

[116] B.P. Singh, S.K. Agarwal, V.N. Moorthy, B.V. Kumaraswamy, R.K. Nayar, and A.V. Narlikar, *J. Mater. Sci.* (1990)**25**, pp4630

[117] H. Zhuang, H. Kozuka, and S. Sakka, *J. Mater. Sci.* (1990)**25**, pp4762

[118] J. Gopalakrishnan, M. A. Subramanian, and A. W. Sleight, *J. Solid State Chem.* (1989)**80**, pp156

[119] M. Nakajima, S. Kawarabuki, T. Sasaki, N. Nojiri, Y. Watababe, H. Ikeda, and R. Yoshizaki, *Jpn. J. Appl. Phys.* (1989)**28**, pp.L943

[120] S. Kobayashi, Y. Saito, and S. Sada, *Jpn. J. Appl. Phys.* (189)**28**, pp.L772

[121] M.A. Señaris-Rodriguez, F. García-Alvarado, E. Morán, M.A. Alarío-Franco, M.A. González, J.L. Vicent, and J. Ibáñez, *Mat. Res. Bull.* (1990)**25**, pp223

[122] M. Matsuda, A. Kikuchi, M. Takata, M. Ishn, T. Yamashita, and H. Koinuma, *Jpn. J. Appl. Phys.* (1989)**28**, pp.L940

[123] W. Gao and J.B. Vander Sande, *Physica C* (1990)**171**, pp69

[124] R. Yoshizaki, H. Ikeda, K. Yoshikawa and N. Tomita, *Jpn. J. Appl. Phys.* (1990)**29**, pp L735

[125] K.H. Song, H.K. Liu, S.X. Dou, C.C. Sorrell, N. Savvides, and G.J. Bowden, *J. Mater. Sci.: Materials In Electronics* (1990)**1**, pp30-33

[126] R.R. Neurgaonkar, J.C. Nelson, I.S. Santha, and M.A. Gawad, *Mat. Res. Bull.* (1989)**24**, pp1541

[127] H. Kumakura, K. Togano, H. Meada, and M. Mimura, *J. Appl. Phys.* (1990)**67**, pp3443

[128] T. Goto and T. Maruyama, *J. Mater. Res.* (1990)**5**, pp1850

[129] C.J. Brinker, G.W. Scherer, *"SOL-GEL SCIENCE"*, Academic Press, Inc., c.1990

[130] A.C. Pierre, *"Introduction Aux procédés Sol-gel"*, SEPTIMA-PARIS, c.1991

[131] M.E. Gross, M. Hong, S.H. Liou, P.K. Gallagher, and J. Kwo, *Appl. Phys. Lett.* (1988)**52**, pp160

[132] E.I. Cooper, E.A. Giess, and A. Gupta, *Mater. Lett.* (1988)**7**, pp5

[133] R.B. Tripathi and D.W. Johnson Jr. *Mater. Lett.* (1990)**10**, pp118

[134] B.S. Khurana, R.B. Tripathi, S.M. Khullar, R.K. Kotnala, Satbirsingh, K. Jain, B.V. Reddi, R.C. Goel, and B.K. Das, *J. Mater.Sci.Lett.* (1989)**8**, pp234

[135] M. Fujiki, M. Hikita, and K. Sukegawa, *Jpn. J. Appl. Phys.* (1987)**26**, pp.L1159

[136] P. Barboux, J.M. Tarascon, L.H. Greene, G.W. Hull, B.G. Bagley, *J. Appl. Phys.* (1988)**63**, pp2725

[137] K. Tanaka, A. Nozue, and K. Kamiya, *Jpn. J. Appl. Phys.* (1989)**28**, pp L934

[138] S.L. Furcone,and Y.-M. Chiang, *Appl. Phys. Lett.* (1988)**52**, pp2180

[139] Y.M. Chiang, D.A. Rudman, D.K. Leung J.A.S. Ikeda, A. Roshka, and B.D. Fabes, *Physica C* (1988)**152,** pp77

[140] C.T. Chu and B. Dunn, *J. Am. Ceram. Soc.* (1987)**70**, pp.c375

[141] R. Sanjinés, K. Ravindranathan , and J. Kiwi, *J. Am. Ceram. Soc.* (1988)**71**, pp.C-512

[142] S.E. Trolier, S.D. Atkinson, P.A. Fuierer, J.H. Adair, and R.E. Newnham, *Am. Ceram. Soc. Bull.* (1988)**67**, pp759

[143] K. Bernhard, G. Gritzner, X.Z. Wang, and D. Bäuerle, *J. Solid State Chem.* (1990)**86**, pp293

[144] T.S. Heh, J.R. Chen, and T.Y. Tseng, *Jpn. J. Appl. Phys.* (1990)**29**, pp552

[145] V.N. Mulay, P.V.L.N. Sivaprasad, K. B. Reddy, M.A. Jaleel., *J. Mater. Sci. Lett.* (1990)**9**, pp1284

[146] A. Manthiram and J.B. Goodenough, *Nature* (1987)**329**, pp701

[147] F.H. Chen and T.Y. Tseng, *J. Am. Ceram. Soc.* (1990)**73**, pp889

[148] F.H. Chen, H.S. Koo, T.Y. Tseng, R.S. Liu, and P.T. Wu, *Mater. Lett.* (1989)**8**, pp228

[149] V. Slusarenko, K.R. Thampi, and J. Kimi, *J. Solid State Chem.* (1989)**79**, pp277

[150] S. Darracq, A.C. Pierre, J. Etourneau, *Bulletin De Société Chimique France* (1989)**2**, pp175

[151] J.V. Mantese, A.B. Catalan, A.H. Hamdi, and A.L. Micheli, *Appl. Phys. Lett.* (1988)**53**, pp527

[152] T.N. Bowmer and F.K. Shokoohi, *J. Mater. Res.* (1991)**6**, pp670

[153] A.H. Hamdi, J.V. Mantese, and A.L. Micheli, *Appl. Phys. Lett.* (1988)**53**, pp435

[154] K.M. Stephens, D.A. Robinson, A. Alvanipour, W.S. Hinton, and A. Morrobel-sosa, *Physica C* (1990)**168**, pp351

[155] S.A. Kramer, G. Kordas, J. Mcmillan, G.C. Hilton, and D.J. Van Harligen, *Appl. Phys. Lett.* (1988)**53**, pp156

[156] S. Kramer, K. Wu, and G. Kordas, *J. Electronic Materials* (1988)**17**, pp135

[157] P. Ravindranathan, S. Komarneni, A.S. Bhalla, R. Roy, and L.E. Cross, *J. Mater. Res.* (1988)**3**, pp810

[158] P. Ravindranathan, S. Komarneni, A.S. Bhalla, and R. Roy, *Mater. Lett.* (1990)**10**, pp153

[159] T. Koyayashi, K. Nomura, F. Uchikawa, T. Masumi, and Y. Uehara, *Jpn. J. Appl. Phys.* (1988)**27**, pp.L1880

[160] S.I. Hirano, T. Hayashi, and M. Miura, *J. Am. Ceram. Soc.* (1990)**73**, pp885

[161] H.S. Horowitz, S.J. Mclain, A.W. Sleight, J.D. Druliner, P.L. Gai, M.J. Vankavelaar, J.L. Wagner, B.D. Biggs, and S.J. Poon, *Science* (1989)**243**, pp66

[162] T. Itaoh and H. Uchikawa, *J. Crystal Growth* (1988)**87**, pp157

[163] C.Y. Shei, R.S. Liu, C.T. Chang, and P.T Wu, *Mater. Lett.* (1990)**9**, pp105

[164] Y.S.N. Murthy, R. Gopalan, S. Raoot, T. Rajasekharan, S. Ravi, and V. Seshubai, *Mater. Lett.* (1990)**9**, pp154

[165] A. Pebler and R.G. Charles, *Mat. Res. Bull.* (1989)**24**, pp1069

[166] Y. Oka, N. Yamamoto, and A. Yuba, *Jpn. J. Appl. Phys.* (1988)**27**, pp.L1429

[167] Powder Diffraction Files, JCPDS-Internation\Center for Diffraction Data

[168] ASTM C914-89, *Annual Book of ASTM Standards* (1990)**15.01**, pp297

[169.1] ASTM E112-85, *Annual Book of ASTM Standards* (1990)**03.01**, pp282

[169.2] ASTM F84-88, *Annual Book of ASTM Standards* (1990)**10.05**, pp147

[169.3] A.C. Pierre, T. Nickerson, and W. Kresic, *J. of Non-crystalline Solids* (1990)**121**, pp45

[170] C.F. Baes and R.E. Mesmer, "*The Hydroysis of Cations* ", Wiley, New York, c.1976

[171] J.C. Boivin, D. Thomas, and G.C.R. Tridot, *Acad. Sci. Ser. C* (1973)**276**, pp1105

[172] W.C. Mackrodt, *Supercond. Sci. Technol.* (1989)**1**, pp343

[173] K. Ma and A.C. Pierre, 91' sintering proceeding, July 24-27, 1991, Vancourver, Canada

[174] T. Uzumaki, K. Yamanaka, N. Kamehara, and K. Niwa, *Jpn. J. Appl. Phys.* (1989)**28**, pp.L75

[175] M. Shiloh, I Wood, M. Brown, F. Beech, and I.W. Boyd, *J. Appl. Phys.* (1990)**68**, pp2305.

[176] H. Pickup, 91' Sintering Proceeding, Jult 24-27, 1991, Vancouver, Canada

[177] C. Herring, *J. Appl. Phys.* (1950)**21**, pp301

[178] K. W. Kingery, H.K. Bowen, D.R. Uhlmann, "*Introduction to Ceramics* " Jhon Wiley &Sons, Inc. c.1976

[179] K.W. Lay, *J. Am. Ceram. Soc.* (1968)**51**, pp373

[180] R.M. German, *"Liquid Phase Sintering"*, Plenum Press, c.1985

[181] P.S. Nicholson, comment on the paper " Phase Transformation of Bi-(Pb)-Sr-Ca-Cu-O superconductor by Sol-Gel.", 1991

[182] Y. Enomoto, T. Murukami, M. Suzuke and K. Muriwaki, *Jpn. J. Appl. Phys.* (1987)**26**, pp.L1248

APPENDIX A

PEROVSKITES[19]

Origins

The original mineral called perovskite is calcium titanate - $CaTiO_3$. It was described in the early nineteenth century by Gustav Rose, who named the ceramic after a Russian mineralogist, L. A. von Perovski. Several natural perovskite minerals exist, but they are rare, however, the production of synthetic perovskites is of considerable importance, especially in new high-T_c ceramic superconductors.

Perovskite Structure

The perovskites include many compositions, like $CaTiO_3$, $AgAnF_3$, $LiBaF_3$, $CsCdBr_3$, $SrTiO_3$ and many more. The general formula for an ideal perovskite is ABX_3, where A and B are metal cations, and X is an anion like oxygen, fluorine, bromine, or chlorine.

A perovskite, in its "ideal" form, has a cubic structure with a relatively large metallic atom (A) at its center, smaller metallic atoms (B) at its corners, and nonmetallic atoms (X) on edge midpoints (Fig. A.1).

The materials involved have been removed because of copyright restriction.

Fig. A.1 Illustration of a unit of an ideal perovskite

Variation from the Ideal Form

The ideal perovskite structure, such as calcium titanate ($CaTiO_3$), is an insulator. Since all the atomic sites are occupied, strong ionic bonds hold the electrons firmly in their positions. This strong bonding also results in a hard mineral that has a relatively high melting temperature. Since the ideal structure is symmetric, it naturally has three-dimensional isotopy. There are, however, variations that lead to marked differences in electrical, mechanical, and optical properties, including anisotropy. These properties may either be useful (as in piezoelectrics) or rather a nuisance (as in the new ceramic superconductors.)

A-B Ion Size Variations

When the central "A" ion is slightly too small compared to the "B" ion at the corners, this can lead to a shifting in the position of the B and X ions. In this instance, the resulting unit cell may appear more like a cluster of polyhedrons than a cube; the structure may "tilt" or "twist" resulting in an electric polarization of the entire crystal or in piezoelectric behavior.

Mixed A or B Sites

Rather than having a single element associated with the A and/or B sites, it is possible to substitute them by foreign elements. For instance, very high pressures and temperatures, such as are found in the earth's interior, either magnesium or iron may fill the "A" site to give magnesium-iron silicate $(Mg,Fe)SiO_3$.

Stoichiometry

It is not uncommon to find materials with X atoms vacancies. This is, in fact, a very important factor in some of the new high-temperature superconductors.

Twinning

In any perovskite specimen that is not of the pure cubic form, a phenomenon called twinning, is commonly seen. This involves, for example, the alignment of the shorter side of one cell with the slightly larger side of an adjacent cell. Twinning is almost always seen in the orthorhombic $YBa_2Cu_3O_{7-d}$ superconductors, and is believed to have significant effects on electrical, magnetic, optical, and mechanical properties.